1 Introduction to Musculoskeletal Imaging

CHAPTER OUTLINE

Part 1: Bones

Bone Anatomy

Bone is composed of mineral (*calcium hydroxyapatite*) deposited on a matrix (*osteoid*) made mainly of collagen. Bones have a thick outer *cortex* that surrounds an inner network of *trabeculae*.

- Synonyms:
  - Cortical bone = compact bone. Dense and strong, accounts for most of the weight of a bone.
  - Cancellous bone = trabecular bone = spongy bone.
- Both cortex and trabeculae are composed of *lamellar bone*, and both contribute to bone strength.
- Precursor to lamellar bone is *woven bone.*
  - Less well ordered, with disordered osteoid and less mineral.
  - Formed initially during intrauterine growth and some fracture healing, later remodels into mature lamellar bone.
  - Woven bone is also seen in high bone turnover conditions and *Paget disease* and hyperparathyroidism (Chapter 13).

LONG BONES (FIG. 1.1):

- *Epiphyses* at the ends.
- *Diaphysis* (shaft) in the middle.
- *Metaphyses* in between, transition between the relatively narrower shaft and wider epiphysis, normally with concave contour.

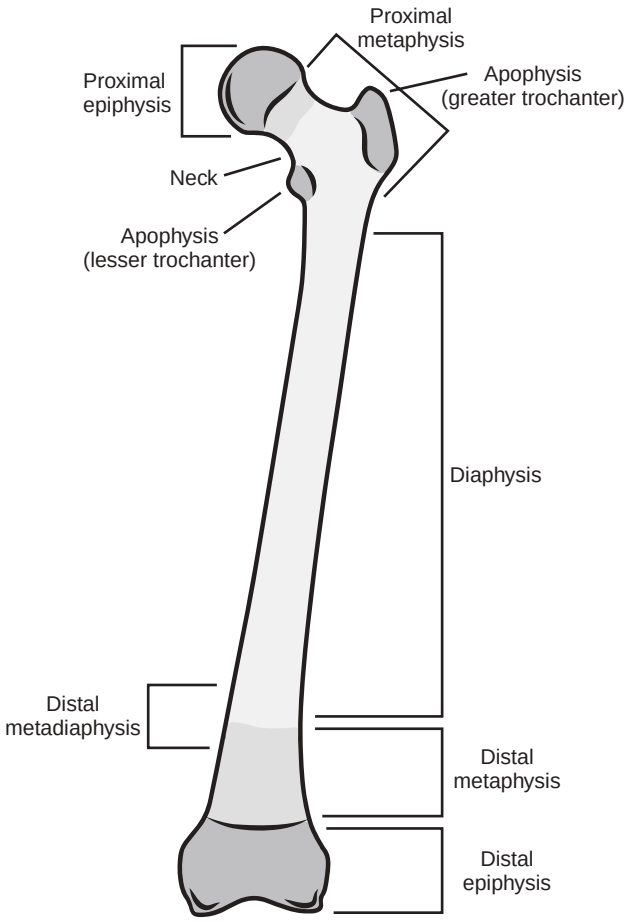

Fig. 1.1 Long bone anatomy.

- *Diametaphysis* = *Metadiaphysis* = the transition between metaphysis and diaphysis.
- Long bones of growing children also have at least one *physis* (*growth plate*, *epiphyseal growth plate*), composed primarily of cartilage, located transversely between a metaphysis and epiphysis.
  - The physis allows for bone elongation during growth.
  - Weaker than surrounding bone, so a frequent site of fracture in children.

MARROW CAVITY

- Contains trabecular bone and varying amounts of cellular and fatty marrow.
- Normal site of hematopoiesis.

PERIOSTEUM

- Covers the bone surface, except at the joints.
- Composed of tough fibrous outer layer and lined with an inner layer (*osteogenic layer*, or *cambium*) that produces bone as needed, allowing bone diameter to increase with growth (and throughout life to some degree), and rapidly in case of fracture.
- Periosteum is tightly bound to underlying bone in adults, but less so in children (except at the physes, where it is tightly bound).
- Cortical bone contains a network of microscopic channels, including *Haversian canals*, that extend through the cortex. Haversian canals provide a route out of the medullary space for tumors or infection, which can elevate the periosteum.

Around joints the *articular cartilage* covers most of the bone surface along with the joint capsule and ligaments.

Embryology and Bone Growth After Birth

- Development of the skeleton begins during the first trimester of gestation.
- *Mesoderm* differentiates into *sclerotome* (eventually forms the bones), *myotome* (muscles), and *dermatome* (skin).
- Aggregation of *mesenchymal cells* during the first trimester forms the limb buds that subsequently become the bones, joints, muscles, and tendons.

BONE FORMATION

Bones are formed by either *intramembranous ossification* or *enchondral ossification*, both of which involve replacement of connective tissues by bone.

Intramembranous Ossification

- Bone is formed by direct transformation of primitive mesenchyme into bone.
- Forms most of the skull, mandible, most of the facial bones, portions of the clavicles, and pubis.
- Contributes to most fracture healing.
- Periosteum can make new bone by intramembranous and enchondral ossification.

Enchondral Ossification

- Bone is formed in a two-step process:
  1. Chondrocytes form a cartilage model
  2. Osteocytes replace the chondrocytes and convert the cartilage model into bone.
- Forms the bones of the extremities, skull base, spine, and most of the pelvis.
- The *physis* (growth plate) in the long bones of children creates bone by enchondral ossification, which allows for long bone growth before and after birth. The physis is reviewed in detail in Part 3 of this chapter.
- Most fracture healing occurs by enchondral ossification.

The bone formed by either process initially is immature *woven bone*. The immature woven bone is subsequently remodeled in a coordinated process of bone resorption by *osteoclasts* and bone formation by *osteoblasts* into stronger, mature *lamellar bone*.

Similar coordinated osteoclast bone resorption and osteoblast bone formation is essential throughout life:

- During growth: *remodels* (reshapes) bones as they grow into the adult configuration.
- Throughout life: maintains bone strength in adults by continuously replacing older bone weakened by microfractures with new bone. This process is called *bone turnover*.

Fig. 1.2 Wolff's law: bone loss as a result of disuse. The hip arthroplasty femoral stem is stiffer than the surrounding proximal femur, effectively shielding the proximal femur from routine stress. The resulting bone loss is seen as cortical thinning *(arrows)*. In contrast, bone loading around the stem tip is increased because stress is concentrated at this point, resulting in new bone formation with cortical thickening *(arrowheads)*. There are many potential causes of bone loss; the stress shielding illustrated here is just one.

Bone growth and bone turnover are governed by multiple factors:

- Hormones, including growth hormone and the sex hormones.
- Genetics.
- Metabolic conditions.
- Mechanical stress.
  - **Wolff's law**: An increase in bone stress shifts the bone resorption/bone production balance toward greater bone production. Cortex thickens. Trabeculae thicken and become more numerous. In contrast, decreased bone loading causes bone resorption to exceed bone production ('use it or lose it'). If unchecked, this leads to decreased bone mass, cortical thinning, and loss of trabeculae (Fig. 1.2).

Pathophysiology: Bone Trauma

Bone is a dynamic tissue performing essential roles in biomechanics, calcium homeostasis, and normal hematopoiesis. The following discussion concentrates on bone trauma.

BASIC BONE BIOMECHANICS

- Normal mature bone is strong and rigid. If enough force is applied, a normal adult bone will break rather than permanently deform.
- Children's bones and, to a lesser degree, adult bones weakened by certain disease states such as *osteomalacia* or *osteoporosis* are 'softer' and can permanently deform without breaking into two separate fragments. Such deformities are the result of numerous microscopic fractures.

There are three primary forces in bone trauma: *compression*, *tension*, and *shear*.

- *Compression* is force that pushes two portions of a bone together.
- *Tension* is the opposite: it is force that pulls two portions of a bone apart.
- *Shear* is force that slides two portions of a bone past one another.

These forces act on both gross and microscopic levels. Any material—be it metal, wood, or bone—has a unique threshold at which it will fail (fracture, in the case of bone) with each of these forces.

- Bones and joints are *anisotropic* (i.e., not the same in each direction). Specifically, bones are stronger in compression and weaker in tension and shear.
- A fracture can be caused by just one of the three basic mechanical forces or by a combination.
- An example of a fracture resulting from *isolated tension*: transverse fracture of the patella, in which violent contraction of the quadriceps muscles places the patella under extreme tension. If the patella fails, the resulting fracture will be transverse (Fig. 1.3).
  - This example illustrates the general rule that fractures resulting from tension tend to occur perpendicular to the direction of the applied force.
- The common cortical avulsion fracture is another example of a tension fracture, due to tension by an inserting ligament.

Pure *compression force* in a long bone usually produces an oblique fracture (Fig. 1.4).

- In the spine, pure compression produces a vertebral body compression or burst fracture (Fig. 1.5).

Fig. 1.3 Transverse fracture of the patella caused by tension failure during extreme quadriceps contraction.

Fig. 1.4 Oblique fracture of the fourth toe proximal phalanx.

Fig. 1.5 Multiple compressions of the lumbar vertebral bodies *(arrows)* in a patient with osteoporosis (sagittal T1-weighted MR image). The irregular transverse low-signal lines within the vertebral bodies are fracture lines.

Shear forces tend to create fracture lines oblique to the line of force. Shear forces are present on a microscopic level in most fractures, because some of the multidirectional bone trabeculae are placed under shear stress regardless of whether the primary force is compression or tension.

Many fractures are caused by some combination of the three basic mechanical forces.

- *Example 1*: Bone bending. If a curved long bone is compressed, the force tries to bend the bone. Tension forces develop along the convex portion of the cortex and compressive forces develop along the concave portion of the cortex. Bone is better able to withstand compression forces than tension forces, so the convex margin tends to fail first. Examples are childhood *pure plastic bowing* fracture and childhood *greenstick fracture* (Fig. 1.6) and the butterfly-shaped comminuted fracture in adults (Fig. 1.7).
- *Example 2*: A twisting or rotational injury in which torsion force is applied around the circumference of a bone. This mechanism combines compression, tension, and shear, resulting in a *spiral fracture* (Fig. 1.8).

An additional important biomechanical property of bone is that the fracture threshold is inversely related to the rate at which a load is applied.

- In other words, bone is more resistant to force that builds slowly than to a rapidly applied force.
- A rapidly delivered, sharp impact such as from a bullet or a direct blow to a bone is more likely to cause a fracture than a greater force that builds slowly.
- On the other hand, because a bone can tolerate a greater load if applied slowly, more energy is stored. If the bone does eventually fracture, the damage may be more severe.
- In the soft tissues a rapidly applied force also is more likely to cause tissue failure. This is why the shock wave from a high-velocity gunshot wound can cause so much damage to the soft tissues.

IMAGING TECHNIQUES IN BONE TRAUMA

Radiographs

- First-line, and often the best and only imaging exam that is needed.
  - Main exception: spine (computed tomography [CT] is better).
- Orthogonal views are needed to detect fracture and characterize deformity.
- A single radiograph as a screening exam decreases sensitivity and is not encouraged.
- Ionizing radiation.
- Radiographs may not provide sufficient fracture characterization to guide therapy.

CT

- Current generation CT with multiplanar reformats has excellent sensitivity.
- More sensitive than radiographs. Useful when radiographs are negative but clinical suspicion is high, especially for body parts where radiography has lower sensitivity such as the midfoot and spine.
- Excellent depiction of fracture fragments.
- Helpful in characterizing complex fractures such as comminuted intraarticular fractures and planning surgery. 3D reconstructions can be useful.
- Fast; often readily available.
- Dual energy CT scanners can identify marrow edema, increasing sensitivity for nondisplaced fractures in osteoporotic patients.
- Ionizing radiation.
- Less sensitive for nondisplaced fractures in osteoporotic patients.
- Can be limited by artifact from orthopedic hardware.

Fig. 1.6 Bowing fractures in children. (A) Pure plastic bowing fracture of the forearm in a 5-year-old. The ulna is laterally bowed *(arrows)* and the radius is dorsally bowed *(arrowheads)*. These bones are normally mildly bowed in these directions, but the degree of bowing, combined with a history of fall and forearm pain, establishes the diagnosis. **(B)** Greenstick fracture of the distal radius. **(C)** Plastic bowing deformities of the ulna and radius. Also note essentially complete radius fracture *(arrowhead)* and the minimal buckle fracture of the distal medial ulna *(arrow)*.

Fig. 1.7 Comminuted fractures. (A) Adult equivalent of bowing fracture: butterfly comminution fracture. *Arrow* points to the butterfly fragment in a humerus midshaft fracture. **(B)** Segmental fracture. Lateral view of the leg shows two fracture sites in the fibula *(arrowheads)* separated by a segment of normal bone. The tibia fracture *(arrows)* is nearly transverse, in this case reflecting a high-force injury.

Fig. 1.8 Spiral fractures. Laterally displaced **(A)** and mildly displaced **(B)** fractures. Note the typical combination of a spiral component *(white arrowheads)* and a straight, longitudinal component *(black arrowheads)*.

Magnetic Resonance Imaging

- Excellent problem solver in acute trauma when other studies are negative due to very high sensitivity and high specificity.
  - Magnetic resonance imaging (MRI) findings in an otherwise occult fracture: Marrow edema on *fluid-sensitive sequences* such as inversion recovery or fat-suppressed T2-weighted images. The low-signal fracture line is often best seen on T1-weighted images (Fig. 1.9)
- Good depiction of larger fracture fragments.
- Can show pediatric fractures through unossified cartilage.
- Also demonstrates soft tissue injuries.
- No ionizing radiation.
- Image quality degraded by motion and metal artifacts.
- Need sedation in younger children.
- Many electronic implants (pacemakers, cochlear implants) are not MRI compatible.

Radionuclide Bone Scan

- Insensitive to acute fractures, but becomes positive after about 3 days (healing response).
- Allows whole body imaging.
- Useful if joint replacement or other metal implant creates artifact on CT or MRI.
- Often used for suspected stress fractures (if negative excludes a stress fracture)
- Can be helpful in suspected child abuse.
- Less sensitive than MRI.

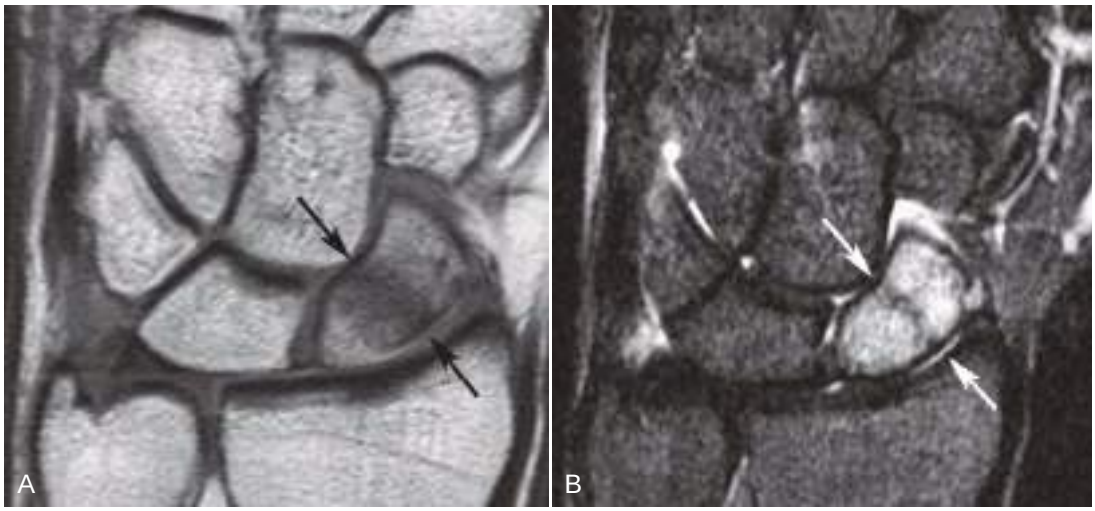

Fig. 1.9 MR imaging of a radiographically occult fracture. Young adult with snuff box tenderness and normal radiographs. Coronal T1-weighted **(A)** and inversion recovery **(B)** images show a scaphoid waist fracture *(arrows)*. Note the diffuse high-signal marrow edema in **B**.

- Ionizing radiation.
- Need sedation in younger children.

FRACTURE DESCRIPTION TERMINOLOGY

Accurate description is extremely important and requires conventional terminology to facilitate communication of the findings.

Fracture Location

- Which bone?
- Which part of the bone (diaphysis, metaphysis, etc.)?
  - Long bone shaft fractures: divide the length of the shaft into thirds. Localize the fracture to the proximal third, the junction of the proximal and middle thirds, the middle third, the junction of the middle and distal thirds, or the distal third.
  - In bones with specific anatomy (neck, trochanter, etc.), use that term.
- Does the fracture extend to a joint surface (*intraarticular*)?
- In children: does the fracture involve a physis? Physeal fractures and their classification system are discussed in Part 3.

Open Versus Closed Fracture

- *Closed fracture*: osseous fragments do not breach the skin surface.
- *Open fracture* is associated with skin disruption and exposure of a bone fragment (Fig. 1.10).
  - Due to infection risk, open fracture is an emergent situation needing lavage and surgical reduction.

Complete Versus Incomplete Fractures

Complete Fractures

- Two or more separate bone fragments.
- *Transverse*: fracture perpendicular or up to 30 degrees oblique to the bone long axis.
- *Oblique*: fracture is at an angle > 30 degrees to the long bone axis.
- *Spiral*: combination of curved oblique and longitudinal.
- *Comminuted*: more than two fragments (only mention when present).
  - *Segmental* fracture: the same bone is fractured in two separate sites, with an intact segment of bone between the fracture sites (see Fig. 1.7B).
  - *Butterfly-comminuted (wedge)* fracture: a wedge-shaped 'butterfly' fragment of intervening bone is present (see Fig. 1.7A). This fragment is at risk for osteonecrosis, and these fractures often require hardware fixation.

Incomplete Fractures

- Cortex is incompletely interrupted.
- Occur most often in children because of the different mechanical properties of bone in children compared with those of adults, as noted earlier.
  - *Buckle fracture*: focal compression of cortex caused by an axial load (Fig. 1.11; see also Figs. 1.1 to 1.5).

Fig. 1.10 Open fractures. (A) Some open fractures are obvious. **(B)** Most are more subtle. Notice the tell-tale subtle low-density soft tissue gas near the tibia fracture *(arrows)*.

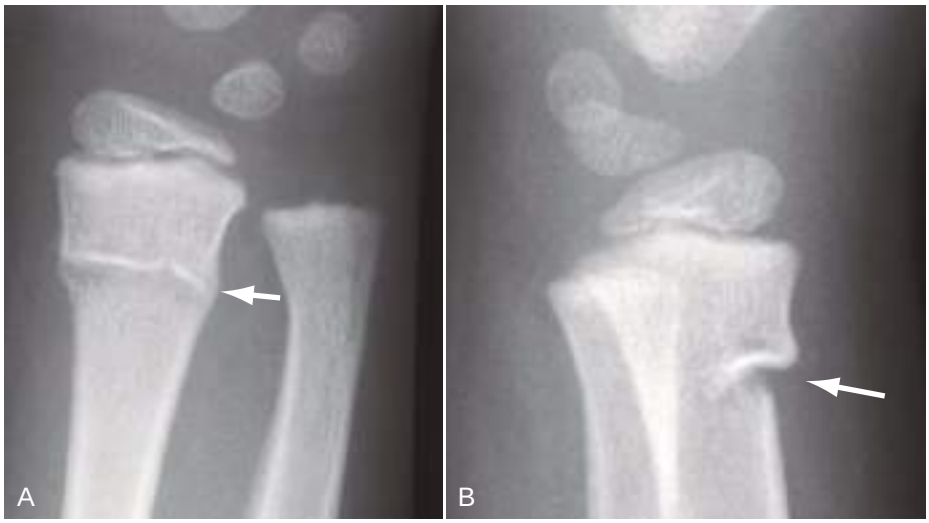

Fig. 1.11 Childhood buckle fracture. PA **(A)** and lateral **(B)** views show a dorsal-distal-radial metaphyseal buckle fracture *(arrows)*.

- *Torus fracture*: circumferential type of buckle fracture.
- *Greenstick fracture*: results from bending force with distraction of cortex fragments on the convex side of the bone (see Fig. 1.6B).
- *Pure plastic bowing deformity (plastic deformation)*: a bending of bone without a visible fracture line (see Fig. 1.6A). This injury represents innumerable microfractures of a long segment of bone.
- *Toddler's fracture*: Usually nondisplaced lower extremity fracture in a newly ambulating toddler. May be difficult to detect on radiographs (Fig. 1.12).

- Incomplete fractures in adults are less common and are usually nondisplaced. Such fractures may have unusual mechanisms or may occur in bone weakened by disease such as osteoporosis or osteomalacia (Fig. 1.13).

Fracture Displacement

By convention, *displacement* is described by the position of the more distal fragment relative to the more proximal fragment.

Translation (Position)

- Anterior/posterior, medial/lateral, proximal/distal.
- Anterior/posterior and medial/lateral displacement can be described in terms of percentage of shaft diameter.
- If displacement is greater than 100% of the shaft diameter, muscle pull can cause the fracture fragments to slide past one another (*overriding, overlap,* or *bayonet apposition*).
- *Distraction* is longitudinal separation of the fracture fragments. This may result from muscle pull or interposed soft tissue.
- The length of any fragment overlap or distraction should be included in the report.

Angular Deformity (Alignment). Directional change of the long axis of the distal fragment relative to the long axis of the proximal fragment. This is described in one of two ways:

1. Orientation of the apex of the angle formed by the fracture fragments

Fig. 1.12 Toddler's fracture. AP radiograph shows an oblique fracture of the distal tibia *(arrows)*. These nondisplaced fractures of the lower extremities of toddlers are always subtle and are often only detected on follow-up radiographs by the development of tell-tale periosteal reaction. Most toddler's fractures occur in the tibia.

2. Orientation of the distal fracture fragment relative to the proximal fragment

Orthopedic surgeons often use the latter system.

- *Medial angulation* (*varus)*: The distal fracture fragment is pointing relatively more toward the midline of the body when compared with the proximal fragment. This is the same as 'apex lateral angular deformity'.
- *Lateral angulation* (*valgus*) is the opposite; the distal fracture fragment is pointing relatively more away from the midline of the body than is the proximal fragment. This is the same as 'apex medial angular deformity'.
  - Anterior and posterior angulation are similar.
  - Other common descriptors: volar/dorsal, radial/ulnar.
- Report the angular deformity in degrees.

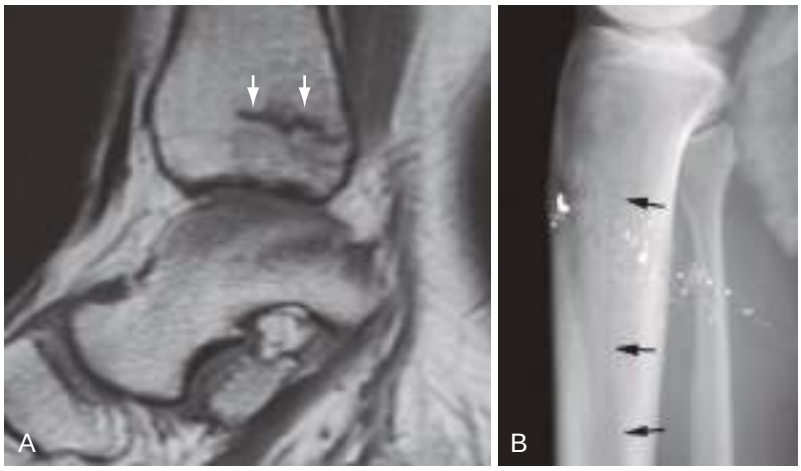

Fig. 1.13 Incomplete fractures in adults. (A) Sagittal T1-weighted MR image shows irregular linear low signal in the distal posterior tibia *(arrows)* representing a nondisplaced, incomplete trabecular fracture, in this case caused by impaction. **(B)** Incomplete tibial fracture in an adult *(arrows)* because of a gunshot wound. Note the metal fragments that mark the bullet tract.

Fig. 1.14 Intraarticular fracture. Shallow oblique AP knee radiograph shows a lateral tibial plateau fracture *(arrow)* with mild diastasis and depression of the lateral fragment.

Rotation or Torsion. Twisting of the distal fracture fragment relative to the proximal around the bone long axis.
- Can be difficult to determine with radiographs.
- Often evaluated clinically.
- MRI or low-dose CT can be helpful in difficult cases (see Fig. 5.33).

Additional Fracture Descriptors

Impaction
- Often with local comminution.

Intraarticular Fracture
- Any fracture that extends to an articular surface.
- Intraarticular fractures are more likely to need surgical intervention and less likely to have a normal outcome (Fig. 1.14).
- Can be very subtle on routine radiographs, requiring special views or CT or MRI for diagnosis or exclusion.
- Hemarthrosis is suggestive but not specific.
  - Fluid-fluid level on horizontal beam radiograph or CT.
  - Cells layer dependently, with lower density serum on top.
- *Fat-fluid level* is specific.
  - Caused by escape of marrow fat into the joint space through an articular fracture.
  - Three levels may be seen: fat on top, serum, and the cellular layer on the bottom (Fig. 1.15).
- *Articular split fracture* cleaves a joint surface into two or more separate fragments.
- *Die-punch fragment*.
  - An articular surface fragment that is driven into the epiphysis or metaphysis.
  - The fragment may be rotated or tilted.
  - Die-punch fragments occur most commonly in distal radius and tibial plateau fractures (Fig. 1.16).

Osteochondral Fracture
- Compression or shear fracture of the subchondral bone and that is confined to the peripheral portion of an epiphysis.
- The equivalent term *osteochondral lesion* is now used.
- Shear injuries may result in a displaced osteochondral fragment. The fragment may remain in or close to its original position or may be displaced into the joint (Fig. 1.17).

One of the most important complications of an intraarticular fracture is posttraumatic osteoarthritis. An articular surface step-off or a gap of more than 2 mm is associated with a significantly increased rate of development of posttraumatic osteoarthritis. Therefore a complete report measures and reports all joint surface gaps and step-offs.

Avulsion Fracture
- Caused by tension (traction) by a tendon or ligament (Fig. 1.18).
- *Chip fracture* is sometimes used to describe any small cortical fragment, but it is more precisely limited to fractures caused by focal impaction or shearing rather than avulsion.

Fig. 1.15 Traumatic joint effusions with fluid levels. (A) Cross-table lateral knee radiograph in a patient with a tibial plateau fracture. Note the fat-fluid level *(arrowheads)* with low-attenuation fat layer on top and the dependent blood below. **(B)** Axial CT image in a different patient with an intraarticular distal femur fracture (not visible on this image) shows three layers *(arrows)*, with low-attenuation fat on top, a dense serum layer in the middle, and a slightly denser layer containing serum and blood cells at the bottom. The layers are not exactly parallel in this image, a temporary phenomenon seen with modern high-speed CT scanners related to patient motion just before the scan and differing fluid viscosities. **(C)** Lipohemarthrosis on MRI. Axial fat-suppressed T2-weighted MR image in the knee of a patient with a tibial plateau fracture shows layering identical to that seen in **B**. The fat layer has low signal intensity because of fat suppression. If this image had been obtained without fat suppression, the fat would be bright. The cellular (most dependent) layer is slightly darker than the serum (middle) layer because of susceptibility artifact due to intracellular hemoglobin. See also Fig. 6.6.

Fig. 1.16 Die-punch fragment. Coronal CT reconstruction of a tibial plateau fracture shows depressed lateral plateau fragment *(arrow)*.

Fig. 1.17 Osteochondral fractures. (A and B) Displaced osteochondral fragment *(arrowheads)* in the knee joint. This is a typical osteochondral fragment in that it is narrow and the subcortical bone is clearly visible. (The cartilage is not visible on radiographs.) Lateral view (**B**) shows the donor site on the lateral femoral condyle *(arrow)*. **(C)** Coronal T2-weighted MR image shows a minimally displaced medial talar dome osteochondral fracture *(arrows)*. Note high T2 signal between the fragment and the talus. **(D)** Displaced osteochondral fragment the hip joint (*arrowhead*) after hip dislocation. Note the donor site (*arrow*).

- Avulsion fractures are more significant, because they may be associated with joint instability.
- Knowledge of the normal sites of ligament attachment can be helpful in distinguishing avulsion fractures from the less significant chip fractures.

Fragility Fracture

- Fracture resulting from a ground level fall or similar minor trauma in bones weakened by osteoporosis, osteomalacia, osteogenesis imperfecta, and other widespread conditions.
- Common sites include the proximal femur, proximal humerus, and distal radius.

Pathologic Fracture

- Fracture caused by normal stresses on an abnormal bone.
- Fragility fractures and insufficiency fractures discussed later technically are pathologic fractures, but in general usage the term *pathologic fracture* is reserved to describe a fracture through bone weakened by a tumor (Fig. 1.19), osteomyelitis, or other focal lesion.
- Pathologic fractures tend to be transverse. Diaphyseal transverse fractures warrant extra scrutiny for a possible underlying lytic lesion.

Trabecular Fracture

- Fracture confined to trabecular bone.

Fig. 1.18 Avulsion fracture. (A) Avulsion fracture of the tip of lateral malleolus *(arrow)* following a supination ankle injury. **(B)** Right anterior inferior iliac spine (AIIS) avulsion. The fragment *(arrow)* is displaced distally by the rectus femoris.

Fig. 1.19 Pathologic fracture through a fourth metacarpal shaft enchondroma.

- May be incomplete and nondisplaced or minimally displaced.
- Typically occur in bone weakened by osteoporosis.
- Subchondral and metaphyseal locations are typical.
- May be visible on radiographs as a sclerotic band.
- MRI: fracture has low signal on T1-weighted images. Surrounding marrow edema may be extensive.

Bone Bruise (Bone Contusion)

- Edema, hemorrhage, and trabecular microfractures caused by a direct blow.
- MRI: marrow edema on fluid-sensitive sequences.

Sample Reports

- Spiral fracture proximal humeral shaft. Distal fragment is displaced medially by greater than one shaft width and the fragments override 3 cm. 15 degrees varus alignment.
- Oblique fracture tibial midshaft. Distal fragment is displaced medially by one-half shaft width with 20 degrees apex anteromedial angular deformity. Adjacent soft tissue gas consistent with an open fracture.
- Buckle fracture dorsal distal radial metadiaphysis with 30 degrees dorsal angulation.
- Transverse fracture proximal femoral shaft through a lytic lesion highly concerning for malignancy.

FRACTURE REDUCTION

- Ideal goal is restoration of anatomic (normal) alignment.
- However, compromises must often be made to achieve the best possible outcome.
- A host of factors determine the desired fragment positions after reduction.
  - Maximize the likelihood of healing.
  - Minimize the risk of complications.
  - Maintaining the function of nearby joints is one of the most important goals.
- Angulation of a long bone shaft fracture is generally undesirable but may be tolerated if it is in the same plane as the motion of an adjacent joint. For example, little if any varus or valgus malalignment or rotation is acceptable in a tibial fracture, because both the ankle and knee are sagittal-plane hinge joints and unable to compensate. The highly mobile shoulder joint is better able to compensate for adjacent deformity.
  - An intraarticular fracture with a step-off or diastasis of greater than 2 mm has a significantly increased risk of developing posttraumatic osteoarthritis.

When reducing a fracture, the orthopedic surgeon reverses the forces that caused the fracture. For example, a *Colles fracture* is caused by compression of the dorsal aspect of the distal radius. When reducing a Colles fracture, the surgeon must distract the dorsal radius, which is accomplished by distraction and palmar flexion of the wrist.

Closed Reduction

- Manipulation to improve alignment.
- The improved alignment is maintained with a cast or splint.

Open Reduction

- Operative access to the injured bone.
  - To assist reduction, especially of intraarticular fragments.
  - To apply fixating hardware.
- The improved alignment may be maintained with hardware fixed to the bone.
- ORIF = open reduction with internal fixation.

Internal Fixation

- Screws that cross an oblique fracture, cortical plate on the bone surface fixed with transverse screws, encircling cerclage wires, or intramedullary fixation with a nail or rod (Figs. 1.20 to 1.22).

External Fixation

- Achieved by pins or wires placed through the skin into the bone remote from the fracture site.
- The pins or wires are fixed to one another externally (Fig. 1.23).
- Used when the fracture site may be infected and, rarely, for fractures near the end of a bone.

Compression across the fracture improves contact between the fragments which speeds healing and reduces the risk of nonunion. A variety of techniques may be used to achieve such compression (Figs. 1.23 and 1.21).

- On the other hand, compression must sometimes be limited.
  - Example: comminuted long bone fracture would telescope and shorten if compressed. The bone length can be controlled by fixation with a cortical plate or an intramedullary nail (rod) with proximal and distal interlocking screws (Fig. 1.22).

Dynamic fixation means that fragment motion is allowed in one direction but constrained in all others. Examples:

- Dynamic hip screw (discussed further in Chapter 5).
- 'Dynamizing' an interlocked intramedullary nail. After a tibial or femoral shaft fracture has partially healed enough to resist compression, bone apposition may be improved by removal of the interlocking

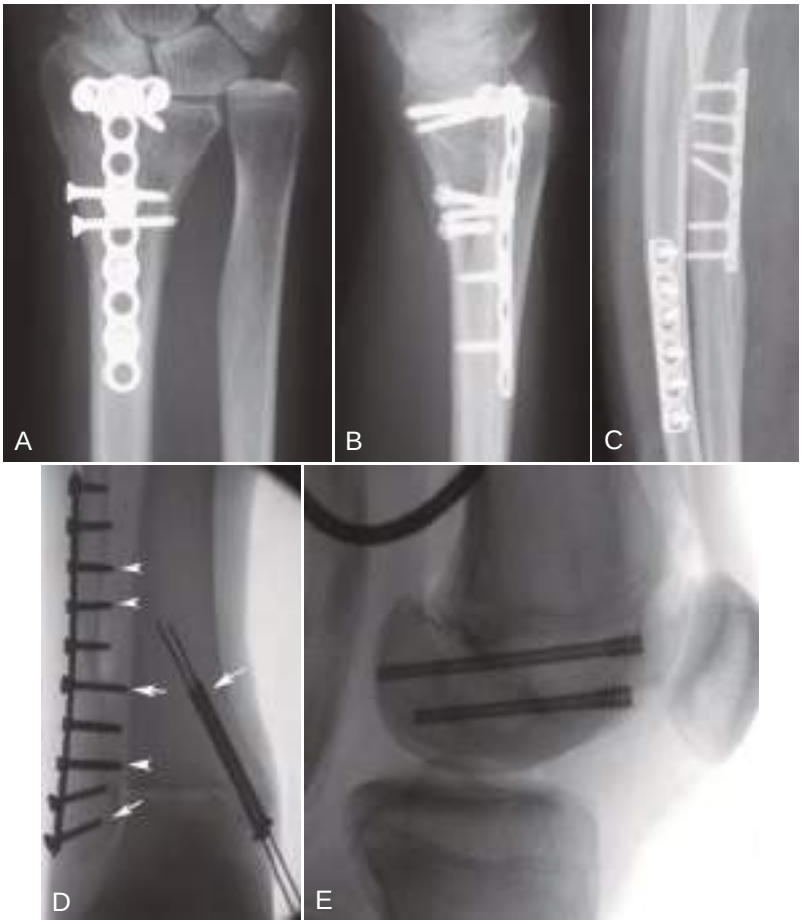

Fig. 1.20 Internal fixation with plates and screws. AP **(A)** and lateral **(B)** radiographs show dorsal T-plate fixation of distal radius fracture. Also note the two lateromedial transverse screws. **(C)** Forearm fractures in adult bones fixed with cortical compression plates. The slots for the screw heads are designed to force the fragments toward the center of the plate. Such compression increases apposition of bone fragments and thus speeds healing. **(D)** Screw types. Screws designed to gain purchase in cortex have fine threads *(arrowheads)*. Screws designed to gain purchase in softer trabecular bone have wider threads *(arrows)*. The medial malleolus screws are lag screws. The gap (lag) between the threads and the head allows compression as the screw is tightened. **(E)** Differential thread screws. This child had a coronal plane fracture across the femoral condyles. The screws were placed from an anterior approach. Note the difference in the threads: the leading edge (more posterior) threads have higher pitch (i.e., are spaced farther apart). As both threads bite, the anterior and posterior bone fragments are compressed together. A similar but smaller screw called a Herbert screw is frequently used to fix scaphoid waist fractures.

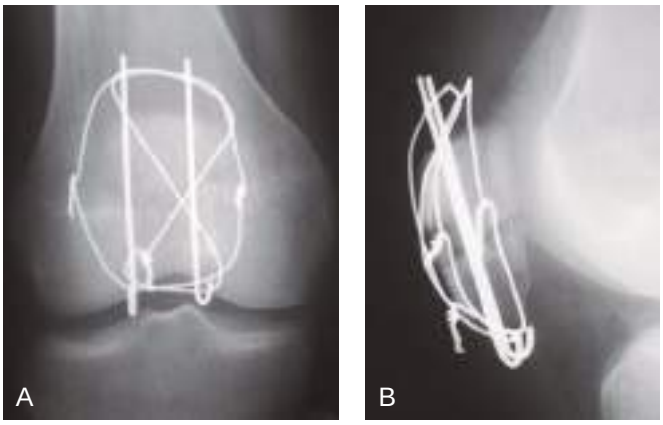

Fig. 1.21 Internal fixation with cerclage wires and pins. (A) AP radiograph and **(B)** lateral radiograph of compression wiring fixation of patellar fracture. Same patient as in Fig. 1.2.

Fig. 1.22 Internal fixation with intramedullary nail. Frontal radiograph of the tibia demonstrates intramedullary rod with interlocking screws *(arrowheads)*, which prevent rotation and shortening after reduction.

Fig. 1.23 External fixation. Note the fixation of the main proximal tibial fragment with crossing wires *(small white arrowheads)*, the main distal fragment with pins *(white arrows)*, and the adjustable external frame *(large white arrowheads)*. This patient also has a tibial plateau fracture that is fixed with two transverse screws *(black arrowhead)*.

screws at one end of the nail. This allows the fragments to slide along the nail and impact against one another (Fig. 1.24), thereby improving bone apposition and healing.

Sample Reports

- Comminuted femoral shaft fracture fixed by an interlocked intramedullary nail. Alignment is anatomic.
- Comminuted intraarticular distal radius fracture has been surgically reduced and fixed with a volar plate and multiple screws.

FRACTURE HEALING

The process described here, known as *secondary fracture healing*, occurs in the large majority of fractures (Fig. 1.25). In contrast, tightly apposed fracture fragments can heal without callus formation (*primary healing*).

The Process

Inflammatory

- Initially a hematoma forms at the fracture site, which provides a source of growth factors and stimulates neovascularization.
- Granulation tissue forms around the fracture site.
  - Contains fibroblasts and stem cells that are supplied in part from the periosteum and endosteum.
- Radiographic findings: Initially none (except for the fracture). Later, blurring or softening of the fracture margins, local demineralization.

Fig. 1.24 Dynamized intramedullary nail. This distal tibial fracture is in the late stages of healing. The fracture was initially fixed with an intramedullary nail with proximal and distal interlocking screws. After the healing process had begun and partial fracture stability was achieved, the distal interlocking screws were removed. This allowed the distal fragment to slide proximally along the nail until fully impacted against the proximal fragment, causing the old screw tracts *(white arrowheads)* to shift proximally relative to the screw holes in the nail *(black arrowheads)*.

Fig. 1.25 Fracture healing in a child. PA **(A)** and lateral **(B)** views show an acute distal radius buckle fracture *(arrows)*. Also note the ulnar styloid avulsion (*arrowhead* in **A**). **(C and D)** Follow-up views obtained 3 weeks later show trabecular healing seen as increased density along the fracture line *(arrows)*. Also note the periosteal new bone formation *(arrowheads)*. The periosteum is loosely adherent to the underlying bone in children, except at the physis, where it is tightly attached. Childhood fractures often result in periosteal elevation because of hematoma associated with the fracture. The elevated periosteum begins to form new bone soon after the fracture. **(E and F)** Follow-up views obtained 5 weeks later show further maturation and remodeling of the periosteal new bone and remodeling of the old fractured cortex (*arrow* in F). On subsequent radiographs (not shown), the bone remodeled to anatomic alignment with no evidence that the fracture had ever occurred.

Repair

- *Primary (immature, soft) callus* forms around the fracture.
  - Contains fibroblasts and chondroblasts that produce cartilage.
- Next, the primary callus is converted to *hard (mature) callus* by enchondral ossification.
  - Woven (immature) bone.
- Note that motion at the fracture site increases callus formation.
- Radiographic findings:
  - *Gap healing*: spaces between fragments fill in with callus.
  - Callus progressively calcifies.
  - The periosteum elevated by hematoma may produce bone that is initially a thin shell and is seen on radiographs as a slender line. (Periosteal new bone formation is also termed *periosteal reaction* or *periostitis*.) The hematoma is eventually converted to bone (Fig. 1.25).

Remodeling

- The callus is remodeled into mature lamellar bone (Fig. 1.25).
- Remodeling goes on for months to years, long after the biomechanical stability is restored, usually toward the prefracture configuration.

- Radiographic findings: amorphous callus replaced by mature bone with cortex and trabeculae.

The *rate of fracture healing* is affected by several factors, including:

- Blood supply.
  - Degree of local bone and soft tissue devitalization.
  - Fracture site.
- Patient age.
  - Children fastest, elderly slowest.
- Fracture location.
  - Metaphysis has the best blood supply.
  - Tibial shaft fractures are notoriously slow to heal (months vs. 6–8 weeks for most fractures).
  - Segmental fractures heal less well.
- Degree of immobilization and apposition of bone fragments after reduction.
  - A small amount of mobility at the fracture site speeds healing.
  - Too much or too little mobility (very rigid internal fixation) slows healing.
  - Too much mobility is also associated with abundant callus formation.
- Smoking slows healing.
- Inadequate nutrition.
  - Vitamin D.
  - Gastric bypass limits calcium absorption.
  - Generalized malnourishment delays healing.
- Drugs.
  - Corticosteroids slow healing and can produce abundant callus (Box 1.1).
  - Nonsteroidal antiinflammatory drugs (NSAIDs) interfere with the early healing process.
- Presence of local complicating factors such as infection or tumor at the fracture site, and bone necrosis.
- Soft tissues interposed between the fracture fragments can delay or block healing.

Interventions that promote fracture healing:

- Electrical stimulation ('bone stimulator').
- Ultrasound (US).
- Various biomaterials, some radiodense, may be placed at the fracture during open reduction. These materials improve fracture healing.

Follow-up Imaging in Routine Uncomplicated Fractures

- Radiographs usually adequate.
  - CT can be used as a problem solver (Fig. 1.26).

Box 1.1 Excessive Callus Formation

Corticosteroids (exogenous, Cushing)
Neuropathic joint
Congenital insensitivity to pain
Paralysis
Osteogenesis imperfecta
Renal osteodystrophy
Burn patients
Subperiosteal bleed in scurvy

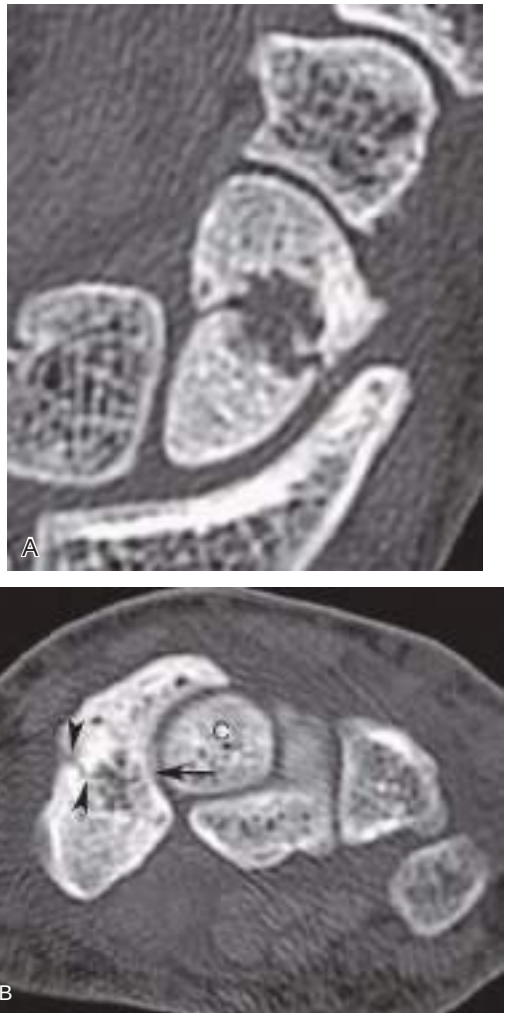

Fig. 1.26 CT for assessing fracture union. (A) Ununited scaphoid waist fracture. Oblique coronal CT reconstruction in a patient who sustained a scaphoid waist fracture 10 weeks previously. No bridging bone was present on this image, nor on any other. **(B)** Partial union of a scaphoid waist fracture. Axial CT image in a different patient obtained several weeks after a scaphoid waist fracture shows partial union, with bridging bone along the medial cortex *(arrow)*, but most of the fracture line is still visible *(arrowheads). C,* Capitate.

- Fragment alignment: report change or no change. If changed, describe.
- Hardware (if present): report change or no change. Look for lucency around screws and other hardware, which is evidence of loosening or infection. This is discussed further below.
- Assess maturity of fracture healing.
  - Earliest: softened fracture lines.
  - Callus first seen at 2+ weeks.
  - Maturing callus.
  - Callus converting to bone (cortex and trabeculae) as early as 3 weeks in children.
  - Late: remodeling (may last for years).

Sample report

- Distal fifth metacarpal fracture is unchanged in position and alignment. Fracture lines have softened and faint callus surrounds the fracture.

FRACTURE HEALING COMPLICATIONS AND IMAGING

Key Concepts

Fracture Healing Complications

Delayed union
Nonunion
Malunion
Osteonecrosis (avascular necrosis)
Soft tissue injury
Infection (open fracture, open reduction, orthopedic hardware)
Hardware failure
Complex regional pain syndrome (reflex sympathetic dystrophy)
Myositis ossificans, heterotopic ossification

DELAYED UNION

- Fracture ununited at 6 months (more or less).
- Delayed union is a clinical diagnosis, with time to union affected by a number of issues that are not evident on the radiograph. These may include:
  - Nutritional status.
  - Alcohol use.
  - Steroids.
  - Smoking.
  - Patient age.
  - Metabolic state.
  - Soft tissue damage.
  - Devascularization.
  - Particular bone involved.
- This term should be used with caution by a radiologist because it may be incorrectly applied to a fracture that is healing slowly but satisfactorily.

NONUNION

- Healing process terminates before osseous union is achieved.
- Radiographic diagnosis.
- No *bridging bone* joining the fracture fragments (Fig. 1.27).
- Can be hypertrophic or atrophic.
  - *Hypertrophic*: sclerotic with excessive new bone formation
  - *Atrophic*: associated with demineralization.
- Rounding and cortication of the fracture edges ('neocortication').
- *Pseudarthrosis* may result.
- *Incomplete union* can be expressed as a percentage, for example '30% osseous union' (Fig. 1.26).

Imaging of suspected nonunion or incomplete union can be difficult in some fractures, even with CT with reformats.

- Comminuted fractures are multiple fractures. Many of the fractures may be well healed, but careful evaluation may show no or only limited continuous bridging bone uniting the most proximal and distal fragments.
- Fixation hardware may obscure fracture lines on radiographs and creates artifact on CT.
  - May need to use much higher CT dose in order to obtain diagnostic images.
  - Dual energy CT and other strategies can reduce this need.

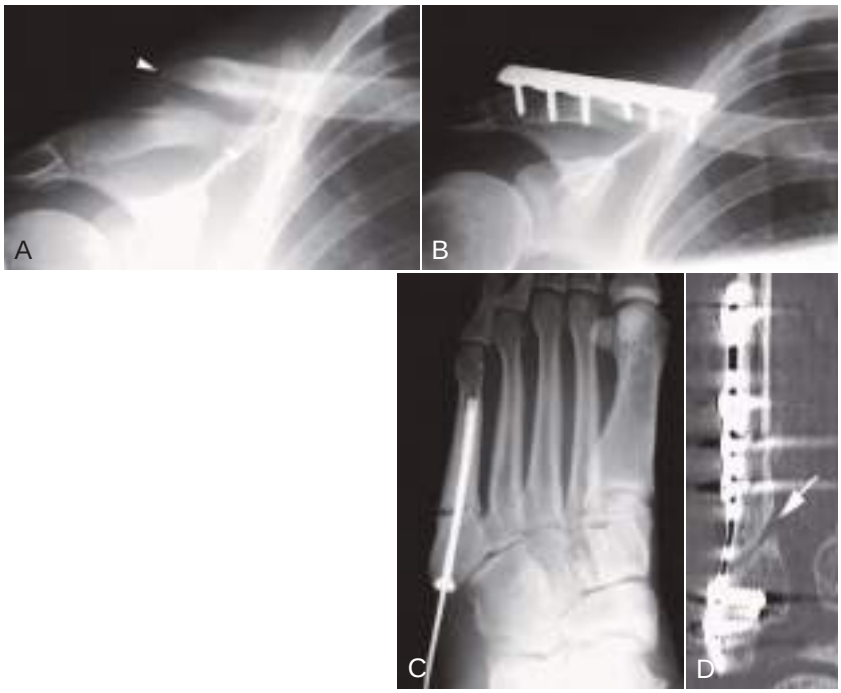

Fig. 1.27 Fracture nonunion. (A and B) Atrophic nonunion of a clavicle fracture. Note the smooth, tapering margins of the fragments (*arrowheads* in A). Surgical fixation was elected **(B)**. **(C)** Nonunion of fracture of the fifth metatarsal proximal shaft. Note the smooth, sclerotic fracture margins. This radiograph also illustrates the technique of placement of a cannulated lag screw. The guide pin is placed under fluoroscopic observation, then the screw is placed over the pin. Because only the tip of the screw is threaded ('lag' screw), tightening the screw compresses the fragments together. (D) Nonunion in an internally fixed distal fibular fracture *(arrow)*.

MALUNION

- Fracture healing with angular or positional deformity.
- Can result in a limb-length discrepancy or limb deformity that may limit function or cause pain.
- As noted in the discussion of fracture reduction, angular deformity in the plane of motion of adjacent joints is better tolerated than angular deformity outside this plane.
- Anterior or posterior angular deformities in children may be corrected over time by the normal remodeling of ongoing bone growth.
- However, varus or valgus angular deformity in children tends to remodel less well and rotational deformity very little.
- Imaging is usually straightforward. CT or MRI can better demonstrate articular surface deformity.

OSTEONECROSIS (AVASCULAR NECROSIS, AVN)

- Potential fracture complication.
- Most common in bones or portions of bones with a tenuous blood supply.
  - Examples include the scaphoid proximal pole (Fig. 1.28), talar dome, and femoral head. These bones have in common extensive covering by articular cartilage, which limits the available sites for blood vessels to enter the bone.
- Diminished bone blood supply can sometimes be detected on radiographs obtained during the initial days and weeks following the fracture.
  - The devascularized bone appears denser than surrounding, vascularized bone.
  - It is not actually denser than that before the fracture. Rather, the vascularized surrounding bone becomes osteopenic due to local hyperemia.
- Although increased fragment density is a sign of AVN, it is not pathognomonic.
  - For example, mild sclerosis of the proximal pole of the scaphoid can be a benign finding in a healing scaphoid fracture.
- Fractures complicated by AVN may require grafting or surgical removal for treatment.
- AVN is discussed further in Chapter 13.

OSTEOMYELITIS

- Open fractures are at especially high risk.
- Risk associated with orthopedic hardware placement is small (Fig. 1.29).
- Look for the development of soft tissue gas, swelling, and bone resorption or other radiographic signs of osteomyelitis.
- Osteomyelitis related to screw placement is usually manifested radiographically as an area of osteolysis surrounding the screw or tract enlargement on follow-up imaging after hardware removal.
- Osteomyelitis is discussed in more detail in Chapter 14.

ORTHOPEDIC HARDWARE LOOSENING AND FAILURE

The potential causes are many. This is a partial list

- Inadequate fracture reduction, which results in undue strain on applied hardware.
- Inadequate hardware.
- Noncompliant patients who place excessive loads on their reduced fractures and hardware before the bone can heal.
- Even the strongest hardware may eventually fail if the fracture fails to heal.
- Imaging findings:
  - Loosening: Look for bone resorption around screws and adjacent to hardware (Fig. 1.30).
  - Hardware fracture (Fig. 1.31).
  - Screw backing out.

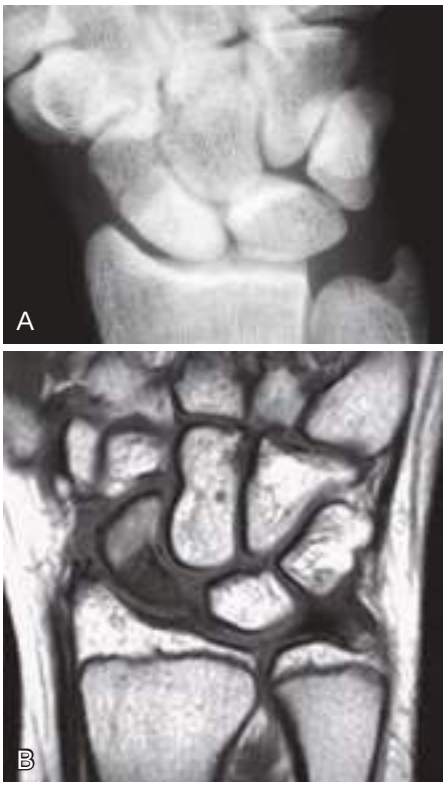

Fig. 1.28 Posttraumatic avascular necrosis. (A) AP wrist radiograph obtained after a nondisplaced scaphoid fracture shows dense proximal pole due to lack of hyperemic healing response. **(B)** Coronal T1-weighted MR image in a different patient shows lack of normal fat signal in the proximal pole because of avascular necrosis.

Fig. 1.29 Antibiotic-impregnated methyl methacrylate beads. After the patient underwent a total hip arthroplasty, the hardware became infected and was removed. The hip is allowed to 'float' during long-term antibiotic therapy before a new arthroplasty is performed. The beads theoretically create high local antibiotic concentration.

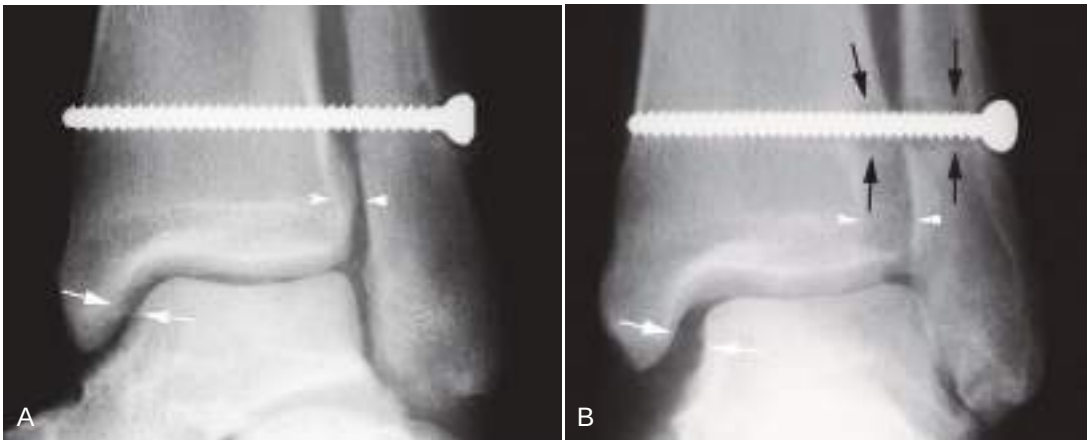

Fig. 1.30 Hardware loosening. (A) Initial AP radiograph of the ankle shows an intact syndesmotic screw fixing a distal tibiofibular diastasis injury. Note the normal alignment of the distal tibiofibular joint *(arrowheads)* and the medial ankle mortise *(arrows)*. **(B)** Radiography repeated several weeks later shows bone resorption seen as lucency around the lateral aspect of the screw, especially in the fibula and lateral tibia *(black arrows)*. Note the widening of the distal tibiofibular joint *(arrowheads)* and the medial mortise *(white arrows)*. Infection or mechanical loosening could cause this appearance.

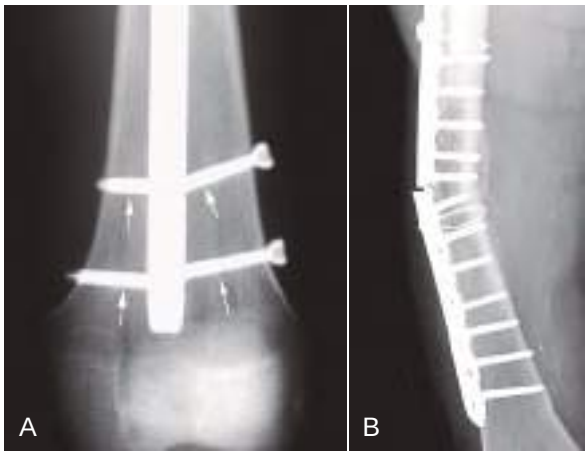

Fig. 1.31 Hardware failure. (A) AP radiograph in a patient with a femoral shaft fracture that was fixed with an interlocking intramedullary nail. He resumed weight-bearing earlier than advised, which placed shearing force across the interlocking screws. The distal screws failed *(arrows)*. **(B)** Hardware fracture. Failed fixation of proximal femur fracture with compression plate and screws.

Fig. 1.32 Stress riser fracture. Oblique proximal femoral shaft fracture near the distal end of intramedullary fixation for a hip fracture. Note that the fracture line crosses—and may have originated at—the hole for the distal interlocking screw *(arrow)*.

Stress Riser (Stress Concentration)

- A small defect in a bone such as an orthopedic screw tract or a foramen where a blood vessel penetrates the cortex can allow force to be magnified at that single point.
- A stress riser can significantly lower the fracture threshold of a long bone shaft, and some fractures begin at a stress riser (Fig. 1.32).
- Orthopedic hardware fractures also often occur at a stress riser in the hardware.

Complex Regional Pain Syndrome (CRPS, Reflex Sympathetic Dystrophy [RSD], Sudeck Atrophy)

- Poorly understood alteration in the nervous system that causes regional hyperemia, pain, osteoporosis, soft tissue trophic changes, and alteration in temperature control.
- Frequently is initiated by a fracture or other trauma.
- This condition is discussed further in Chapter 13.

Soft tissue Injury Associated With Fracture

- Frequently occurs with a fracture, particularly if there is significant fragment displacement or associated dislocation.
- Suspected arterial injury is an indication for emergent angiography, usually CT angiography.
- Nerve or ligament injury can result in poor limb function despite satisfactory fracture healing.
- Additional forms of posttraumatic soft tissue injury are discussed in Part 2.

Stress Injury

- *Fatigue fractures* result from abnormal stresses placed on normal bone.
- *Insufficiency fractures* result from normal stresses placed on bone that is weakened by a generalized process such as osteoporosis.

- The term *stress fracture* is usually reserved for fatigue fractures, although this is not universally agreed upon. Many authors regard both fatigue and insufficiency fractures as stress fractures.
- In some cases, the distinction between fatigue fracture and insufficiency fracture is blurred. An example is lower extremity stress fracture in a young female runner with the *female athletic triad* of eating disorder, diminished or absent menses, and deceased bone mineral density. These stress fractures have features of both fatigue and insufficiency fractures.
- *Stress injury* is an umbrella term that covers the wide clinical and imaging spectrum from minimal injury to complete fracture.

Fatigue Fractures

Occur when abnormal stresses are placed on normal bone, typically multiple and frequent repetition of an otherwise normal force.

- Contributing factors:
  - Muscles, tendons, and ligaments normally help to redistribute forces applied to the bones and joints. Muscle fatigue during prolonged exercise diminishes this protection.
  - Increased bone loading stimulates a normal adaptive process that leads to new bone formation (Wolff's law). The shift toward greater bone formation requires the activity of both osteoblasts and osteoclasts. Unfortunately, the osteoclasts begin first, so an increase in bone stress such as increased physical activity initially results in the bones becoming weaker for a few weeks before ultimately becoming stronger. This creates a window of vulnerability during which microfractures already present can coalesce into a discrete fracture.

Stress Fractures Evolve Over Time

- Begin as microcracks on the bone surface. Undetectable on clinical imaging studies at this stage.
- Initial healing response removes some cortical bone and may incite a periosteal reaction. This stage is sometimes termed a *stress reaction* or, in the tibia, a *shin splint*, but the terminology is not standardized.
  - Radiographs at this stage are usually normal, but faint cortical resorption may be seen.
  - MRI: periosteal edema that may be subtle. Normal marrow signal
  - Bone scan: longitudinal cortical tracer uptake.
- With injury progression, microfractures in a focal segment within the stress reaction may weaken more rapidly. This weaker segment becomes a focal point for bone deformation during repeated loading, because it is less able to resist deformation than adjacent bone. This concentration of microscopic bone deformation at the focally weakened segment has two important consequences.
  - First, the stresses applied to the remainder of the bone are partially relieved, potentially allowing these portions of the bone to heal.
  - Second, the microfractures in the weakened segment are subject to greater deformation, so they are more likely to progress.
  - Radiographs at this stage show periosteal reaction (new bone formation) and cortical demineralization.
  - MRI: periosteal and endosteal edema.
  - Bone scan: trace uptake becomes focal.
- If the injury progresses, there is further fracture progression through the cortex into the medullary space.
  - Radiographs at this stage show cortical bone loss.
  - MRI: more extensive marrow edema. Cortical edema may also be seen.
  - Bone scan: focally hot.
- Further fracture progression results in the fracture line visible on radiographs (the *dreaded black line*). The fracture line may be very faint, but in any terminology this is a true stress fracture (Figs. 1.33 to 1.39).

If untreated, a stress fracture can progress to a complete fracture.

- *Tensile stress fracture* is a stress fracture at a site of distracting force, for example, on the convex side of a curved weight-bearing long bone. Examples include

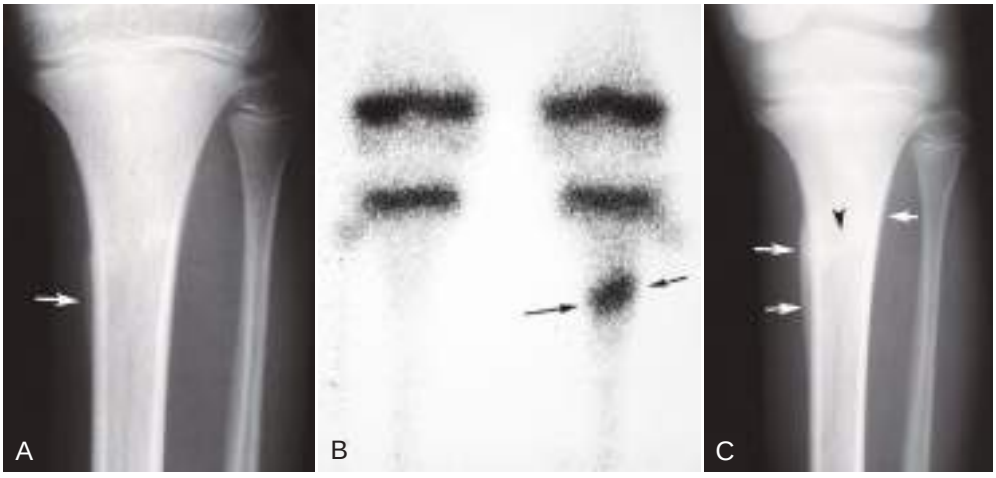

Fig. 1.33 Proximal tibia stress fracture. (A) Radiograph shows ill-defined lamellar periosteal bone formation in proximal medial tibial diaphysis *(arrow)*. **(B)** Bone scan shows oblique transverse stress fracture in the proximal tibia *(arrows)*. **(C)** Frontal tibial radiograph obtained 3 weeks later demonstrates progressive formation of periosteal new bone formation *(arrows)* and appearance of subtle linear sclerosis at the stress fracture site *(arrowhead)*.

Fig. 1.34 Tibia shin splint progressing to stress fracture in a long-distance runner. (A) Initial axial fat-suppressed T2-weighted MR image shows subtle periosteal edema on the posterior tibial shaft *(arrows)*. **(B)** Bone scan obtained the next day confirms classic stress reaction pattern with localized longitudinal tracer uptake in the posterior proximal tibial cortex *(arrow)*. Despite these findings, the patient chose to continue running. **(C)** Repeat MRI using the same sequence 3 weeks later shows intense bone marrow and periosteal edema of a stress fracture.

Fig. 1.35 Foot stress fractures. (A) Metatarsal stress fracture ('march fracture'). Note the periosteal new bone formation in the metatarsal shaft *(arrows)* and the subtle sclerosis caused by healing response to the metatarsal fracture. **(B)** Healing metatarsal stress fracture. Radiographs 3 weeks earlier were completely normal, but the diagnosis was made with MRI and the foot was casted. (C–E) Calcaneus stress fracture. **(C)** Note the sclerotic incomplete fracture line *(arrow)*. **(D)** A sagittal fat-suppressed T2-weighted MR image shows low-signal fracture and intense surrounding bone marrow edema. **(E)** Sagittal T1-weighted MR image also shows low-signal fracture. **(F)** Calcaneus stress fracture in a young child. Note the sclerotic zone in the posterior calcaneus *(arrowheads)*. This can be considered a type of toddler's fracture.

Fig. 1.36 Femoral shaft stress fracture. Coronal inversion recovery image shows medial periosteal edema *(arrow)* and bone marrow edema.

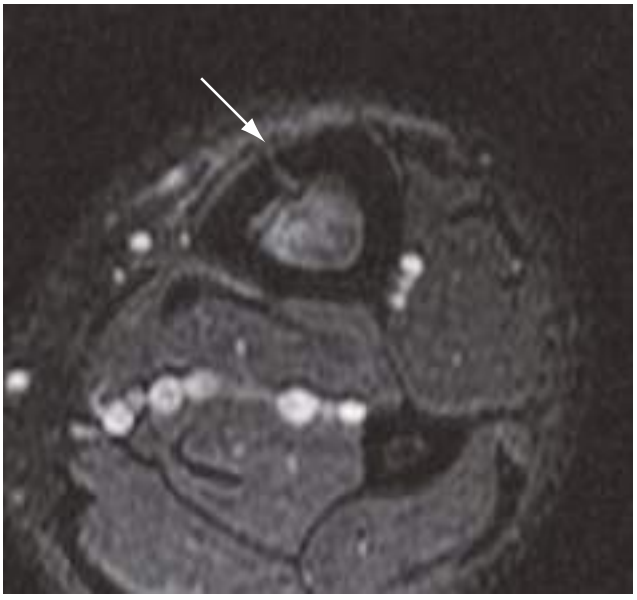

Fig. 1.37 Some stress fractures are oriented longitudinally. This axial fat-suppressed T2-weighted MR image shows interruption of the anterior tibial cortex *(arrow)*. This finding was present on multiple consecutive images. Radiographs were normal.

the anterior tibia, superior femoral neck, and proximal femoral shaft. These fractures are at high risk for completion.

- *Compressive stress fracture* is a stress fracture at a site of compressive force, for example, the inferior femoral neck. These fractures are at low risk for completion.

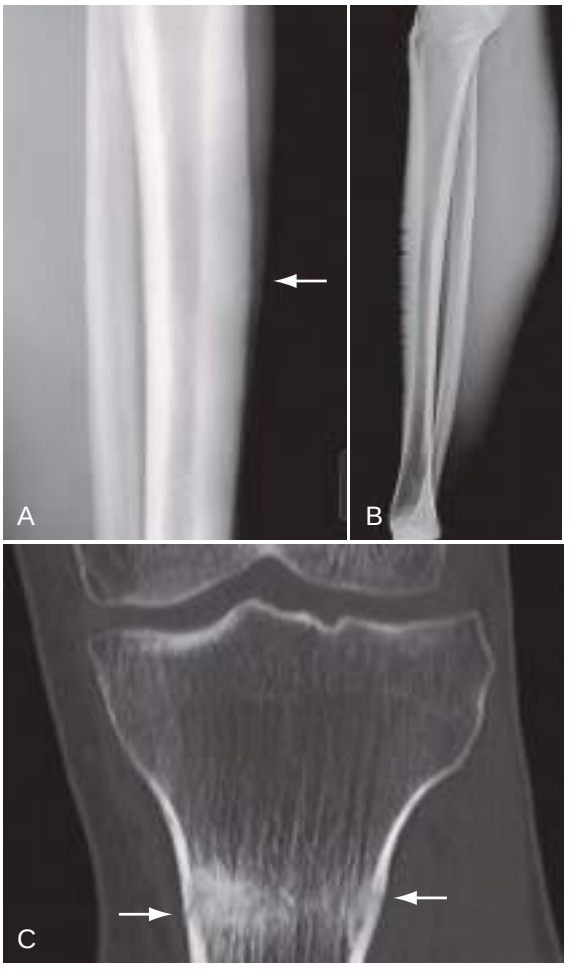

Fig. 1.38 Severe tibial stress fractures. (A) Lateral radiograph shows a visible transverse cleft in the thickened anterior tibial cortex *(arrow)*. **(B)** Unusual example with multiple visible anterior cortical stress fractures. **(C)** Coronal CT reconstruction shows nondisplaced complete stress fracture across the proximal metadiaphysis *(arrows)*.

Stress Injury Imaging

- Radiographs are insensitive and do not accurately evaluate injury severity. However, they are obtained as a first-line test, in part to search for alternative diagnoses such as a lytic lesion.
- CT is more sensitive than radiographs in demonstrating the fracture, periosteal elevation, and surface or endosteal callus.
- Radionuclide bone scanning with TC99m tagged bisphosphonates has high sensitivity and a negative scan has very high negative predictive value. Specificity is lower.
- MRI is highly sensitive for stress injury and fracture because of the associated marrow, periosteal, and/or cortical edema, and it is highly specific when a fracture line is shown. MRI also may demonstrate an injury in an adjacent tissue, such as a muscle strain that clinically simulates a bone stress injury. MRI has the additional advantage of no ionizing radiation. MRI is now generally obtained rather than bone scan when the region of concern is a single site or adjacent sites such as bilateral tibias.

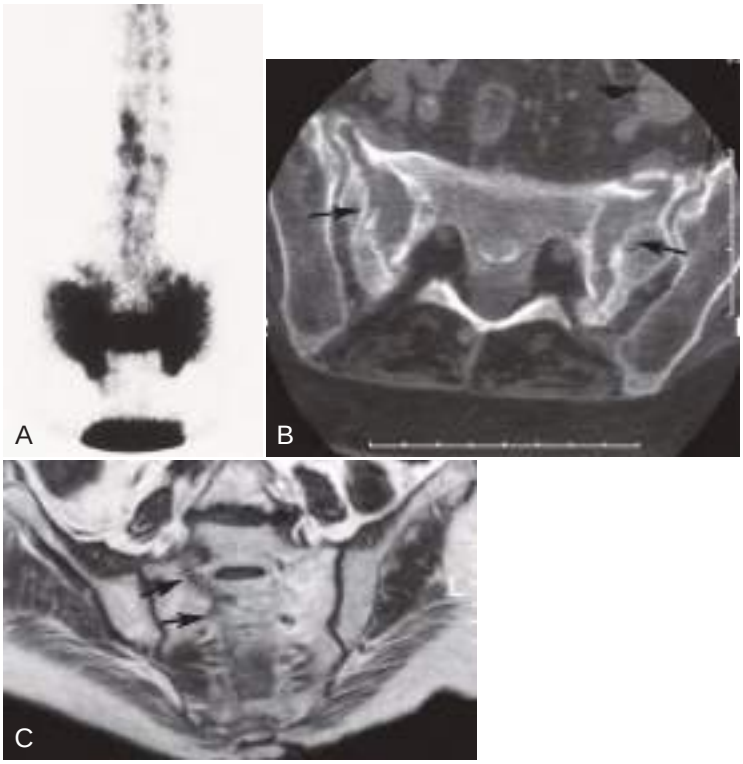

Fig. 1.39 Insufficiency fracture of the sacrum. (A) Radionuclide bone scan demonstrates intense uptake in sacrum in an H configuration. This pattern is typical of sacral insufficiency fracture. **(B)** Axial CT image of the same patient demonstrates chronic fractures in both sacral alae *(arrows)*. Sclerotic opposing margins indicate chronic nature of these insufficiency fractures. **(C)** Oblique coronal T1-weighted spin-echo image in a different patient demonstrates low-signal insufficiency fracture line in the right sacral wing *(arrows)*.

Stress fractures can occur in almost any stressed bone. Some classic locations include:

- Femoral neck.
- Tibial shaft.
- Metatarsals (*march fracture*; see Fig. 1.35A and B).
- Femoral shaft.
- Fibular shaft.
- Calcaneus.
- Tarsal navicular.
- Lumbar spondylolysis in activities with forceful spine hyperextension.
- Some bifid first metatarsophalangeal sesamoid bones are stress fractures.
- Some less common sites have particular associations:
  - Hamate hook in golf, baseball, and tennis players.
  - Medial pubic bone in soccer players and gymnasts.
  - Obturator ring and pediatric wrist in gymnasts.
  - Proximal humerus and around the elbow in pediatric baseball pitchers.
  - Ribs in rowers.

Stress Fracture Mimics

- Osteoid osteoma is painful and produces periosteal new bone with marrow edema.
- Other bone tumors.
- Osteomyelitis, especially in children.

Stress Fracture Management

- Rest and, in more advanced cases, immobilization.
- Internal fixation for the most severe cases.
- Successful conservative treatment requires the cooperation of the patient.
  - Many stress fractures are self-inflicted overuse injuries in which patients ignore the warning signs because of their passion for the injurious activity (see Fig. 1.34). Knowledge that earlier intervention results in more rapid healing may help to persuade the injured patient to allow the fracture to heal.

Insufficiency Fracture

- Caused by normal stresses placed on bone that is weakened by a generalized process such as osteoporosis.
- Also seen in osteomalacia, hyperparathyroidism, corticosteroids, Paget disease, and numerous other conditions that weaken bones.
- Like a fatigue-type stress fracture, an insufficiency fracture can often be diagnosed by clinical history, but imaging is helpful for confirmation and assessment of severity.
- As with fatigue-type stress fracture, tensile fractures are at greater risk for completion than compressive fractures.
- Most common at sites with high trabecular bone content because trabecular bone is disproportionately lost in osteoporosis.
- Common locations:
  - Vertebral osteoporotic compression fracture (Fig. 1.5)
  - Ends of weight-bearing long bones.
  - Pelvic ring.
  - Sacrum.
    - Sagittal plane alar fractures.

  - Transverse fracture across the mid-upper sacrum.
  - These may coalesce into an H-shaped pattern (Fig. 1.39).
- Proximal lateral femoral shaft, associated with long-term bisphosphonate therapy for osteoporosis. A characteristic laterally oriented spike of bone resembling a beak is usually seen at the fracture line. These fractures can be bilateral.

Insufficiency Fracture Imaging

- Radiographs are insensitive. Detection of a nondisplaced insufficiency fracture on radiographs can be quite difficult because of osteopenia. Initial films are negative approximately 80% of the time.
- CT is much more sensitive than radiographs, but less sensitive than bone scan or MRI. Findings may include lucent fracture line, cortical interruption, deformity, increased trabecular bone density (healing response in trabecular fractures), and subtle callus adjacent to the cortex. Dual energy scanners can detect marrow edema in osteoporotic bones, increasing sensitivity.
- Radionuclide bone scanning is sensitive but less specific unless a specific pattern of tracer uptake can be identified, such as the H-shaped pattern of activity seen with a sacral insufficiency fracture (Fig. 1.39).
- MRI is highly sensitive to the presence of a fracture and more specific than radionuclide imaging because a fracture line usually can be shown.

Insufficiency Fracture Management

- Rest.
- Internal fixation for some.
- Methyl methacylate injection for acute vertebral and sacral fractures (vertebroplasty, kyphoplasty, sacroplasty).
- Management of the underlying condition (usually osteoporosis).

Part 2: Joints and Soft Tissues

Joint Basics
Ligament Basics
Tendon Basics
Muscle Basics
Articular Cartilage Basics
Nerve Basics
Foreign Body Imaging

This section provides an overview of imaging findings in normal and injured musculoskeletal soft tissues. Many of the generalizations and specific injuries introduced in this section are discussed in greater detail in later chapters.

Joint Basics

- Structures that connect adjacent bones.
- Function: allow motion.

There are three types of joints:
Synovial joint (diarthrosis)

- Most of the joints of the extremities, facet joints of the spine, inferior portion of the sacroiliac joints.
- Freely mobile with a wide range of motion.
- Three basic components:
  - Articular cartilage covering the ends of the bones.
    - Cushions the bones and allows for nearly frictionless joint motion.
  - Flexible, synovium-lined fibrous joint capsule.
    - Synovium produces synovial fluid, which lubricates and nourishes the articular cartilage.
  - Stabilizing ligaments.

Cartilaginous joint

- Intervertebral discs of the spine, symphysis pubis.
- Limited range of motion.
- Articulating bones are covered with fibrocartilage.
- No synovial lining.
- Usually invested with a central disc.

Fibrous joint

- Cranial sutures, superior portions of the sacroiliac joints.
- Strongest type of joint.
- Allows almost no motion and has only fibrous tissue between the bones.

JOINT PATHOLOGY TERMINOLOGY (PARTIAL LIST)

Valgus

- Abnormal angulation of the distal bone away from the midline, for example, genu valgum (knock knees).
- The term is used in context, as some valgus is present normally in the adult knee and elbow.

Varus

- Distal bone is oriented more toward the midline than normal, for example, genu varum (bow legs).
- The term is used in context, as some varus is present normally in the pediatric knee.

Dislocation

- Complete loss of contact between the articular surfaces.

Subluxation

- Partial loss of contact between the articular surfaces.
- Causes:
  - Acute or chronic ligamentous injury (Fig. 1.40).
  - Laxity due to a generalized process such as Ehlers–Danlos syndrome (discussed in Chapter 15).
  - Articular cartilage thinning in the setting of arthritis.

Diastasis

- Separation or widening of a slightly mobile joint such as the acromioclavicular joint or the symphysis pubis.
- The term *diastasis* is also used to describe gaps between articular surface fragments of an intraarticular fracture.

Internal Derangement

- Disruption of normal joint anatomy.
- In common usage also associated with pain and/or limited joint function.
- Examples: rotator cuff tear in the shoulder, meniscal tear in the knee.

Fig. 1.40 Instability of the thumb metacarpophalangeal (MCP) joint related to chronic ulnar collateral ligament tear. Radiograph without stress was normal (not shown). Valgus stress *(arrows)* applied across the thumb MCP joint by the examiner's gloved hands results in valgus alignment across the joint.

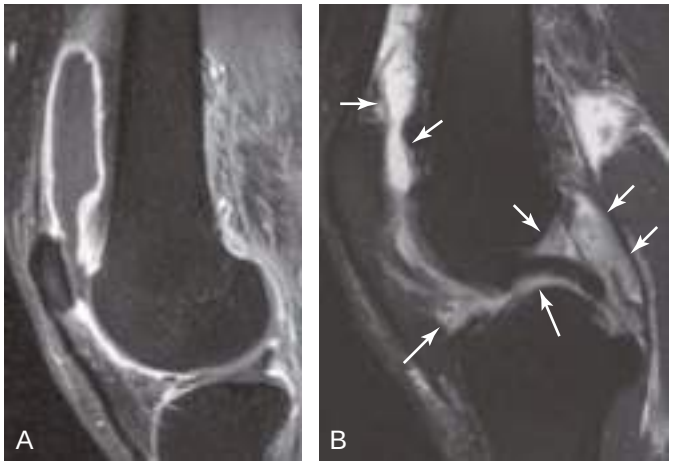

Fig. 1.41 Synovitis. (A) Sagittal fat-suppressed gadolinium-enhanced T1-weighted MR image of the knee in a patient with a septic knee shows intense enhancement of uniformly thickened synovium. **(B)** Sagittal fat-suppressed T2-weighted MR image of the knee in a different patient with new onset of inflammatory arthritis shows bulky synovial hypertrophy. The thickened synovium is seen as intermediate signal intensity *(arrows)*, compared with the higher signal intensity of joint fluid.

Synovitis

- Synovial inflammation.
- Many potential causes, including infection, autoimmune, intraarticular hemorrhage, and trauma.
- Synovium can thicken and become hyperemic (Fig. 1.41).

JOINT IMAGING TECHNIQUES

- Radiographs: evaluate alignment, detect intraarticular fractures, joint effusion, degenerative changes.
- CT: same as radiographs, but much more sensitive than radiographs for joint effusion and intraarticular fracture.
- US: effusion, synovial hypertrophy, can detect some ligament injuries.
- MRI: same as CT combined with US, plus better detection of many soft tissue injuries (Fig. 1.42).
- CT and MR arthrography: enhanced detection of some internal derangements such as labral or meniscal tears and articular cartilage defects. Can also be helpful in postoperative imaging.

Fig. 1.42 Ankle ligament sprain. Coronal fat-suppressed T2-weighted MR image of the right ankle in a 30-year-old woman who sustained an ankle inversion injury shows edema in the deltoid ligament (between *arrows*). Also note bone marrow edema in the medial malleolus and talus at the ligament insertions *(arrowheads)*. *calc*, Calcaneus; *f*, fibula; *tal*, talus; *tib*, tibia.

INTRAARTICULAR BODIES (LOOSE BODIES)

- Can cause joint pain and locking (Fig. 1.43; see also Fig. 1.17).
- A common source is displaced articular cartilage fragments or, in the knee, a displaced meniscal fragment.
- Not all intraarticular bodies are truly loose, because many are fixed to the synovium.
- May grow, change shape, calcify, or ossify over time.

Imaging of Intraarticular Bodies

- Radiography and CT:
  - Visible if calcified or ossified.
  - Bone portion of an acute, displaced osteochondral fragment also visible.
  - CT arthrogram can show low-density bodies.
- US can show intraarticular bodies but is not a first-line test.
- MRI: often low signal on all sequences. Ossified bodies may contain marrow fat.

Ligament Basics

- Strong, flexible bands or cords of fibrous tissue composed of highly ordered collagen fibers.
- Anisotropic (not the same in every direction).

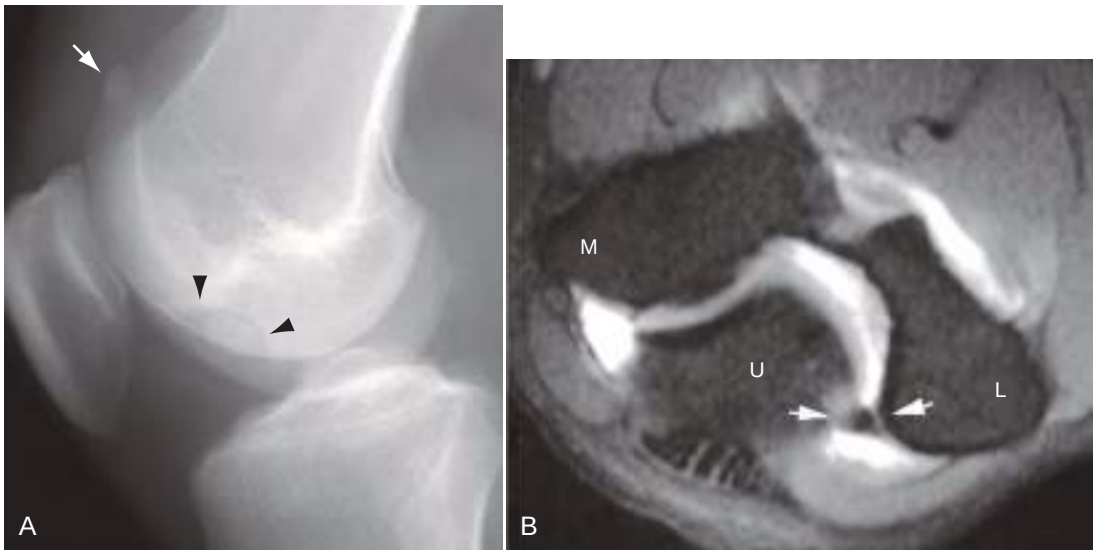

Fig. 1.43 Intraarticular bodies. (A) Lateral knee radiograph shows a small bone fragment in the superior joint recess *(arrow)*. Also note the donor site of this osteochondritis dissecans fragment on the medial femoral condyle defect *(arrowheads)*. **(B)** Elbow intraarticular body diagnosed by use of MR arthrography. Axial fat-suppressed T1-weighted MR arthrogram shows a small filling defect (between *arrows*) between the ulna and humerus in the lateral aspect of the olecranon fossa. This body caused pain on the elbow extension and therefore was removed. *L*, Lateral epicondyle; *M*, medial epicondyle; *U*, ulna.

- Connects a bone to another bone.
- Function: provides joint stability by resisting tension.
- Most ligaments are contiguous with the joint capsule.
  - Notable exceptions are the *anterior* and *posterior cruciate ligaments* of the knee, which are located inside the joint capsule (although they are technically extraarticular because they are separated from the joint compartment by the synovium)

Enthesis

- The site of attachment of a ligament or a tendon to a bone.
- Two types:
  - *Fibrous* (most common).
    - Calcified collagen fibers (*Sharpey fibers*) form the intraosseous root.
  - *Fibrocartilagenous*.
    - Complex anatomy allows stresses to be spread over a larger volume.
    - Example: rotator cuff.

LIGAMENT INJURY (SPRAIN)

- Occurs with tension.
- Simplified grading system:
  - Grade 1: injury without macroscopic tear.
  - Grade 2: partial tear.
  - Grade 3: complete ligament interruption.
- *Avulsion fracture:*
  - Ligament and its bony attachment are detached, with intact or partially intact ligament (Fig. 1.18A).
  - The associated bone fragment is usually small and can be difficult to identify on radiographs and invisible on MRI.
    - Knowledge of the sites of ligament attachments to bone is helpful.
- A complete ligament tear or avulsion often occurs with transient joint subluxation or dislocation.
- Traumatic dislocation with residual joint subluxation or distraction generally implies the presence of significant ligament injury and the potential for chronic joint instability.

IMAGING OF LIGAMENT INJURIES

Radiographs and CT

- Limited direct visualization.
- Secondary findings:
  - Malalignment (Fig. 1.40).
  - Subtle avulsion fracture fragment.
  - Adjacent soft tissue edema and swelling, joint effusion.

US

- Excellent for superficial ligaments.
- Can distinguish partial from complete tears.
- Real-time stress imaging increases sensitivity.
- May detect a small avulsion fragment that is invisible on MRI.

MRI

Most normal ligaments and tendons are dark on all MRI sequences because of their highly ordered, *anisotropic ultrastructure*. This is discussed further in the section on 'normal tendon imaging'.

- Fluid-sensitive sequences demonstrate sprain severity.
  - Mild sprains (grade 1): edema with intact fibers (Fig. 1.42).

- Partial tears (grade 2): edema and some of the ligament fibers may appear to be lax, wavy, or obviously interrupted. Surrounding edema and hemorrhage frequently present.
- Complete ligament tears (grade 3): may show either obvious interruption or edema with laxity of all fibers. Surrounding edema and hemorrhage are variable and may be extensive.
- Avulsion fracture of a ligament insertion may mimic a complete ligament tear on MR images, with a ligament clearly discontinuous from bone. Marrow edema at the avulsion donor site is usually minimal, in contrast to the intense and extensive edema associated with bone bruises due to impaction. When visible, the small cortical avulsion fragment is low-signal, thin, and linear or curvilinear.

Note that while imaging plays a major role in evaluation of ligament injuries, clinical examination for pain and stability is the gold standard.

Tendon Basics

- Tendons connect a muscle to a bone.
- Function: allows muscle contraction to act on a bone.
- Structurally and biomechanically similar to ligaments.
  - Surgeons routinely exploit this similarity by harvesting a tendon to replace a damaged ligament.
- Some tendons are surrounded by a synovial lined *tendon sheath.*
  - Examples: most tendons of the hand, wrist, feet, and ankles.
  - Allows the tendon to glide without friction around corners and in narrow spaces such as the carpal tunnel and around bony prominences such as the malleoli of the ankles.
  - Prone to wear-and-tear injuries (poor blood supply) and laceration (superficial and peripheral location).
- Other tendons have no sheath.
  - Examples: quadriceps, patellar, Achilles.
  - Loose fatty tissue (*paratenon*) surrounds the tendon.
    - Better blood supply, heal well.
  - Prone to injuries at the insertion and myotendinous junction.

Tendon attachment to bone:

- Is an enthesis, just like ligament attachments.
- Sometimes termed the *tendon footprint.*
- Generalization: tendons that attach to an epiphysis or an apophysis have a wide range of angular motion at the insertion through the range of motion.
  - This makes them more vulnerable to overuse and wear-and-tear injury.
  - Examples: rotator cuff, distal biceps tendon, Achilles.
- In contrast, tendons that attach to a long bone metaphysis or diaphysis generally have a narrow range of insertion angle.
  - Less prone to injury at the insertion.
  - Example: deltoid insertion on the humerus.

IMAGING OF NORMAL TENDONS (AND LIGAMENTS)

Key Concepts

Normal Tendon

US: echogenic, uniform pattern of parallel fibers
MRI: normally dark on all sequences
Exceptions:
1. Specific areas of normal variation, often where tendons fan out or merge
2. Magic angle. Solution: evaluate tendons with T2-weighted images

US

- Excellent for superficial tendons.
- Readily displays the parallel fibers of a normal tendon.
- Tendon echogenicity depends on the angle of the transducer.
  - If the transducer is held exactly perpendicular to a normal tendon, the tendon appears hyperechoic because of specular reflections from the parallel tendon fibers (Fig. 1.44).
  - Inability to induce these specular echoes can indicate tendon pathology.

MRI

- Normal tendons and ligaments are dark on all MRI sequences because of their highly ordered, anisotropic ultrastructure (Fig. 1.45). Explanation: The extremely highly ordered, anisotropic ultrastructure of tendons and ligaments results in very rapid T2 signal decay, markedly diminishing signal intensity on T2-weighted images. In other words, the normal low signal of ligaments and tendons on MRI can be considered an artifact, albeit a very useful artifact.
- Intermediate or high signal intensity in a tendon or ligament usually indicates loss of the normal highly ordered anisotropic ultrastructure and thus tendon injury.
- Important exceptions:
  - Some tendons normally have intermediate signal at or near the insertion or origin or at sites where the tendon normally fans out or merges with other tendons. The

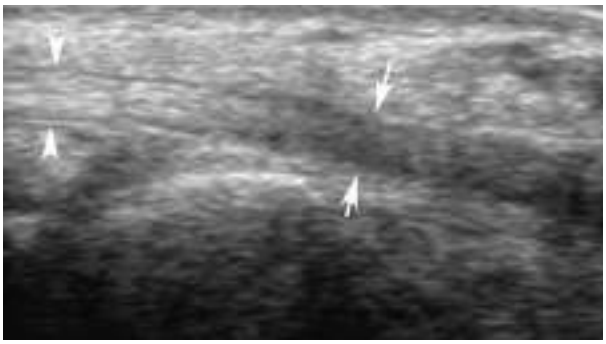

Fig. 1.44 Normal tendon on US. Normal flexor hallucis longus tendon in the foot. Note the normal high echogenicity of normal tendon that is perpendicular to the transducer (between *arrowheads*) and lower echogenicity of tendon that is not perpendicular to the transducer (between *arrows*).

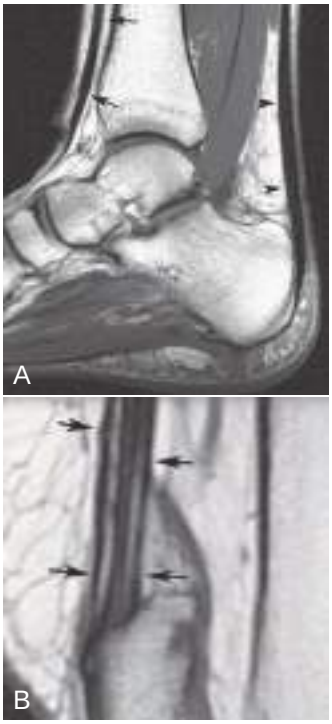

Fig. 1.45 Normal tendons on MRI. (A) Normal tendons have low signal intensity on all MRI sequences, with a few specific exceptions. Sagittal T1-weighted MR image of the ankle and hindfoot shows normal Achilles *(arrowheads)* and tibialis anterior *(arrows)* tendons. **(B)** As shown in this sagittal T1-weighted MR image, one exception is the distal quadriceps tendon, which is formed from four muscles in three layers *(arrows)*.

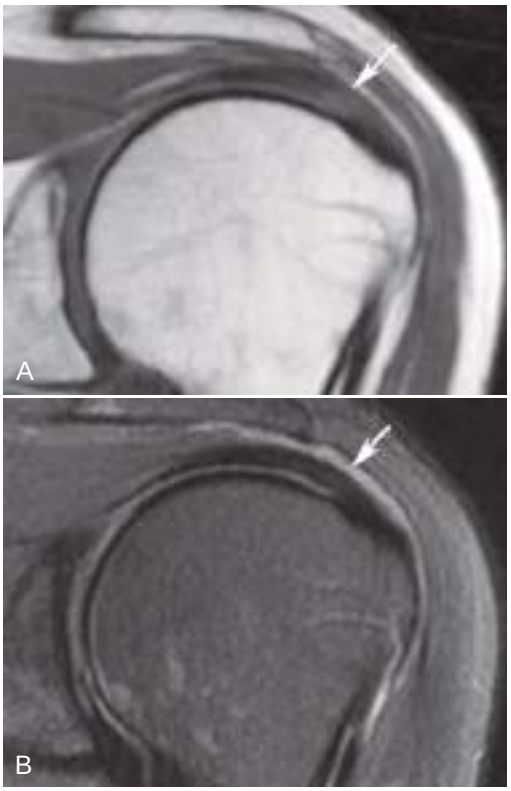

Fig. 1.46 Magic angle effect. (A and B) Oblique coronal T1-weighted **(A)** and fat-suppressed fast spin-echo T2-weighted **(B)** (echo time effective, 60 msec) MR images show the normal curved course of the supraspinatus tendon over the humeral head. Images were obtained in a high-field magnet with β_0-oriented head-to-toe. Note increased tendon signal in A but normal low signal in B, where the tendon is oriented about 55 degrees away from β_0 *(arrow)*.

tendon fibers at these sites are less anisotropic and thus do not normally have low signal. Example: the distal semimembranosis tendon at the proximal tibia.

- The distal quadriceps tendon often has a striated appearance on sagittal images as a normal finding. This reflects the quadriceps anatomy, because this tendon is formed from the tendons of four muscles.
- *Magic angle*: Due to a quirk in MRI physics, a normal ligament or tendon will have an intermediate or bright signal when oriented 55 degrees relative to the bore of the magnet (β_0) on short-echo time (TE) sequences such as gradient echo, T1, or proton density. This is known as the *magic angle effect* or *phenomenon* (Fig. 1.46). The magic angle effect occurs in the ankle tendons as they curve around the malleoli and in the supraspinatus tendon as it curves over the humeral head. Increasing TE reduces magic angle effect, so T2-weighted images are essential when imaging the rotator cuff and ankle.

Radiography and CT

- Tendons have higher attenuation than joint fluid and muscle

TENDON INJURY AND ASSOCIATED IMAGING FINDINGS (BOX 1.2)

Tendons can be injured by acute or chronic overloading, extrinsic compression such as impingement, laceration, tenosynovitis, infection, crystal deposition, and tumors. Tendons have a poor blood supply, so an injured tendon tends to heal poorly, especially sheathed tendons in the extremities. Microscopic injuries may accumulate over many years, with associated gradual tendon weakening. Thus, clinically apparent tendon injuries in patients in their 20s and 30s tend to be associated with a high-force acute injury, whereas tendon injuries in older patients often present after minimal trauma or overuse.

Tendon Tears

- May be complete or partial.
- An *intrasubstance tear* is a partial tear that does not extend to a tendon surface.
  - Some intrasubstance tear subtypes (terminology varies):
    - *Interstitial tear*: longitudinally oriented along the course of the tendon.
    - *Laminar* or *cleavage tear*: a sheetlike interstitial tear in a flat tendon such as the rotator cuff.

Imaging Findings

RADIOGRAPHS

- Direct tendon evaluation is limited.
- Some injuries visible on radiographs can imply a tendon tear.
- Examples: extreme patella alta (high position of the patella) in patellar tendon tear or patella baja (low position of the patella) with quadriceps tendon tear.

Box 1.2 Tendon Injury Patterns

Complete tear

MRI

Tendon interruption visible
Bright T2 signal (fluid or granulation) fills the gap between torn tendon fragments
Retraction may or may not be present
Chronic tear: Muscle fatty atrophy

US

Tendon interruption visible
Anechoic or hypoechoic fluid may fill gap between tendon fragments
Fragments move separately
Retraction may or may not be present

Partial tear

Similar to complete tear, but tendon partially intact

Chronic partial tear

Tendon may be too thick or thin, with normal signal

Tendinosis

Spectrum of abnormal findings due to degeneration, tendinitis, partial tears, repair
Too thick
Too thin
Abnormal signal/echogenicity

Tenosynovitis

Increased fluid and/or synovial hypertrophy in the tendon sheath

Stenosing tenosynovitis

MRI and US

Focal tendon thickening or fibrosis adjacent to the tendon sheath
US can show tendon tethering in real time
Tendon sheath fluid may be in pockets or absent
Fibrosis may be visible around sheath

Calcific tendinitis

Radiography: Amorphous calcification
MRI: Low signal on all sequences
US: Hyperechoic with shadowing

MRI, magnetic resonance imaging; *US,* ultrasound.

Fig. 1.47 Complete tendon tears. (A) MR image of Achilles tendon rupture. Sagittal T2-weighted spin-echo image shows a complete tear at the musculotendinous junction of the Achilles. Note wide, fluid-filled gap due to retraction of the distal muscle fibers *(arrows).* **(B)** Ultrasonogram of complete tear of the posterior tibial tendon in the foot. Note normal tendon proximally (*black arrowheads*, at the left side of the image), but low echogenicity at the torn tendon margin *(white arrows)* and empty tendon sheath more distally *(black arrows)*. Also note the medial cortex of talus *(white arrowheads)*.

US AND MRI

- A completely interrupted tendon usually has fluid or granulation tissue between the torn fragments that has very bright T2 signal, or on US has low echogenicity (see Fig. 1.47).
- Partial tendon tears may be seen as a focal defect or tendon thinning, but not all partial tears are readily demonstrated.
- Some chronic partial tears manifest only as tendon thickening, thinning, and/or elongation.

Tendinosis

- Umbrella term for chronic tendon tearing and repair.
- Histologically, there is replacement of normal collagen fibers with mucoid tissue, granulation, or fibrosis.
- The tendon may become thicker or thinner, or have variable thickness.
- Loss of normally highly ordered ultrastructure and tendon edema.
  - US: loss of normal specular echoes, decreased echogenicity.
  - MRI: variably increased signal on fluid-sensitive sequences, but usually less bright than fluid (Fig. 1.48)
- *Tendinitis* is a clinical term for a tender, painful tendon. Tendinitis is usually associated with imaging findings in the tendinosis spectrum.

Impingement

- Abnormal tissue compression.
- In sports medicine, the term is most often applied to transient pathologic compression of soft tissues in or near a joint that occurs with a specific motion or activity, and that has the potential to cause pain and lead to more serious injury.
- Example: the supraspinatus tendon of the shoulder is vulnerable to impingement between the humeral head and the acromion, especially during overhead activities such as throwing a ball.
- Impingement is a clinical diagnosis.
- It is a common condition.

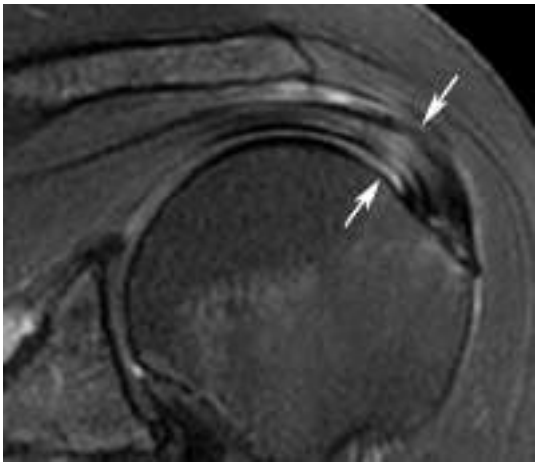

Fig. 1.48 Tendinosis. Compare with Fig. 1.46B. Coronal fat-suppressed T2-weighted fast spin-echo MR image shows increased signal intensity in the rotator cuff (between *arrows*). This is an example of mild tendinosis. More severe cases might show tendon thickening or thinning.

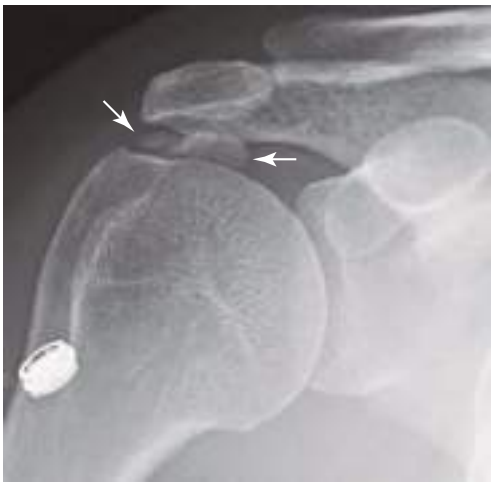

Fig. 1.49 Calcific tendinitis. Left shoulder AP radiograph shows the typical uniform calcification *(arrows)* of calcific tendinitis of the rotator cuff.

- Most imaging studies may not directly demonstrate impingement that occurs transiently during joint motion; instead, we search for associated anatomic features and tissue injury patterns.
- US has the potential to directly visualize some types of impingement.
- Imaging findings depend on the specific site and are reviewed later in this book.

Tendon Subluxation and Dislocation

Many tendons, as they curve around osseous structures at a joint, are held in position by a groove in the adjacent bone and an overlying retinaculum. If the bony groove is malformed or the retinaculum is lax or deficient, the tendon may sublux or dislocate from its normal position, either transiently or continuously.

Examples:

- Extensor carpi ulnaris (ECU) at the ulnar styloid.
- Peroneus longus and brevis at the lateral malleolus.
- Tibialis posterior at the medial malleolus.
- Biceps long head tendon from its groove between the humeral tuberosities in the setting of a subscapularis tendon tear.
- Recurrent subluxation may cause tendon degeneration, dysfunction, and pain.

Imaging: tendon is displaced, and may also have abnormal appearance due to related injury.

Calcific Tendinitis

- Calcium hydroxyapatite deposits within a degenerated tendon.
- Can be very painful.

Imaging

- The calcium deposit usually has uniform high density on radiographs (see Fig. 1.49), is hyperechoic with posterior acoustic shadowing on US, and has low signal intensity on all MRI sequences (which can be subtle or confusing until the radiographs are reviewed).
- The involved tendon often is highly edematous on MRI. The calcium deposit has low signal on all sequences.
- Calcific tendinitis is discussed further in Chapter 2, because the rotator cuff is the prototypic site for this condition. The numerous causes of soft tissue calcification are listed in Box 1.3 and are discussed throughout this book.

Tenosynovitis

- Inflammation of a tendon sheath.
- Tenosynovitis may result from more generalized synovitis (e.g., rheumatoid arthritis) or may be localized because of tendon degeneration, inflammation, tear, overuse, or tendon sheath trauma or infection.
- An effusion and/or thickening and hyperemia of the synovium may be present.
- Imaging: US and MRI show tendon sheath effusion and/or synovial hypertrophy (Fig. 1.50).

Stenosing Tenosynovitis

- Abnormal friction between a tendon and surrounding the tendon sheath.
- May be due to focal tendon thickening or tendon sheath narrowing.
- Examples:
  - *Trigger finger*, which classically occurs in the ring finger long flexor tendon
  - *De Quervain's tenosynovitis* in the abductor pollicis longus and extensor pollicis brevis tendons (wrist first extensor compartment)
- Also termed *tendon entrapment.*

Tendon Entrapment Between Fracture Fragments

- Different from stenosing tenosynovitis.
- A tendon may be trapped between bone fragments following a fracture or fracture reduction, notably at the ankle.
- The entrapped tendon may be visible on CT due to its relatively high density.
- Detection requires diligent review of all tendons—are they all where they should be?

Box 1.3 Soft Tissue Calcification

1. Trauma
   a. Heterotopic ossification: Most often after trauma or surgery. Also seen with brain or spinal cord injury, especially about the hips
   b. Myositis ossificans: Distinctive subtype of heterotopic ossification. Characteristic timing and maturation with peripheral calcification
   c. Burns: Often associated with contractures and acroosteolysis
   d. Frostbite: Thumb is often spared; acroosteolysis
2. Tumor
   a. Synovial cell sarcoma
   b. Liposarcoma
   c. Fibrosarcoma and malignant fibrous histiocytoma
   d. Soft tissue osteosarcoma
   e. Phleboliths in vascular tumors
   f. A soft tissue tumor may have dystrophic calcification.
3. Collagen vascular diseases
   a. Scleroderma: Usually subcutaneous, with other changes including acroosteolysis
   b. Dermatomyositis: Sheetlike in muscle or fascial planes, but other calcification patterns are also seen
   c. Systemic lupus erythematosus: Calcification is uncommon, but may occur, especially in lower extremities; consider when avascular necrosis is also seen
   d. CREST syndrome: Calcinosis cutis, Raynaud phenomenon, esophageal dysmotility, scleroderma, telangiectasias
   e. Calcinosis cutis
4. Arthritis
   a. Calcium pyrophosphate deposition arthropathy: triangular fibrocartilage complex, menisci, pubic symphysis, hyaline cartilage
   b. Hydroxyapatite deposition disease: Especially calcific tendinitis, bursitis, juxtaarticular
   c. Gout: Tophus is usually juxtaarticular
   d. Synovial chondromatosis: Intraarticular
5. Congenital
   a. Tumoral calcinosis: Periarticular
   b. Myositis ossificans progressiva: Usually axial, bridging between bones of the thorax
   c. Pseudohypoparathyroidism, pseudo-pseudohypoparathyroidism
   d. Progeria
   e. Ehlers–Danlos disease
6. Metabolic disorders
   a. Hyperparathyroidism (primary or secondary)
   b. Hypoparathyroidism
   c. Renal dialysis sequelae: Periarticular
7. Infectious disorders
   a. Granulomatous: Tuberculosis, brucellosis, coccidioidomycosis
   b. Dystrophic calcification in abscesses
   c. Leprosy: Linear calcification in digital nerves
   d. Cysticercosis: Small calcified oval bodies in muscle
   e. *Echinococcus* infection: Usually liver or bone, but occasionally in soft tissue
8. Drugs
   a. Hypervitaminosis D
   b. Milk-alkali syndrome

Bursa

- Synovium-lined potential space that allows reduced friction so that adjacent tissues such as ligaments or tendons can slide easily past one another or an adjacent bone.
- Also common between skin and bony prominences.

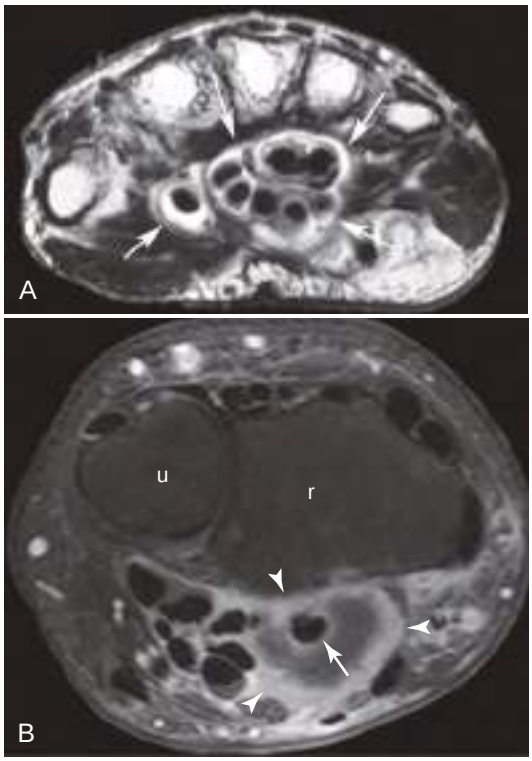

Fig. 1.50 Tenosynovitis. (A) Carpal tunnel tenosynovitis due to overuse. Axial T2-weighted fast spin-echo MR image shows fluid distention of the carpal tunnel tendon sheaths *(arrows)*. **(B)** Infectious tenosynovitis. Axial fat-suppressed contrast-enhanced T1-weighted MR image through the distal forearm at the distal radioulnar joint shows distended, enhancing tendon sheath *(arrowheads)* and low–signal-intensity fluid surrounding the flexor pollicis longus tendon *(arrow)*. The nonenhancing fluid in the tendon sheath in this case was pus related to *Staphylococcus aureus* infection. *r*, Radius; *u*, ulna.

- In addition to the numerous normally occurring bursae, bursae may be created de novo in areas of unusual shear stress (*adventitial bursa*), for example, around the ankles in figure skaters.

Bursitis

- Inflammation of a bursa.
- Causes: trauma, calcium salt deposition (*calcific bursitis*), infection, or causes of generalized synovial inflammation such as rheumatoid arthritis.
- Normal bursae are nearly invisible on imaging studies, but an inflamed bursa is readily apparent because of the presence of fluid, synovial thickening, and/or calcification (Fig. 1.51).

Skeletal Muscle Basics

- Function: allows motion through contraction.
- Composed of ordered bundles of muscle fibers and an investing fascial sheath.
- Supplied by blood vessels, lymphatics, and nerves.
- Attaches to bone by a tendon. The tendon usually extends far into the muscle belly.
  - *Myotendinous junction* is the junction of tendon and muscle.

Fig. 1.51 Bursitis. (A) Sagittal fat-suppressed T1-weighted MR image with intravenous gadolinium of the left shoulder shows synovial enhancement of subacromial subdeltoid bursa *(arrows)* in this patient with bursitis. The bursal fluid *(asterisk)* does not enhance. Also note enhancement of granulation tissue *(arrowheads)* in a supraspinatus tendon tear. **(B)** Sagittal fat-suppressed T2-weighted MR image shows a hemorrhagic effusion with a fluid-fluid level in the infrapatellar bursa *(arrow)* and a smaller effusion in the prepatellar bursa *(arrowhead)*.

IMAGING OF NORMAL SKELETAL MUSCLE

- Radiography: soft tissue density.
- CT: muscle attenuation is lower than tendons. Fat may be found between the muscle fibers, especially in obese patients or in chronically injured muscle. Intravenous contrast is very useful for evaluating certain conditions such as intramuscular abscess.
- US: excellent demonstration of the normal multibundle anatomy.
- MRI: intermediate signal on T1w and low to intermediate signal intensity on T2w images (Fig. 1.52). As with CT, intramuscular fat may be present.
- Nerves and blood vessels are visible and may be assessed with US, CT, and MRI.

MUSCLE PATHOLOGY AND ASSOCIATED IMAGING FINDINGS

- MRI is the most sensitive modality for evaluating most types of muscle injuries.
- US can show many of the same injuries as MRI, in superficial muscles, but with much lower contrast.
- Radiography and CT can display intramuscular calcification, which can be a subacute or late finding after many types of muscle injury. These modalities also allow assessment of the pattern of calcification, as in the peripheral calcification of myositis ossificans or the streaky, sheetlike pattern of polymyositis.

Muscle Strain

- An *intrinsic* muscle injury that is produced by an intrinsic force generated by the muscle itself (in contrast with an *extrinsic injury* such as a contusion or stab wound).
- Strains are most common in muscles that elongate while they contract (*eccentric contraction*), such as the hamstrings and the biceps.
- A strain begins as a microscopic muscle fiber tearing, usually at the musculotendinous junction, caused by forceful contraction while under load. More severe strains include tearing of the myotendinous junction and can, when still more severe, extend into the muscle belly.

Imaging

- MRI is most sensitive due to high contrast (Box 1.4). US can detect many of the same findings, especially in more severe strains, but the findings are more subtle.
- Mild (grade 1) strain: feathery edema between the muscle fibers, usually centered along the musculotendinous junction (see Fig. 1.53).
- Moderate (grade 2) strains: have more extensive edema and fluid collections (see Fig. 1.54).
- Severe (grade 3) strains involve disruption of the musculotendinous junction with loss of muscle function. Both

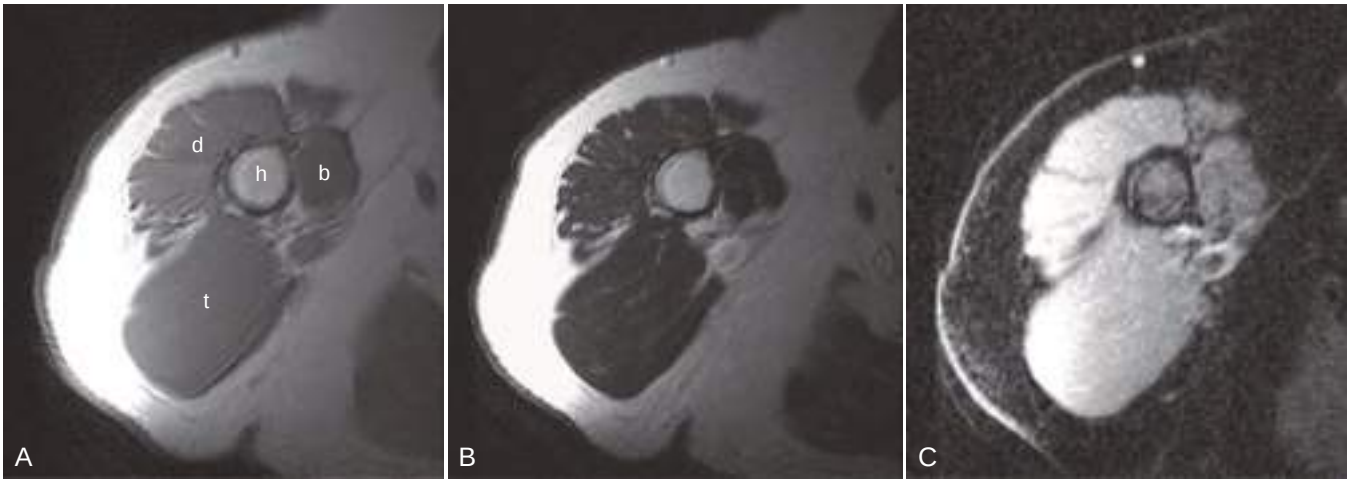

Fig. 1.52 Normal muscle and fat. (A–C) Axial MR images obtained through the proximal right arm. T1-weighted (A), T2-weighted **(B)**, and inversion recovery **(C)** images. Note intermediate signal intensity of muscle on all sequences. Fat is much brighter than muscle, except on the inversion recovery sequence **(C)**, which uses an inversion time of 140 msec at 1.5 T to null fat signal. A selective presaturation pulse can accomplish the same effect. Inversion recovery using a shorter inversion time of 110–130 msec suppresses but does not eliminate fat signal, resulting in images that many radiologists find easier to interpret. Most of the inversion recovery images in this text use a shorter inversion time. The fat signal intensity in **A** and **B** and muscle signal in **C** artifactually much higher laterally because of proximity to the receiver coil. *b*, Biceps; *d*, deltoid; *h*, humerus; *t*, triceps.

Box 1.4 Muscle Injury Patterns

Localized fluid collection at musculotendinous junction

Strain

Anywhere

Hematoma
Abscess
Myonecrosis
- Myonecrosis causes
  - Severe trauma
  - Compartment syndrome
  - Infection
  - Autoimmune disorders
  - Diabetes mellitus

Edema without fluid collection

Diffuse

Overuse (delayed-onset muscle soreness [DOMS])
Subacute denervation (after 2–4 weeks)
Radiation therapy

Focal

At musculotendinous junction:
- Strain

Anywhere:
- Trauma
- Early myonecrosis
- Infection without abscess
- Tumor

Atrophy with fatty infiltration

Paralysis, chronic denervation
Chronic tendon tear
End-stage autoimmune disease
Muscular dystrophy
Chronic corticosteroid use

Muscle calcification

Mass with peripheral calcification: Myositis ossificans
Sheetlike: Autoimmune disorder
Small nodules: Parasites
Tumors: Various patterns

Fig. 1.53 Muscle strain. Coronal inversion recovery (short-tau inversion recovery [STIR]) MR image of the right thigh shows quadriceps strains. Note edema within the vastus lateralis oriented with the muscle fibers (between *arrowheads*), small fluid collection in a musculotendinous junction tear *(long arrow)*, and intense edema along the vastus intermedius femoral origin *(short arrows)*. The femur bone marrow signal is normal.

Fig. 1.54 Muscle strain in an elderly patient who fell. Coronal inversion recovery MR image shows high signal intensity in the left hip adductors. (Reprinted with permission from May DA, Disler DG, Jones EA, et al. Abnormal signal within skeletal muscle in magnetic resonance imaging: patterns, pearls, and pitfalls. *Radiographics*. 2000;20:S295–S315.)

MRI and US images reveal the musculotendinous disruption, as well as fluid collections and extensive regional edema (Box 1.4).

Extrinsic muscle injuries caused by trauma include contusion or penetrating injuries such as a knife wound. Intramuscular hematoma may result.

- A **muscle contusion** produces intramuscular edema and small fluid collections, usually centered at the site of injury.
- An **intramuscular hematoma** may contain a fluid-fluid level and/or have high signal on T1-weighted images because of the presence of methemoglobin (Fig. 1.55). An older hematoma may have a low signal intensity rim resulting from the presence of hemosiderin which results in marked signal loss on all MRI sequences, especially gradient-echo images.

Heterotopic Ossification

- Bone formation in soft tissue (Fig. 1.56).
- Common sites include around the hip or knee joint after arthroplasty, or around the hip after placement of an intramedullary nail in the femur. Soft tissues around the elbow are especially vulnerable to heterotopic ossification (HO).
- Can also occur when joint motion is profoundly reduced as, for example, in patients paralyzed by a spinal cord or brain injury.
- Rare progressive genetic forms also exist.
- Initial presentation is pain with an appropriate history. Late presentation is painless reduced range of motion.
- Heterotopic bone can limit the range of motion of an adjacent joint and, in extreme cases, effectively fuse the joint.
- Early management is with indomethacin or other NSAIDs.
- Preoperative or postoperative radiation is sometimes used as prophylaxis before hip arthroplasty. The effectiveness of this therapy is debated.

Fig. 1.55 Muscle laceration and hematoma. MR images in a patient with brachialis muscle injury. Sagittal fat-suppressed T2-weighted MR image **(A)** shows bright edema signal interposed between brachialis muscle fibers *(arrowheads)*. A masslike hematoma *(arrows)* with complex signal is located between interrupted muscle fibers. Coronal T1-weighted image **(B)** shows elevated signal of methemoglobin in the hematoma *(arrows)*. *h*, Distal humerus; *r*, proximal radius.

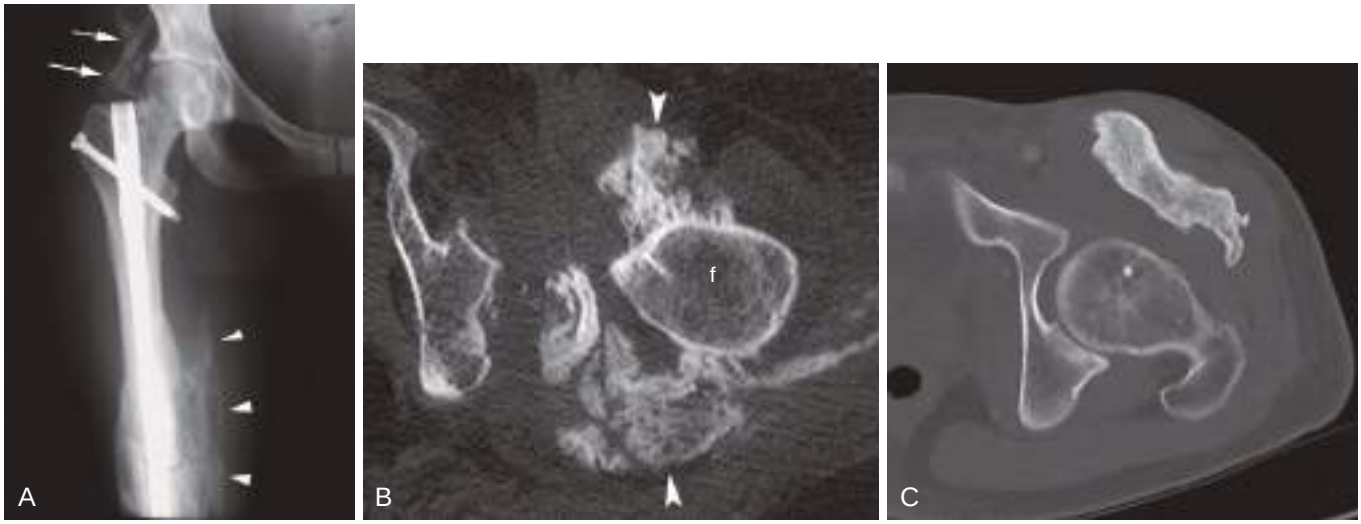

Fig. 1.56 Posttraumatic heterotopic ossification. (A) AP radiograph of the right thigh and hip shows mature bone above the femoral neck *(arrows)* and medial thigh *(arrowheads)*. **(B)** Heterotopic ossification *(arrowheads)* surrounding chronically dislocated left hip. **(C)** Heterotopic ossification anterior to the proximal left femur. *f*, Proximal femur.

- Imaging in early HO:
  - Radiography: soft tissue calcification develops 3–4 weeks after onset of symptoms.
  - Bone scan allows earlier diagnosis.
  - US also can detect calcification before radiographs: echogenic interface and limited posterior acoustic shadowing.
- Imaging in late HO: mature bone with cortex, trabeculae, and marrow.

Myositis Ossificans

- A distinctive and poorly understood form of HO that occurs in muscle after blunt trauma or intramuscular hematoma (Fig. 1.57).
- Trauma initiates conversion of local cells into osteocytes and chondrocytes.
- Bone formation may be detected by bone scan or US as early as 2 weeks. US initially shows a hypoechoic mass with subtle peripheral hyperechogenicity with limited posterior acoustic shadowing. Bone scan is initially hot on blood flow and blood pool, but becomes progressively hotter on delayed images as the lesion matures.
- At 3–4 weeks, sometimes later, soft tissue calcification becomes visible on radiographs.
  - Initially it is amorphous.
- After about 8 weeks, soft tissue calcification evolves into characteristic maturing *peripheral* calcification that reveals the true, benign nature of this process.
- There also may be periosteal reaction new bone formation in an adjacent long bone, but no bone destruction is seen.
- Over the course of weeks to months, the soft tissue bone may resolve or diminish, migrate toward and

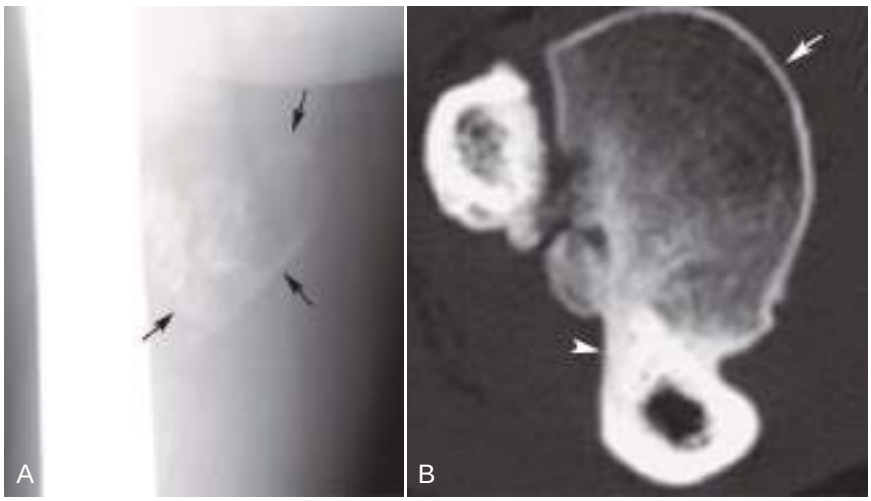

Fig. 1.57 Myositis ossificans. (A) AP radiograph of the right midthigh shows calcification that is densest at the periphery *(arrows)*. **(B)** Axial CT image in a different patient with myositis ossificans in the forearm shows mature ossification with cortex and trabeculae *(arrow)* that is fusing with the ulna *(arrowhead)*. (**A** reprinted with permission from May DA, Disler DG, Jones EA, et al. Abnormal signal within skeletal muscle in magnetic resonance imaging: patterns, pearls, and pitfalls. *Radiographics*. 2000;20:S295-S315. **B** courtesy of William Pommersheim, MD.)

ultimately merge with the adjacent bone, or remain unchanged.
- MRI can be misleading, showing a masslike intramuscular lesion that can be confused at imaging and at biopsy with an aggressive sarcoma. Careful evaluation that includes patient history may mitigate potentially confusing biopsy findings.
- Myositis ossificans is discussed in greater detail in Chapter 12.

Key Concepts

MRI to evaluate an unknown myopathy

Axial T1 is used to assess for fatty infiltration (usually indicates nonspecific end stage).

Axial fluid-sensitive sequence such as T2 with fat suppression or inversion recovery is used to assess for edema.

Including both sides for comparison can be helpful.

Use gadolinium enhancement if necrosis or abscess is suspected.

Edema without fatty infiltration indicates a good site for biopsy.

Denervation

- Muscle deprived of normal innervation undergoes degeneration and atrophy.
- MRI is highly sensitive in detection of muscle denervation and can provide prognostic information (Fig. 1.58).
- During the first 2–4 weeks after denervation, muscle signal is normal.
- After about 2–4 weeks, the denervated muscle becomes diffusely and uniformly edematous, with elevated signal on fluid-sensitive images.
- If normal innervation is restored within a few weeks, the muscle returns to normal both clinically and on MR images.
- However, denervation that persists for several weeks to months results in irreversible muscle wasting that manifests as fatty atrophy.
  - CT and MRI show decreased muscle bulk with fatty infiltration (*muscle fatty atrophy*). A chronic complete tendon tear results in a similar appearance but may also show muscle and tendon retraction

Other causes of muscle fatty atrophy:

- Long-term high-dose corticosteroid use, especially in trunk and proximal extremity muscles.
- Degenerative neuromuscular conditions (e.g., muscular dystrophy).
- Autoimmune inflammatory conditions (e.g., *dermatomyositis* or *polymyositis*) may also progress from edema during the active phase of the disease to end-stage irreversible fatty atrophy. These processes may be patchy or irregular in distribution.
- MRI is useful in guiding a biopsy when these conditions are suspected, because an optimal biopsy site should not show nonspecific end-stage fatty atrophy but rather edema related to active inflammatory cell infiltration.
- Late-stage dermatomyositis or polymyositis may show streaky or sheetlike calcifications.
- These conditions are illustrated and discussed further in Chapter 9.

Muscle infection may cause diffuse or focal edema.

- Infectious myositis due to pyogenic organisms can result in formation of an intramuscular abscess (Fig. 1.59). This condition is well known in the tropics but also occurs in temperate climates. Patients with immune dysfunction are the most vulnerable.
- An intramuscular abscess is similar in appearance to an abscess elsewhere in the body, with central fluid surrounded by an enhancing margin.
- Intramuscular gas bubbles suggest infection with a highly aggressive organism such as a *Clostridium* species; this condition is a surgical emergency requiring prompt debridement.
- Muscle infection is discussed further in Chapter 14.

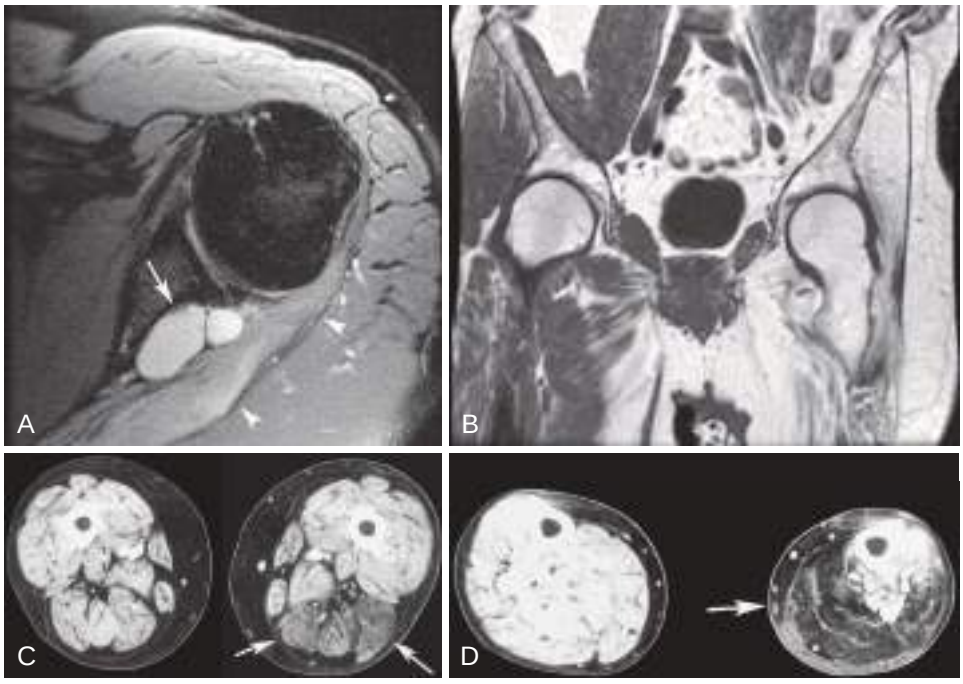

Fig. 1.58 Muscle denervation. (A) Acute muscle denervation. Acute infraspinatus denervation caused by nerve compression. Axial fat-suppressed T2-weighted MR image shows diffusely increased signal intensity in the infraspinatus muscle *(arrowheads)* caused by compression of the suprascapular nerve in the scapular spinoglenoid notch by a large paralabral cyst *(arrow)*. T1-weighted images (not shown) showed no fatty infiltration, indicating that the muscle injury is reversible. **(B)** Chronic muscle denervation, coronal T1-weighted MR image in an adult who had polio as a child shows profound fatty atrophy of left pelvic and thigh musculature. **(C and D)** Sciatic nerve injury. Axial CT images in the thighs **(C)** and calves **(D)** show fatty atrophy *(arrows)* of the hamstrings in **C** and ankle flexors in **D**. Fatty atrophy indicates irreversible muscle injury.

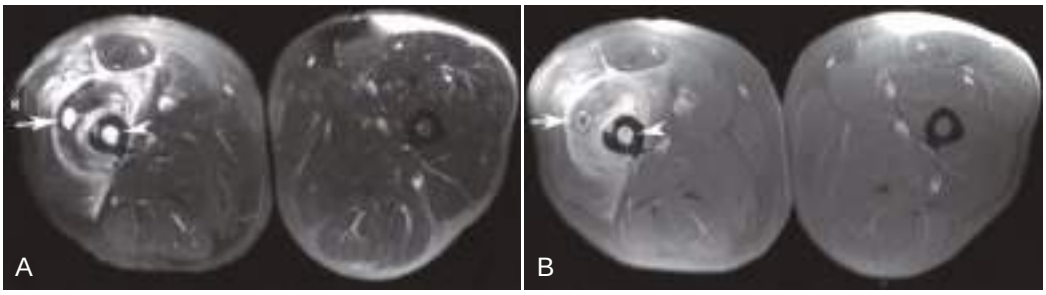

Fig. 1.59 Infectious myositis, intramuscular abscess, and osteomyelitis. Axial fat-suppressed T2-weighted (A) and contrast-enhanced fat-suppressed T1-weighted (B) MR images show small abscess in the right vastus intermedius *(arrow)* with surrounding muscle edema and enhancement, and femur midshaft marrow edema and enhancement *(arrowheads)* due to *Staphylococcus aureus* infection. (Reprinted with permission from May DA, Disler DG, Jones EA, et al. Abnormal signal within skeletal muscle in magnetic resonance imaging: patterns, pearls, and pitfalls. *Radiographics*. 2000;20:S295–S315.)

Necrotizing Fasciitis

- Infection along fascial planes that can be explosively progressive and highly lethal.
- When suspected, there is no time for imaging. The patient is taken directly to the OR for extensive debridement.
- Should imaging be obtained, fluid accumulation along fascial planes with or without enhancement may be seen. Gas bubbles may be present.

Myonecrosis

- Imaging findings vary: can resemble a mass on noncontrast CT and MRI.
- With intravenous contrast, a nonacute muscle infarct may resemble an abscess, with an enhancing rim surrounding a central region of edema or fluid.
- Outcomes also vary, can range from permanent muscle loss to complete recovery.
- Potential causes include:
  - Sickle cell disease.
  - Rhabdomyolysis.
  - Severe blunt trauma.
  - Venomous snake bite.
  - *Compartment syndrome* (discussed later in this chapter).
  - *Diabetic myonecrosis.*
    - An incompletely understood condition that resembles severe infectious myositis in imaging studies (Fig. 1.60).
    - Not due to infection and does not require aspiration, antibiotics, or surgical drainage. Extremely

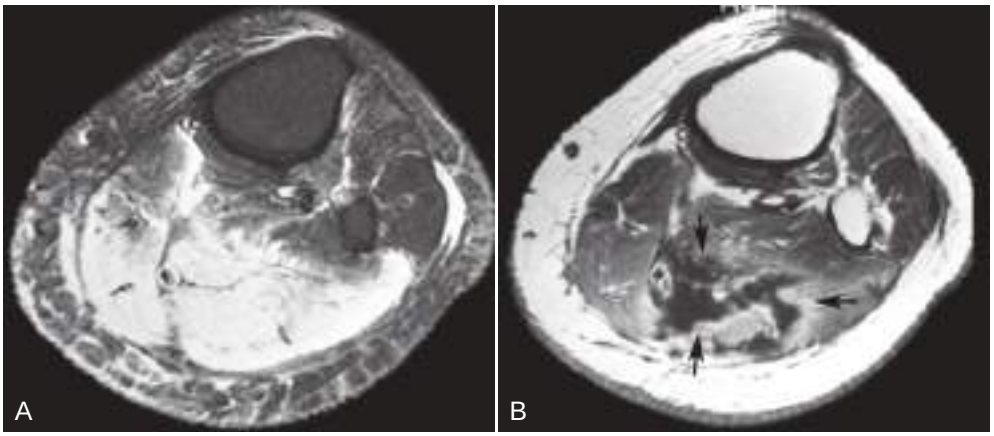

Fig. 1.60 Diabetic myonecrosis. Axial fat-suppressed T2-weighted **(A)** and contrast-enhanced T1-weighted **(B)** MR images show intense edema in the left soleus in **A** and heterogeneous enhancement and an irregularly shaped muscle infarct (*arrows* in **B**). (Reprinted with permission from May DA, Disler DG, Jones EA, et al. Abnormal signal within skeletal muscle in magnetic resonance imaging: patterns, pearls, and pitfalls. *Radiographics*. 2000;20:S295-S315.)

painful. Additional clues to the diagnosis are a history of poorly controlled diabetes mellitus and a normal or near-normal leukocyte count.

Acute Compartment Syndrome

- Muscles of the leg and volar forearm, as well as several other sites in the extremities are invested in indistensible fascia.
- Fracture, blunt or sharp trauma, a surgical procedure, or other insult can cause muscle swelling or hemorrhage that in extreme cases lead to a vicious cycle of increasing intracompartmental pressure, ischemia, more edema and swelling, further increased pressure, and, ultimately, tissue necrosis due to ischemia.
- If undetected, the compartment contents including muscles and nerves atrophy and scar, with contracture and irreversible complete loss of function. Early detection is imperative to avoid this devastating outcome.
- Acute compartment syndrome is treated by decompression with fasciotomy.
- When acute compartment syndrome is suspected, direct measurement of intracompartmental pressure is the appropriate test. This should not be delayed to obtain MRI or other imaging studies. If obtained, MRI shows muscle edema.

Exertional Compartment Syndrome

- Reversible muscle ischemia that manifests as reproducible pain during exercise.
- Running athletes.
- Anterior compartment of the leg is a common site.
- Sometimes can be detected with MRI. The symptomatic extremity can be scanned during or immediately after the offending activity. Muscle edema, often subtle, develops transiently in the affected muscle.
- The main role of MRI is to exclude other pathology.

Subacute compartment syndrome and *chronic compartment syndrome* are less precise terms that are sometimes used for milder cases of compartment syndrome (Fig. 1.61) or for exertional compartment syndrome. Some may still require fasciotomy.

A tight cast can produce compartment syndrome–like symptoms, due to swelling after cast placement. Treatment is simple: The cast is revised or simply divided longitudinally into two pieces ('bivalve' the cast, like a clam's shell) and wrapped with elastic wrap. This allows the soft tissues to swell without necessitating replacement of the cast.

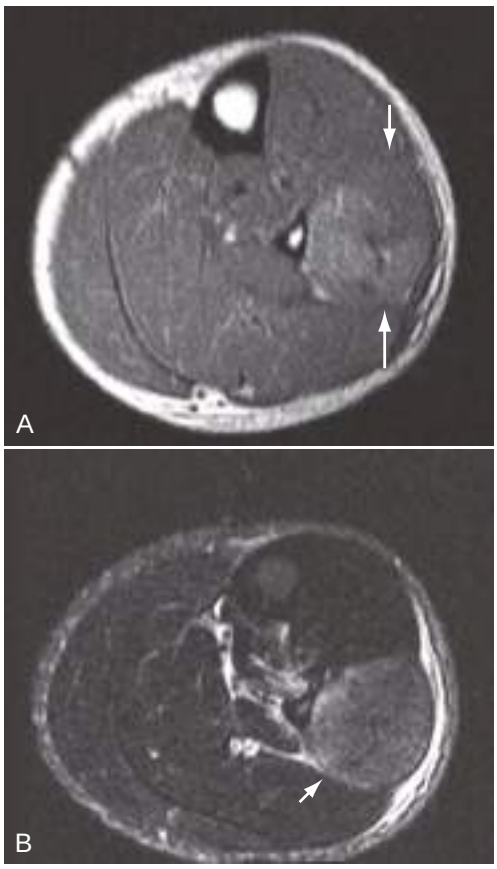

Fig. 1.61 Chronic compartment syndrome. Axial T1-weighted **(A)** and axial inversion recovery **(B)** MR images show enlargement of the peroneus longus muscle in the proximal lateral calf *(arrows)*. Note edema signal in **B** and mildly elevated T1 signal in **A** suggesting hemorrhage.

Radiation Therapy

- Produces long-lasting soft tissue edema throughout the radiation field.
- MR images often show a sharp, straight margin between the edematous radiated tissue and the normal adjacent tissue (Fig. 1.62). This finding helps to distinguish incidental radiation therapy–induced edema from other causes of muscle and adjacent soft tissue edema.

Myofascial Defect

- Presents as a bump or protrusion along the surface of a muscle, often in the calf.
- Caused by muscle bulging through a defect in the muscle fascia (Fig. 1.63).
- Often incidental but may cause concern for a neoplasm and occasionally are symptomatic during exercise.
- Because some lesions can be reproduced with muscle contraction, US or rapid MRI with the muscle relaxed and contracted may show the muscle bulging through the defect.
- Symptomatic defects occasionally show muscle edema on MRI.

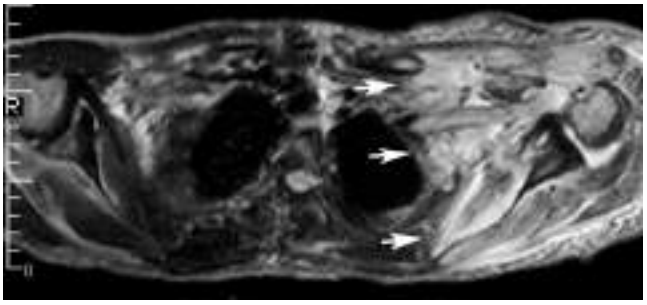

Fig. 1.62 Radiation therapy. Axial T2-weighted MR image of the upper chest in a patient previously treated with radiation therapy to the left shoulder and axilla region shows diffuse edema in the radiated soft tissues. Note sharp, straight margin between the radiated and normal tissues *(arrows)*. (Reprinted with permission from May DA, Disler DG, Jones EA, et al. Abnormal signal within skeletal muscle in magnetic resonance imaging: patterns, pearls, and pitfalls. *Radiographics*. 2000; 20:S295-S315.)

Fig. 1.63 Myofascial defect. Axial **(A)** and coronal **(B)** T1-weighted MR images in a 25-year-old patient with a palpable lump in the anterior proximal right calf show subtle anterior muscle protrusion *(arrows)*.

- More often, MRI shows nothing at all. The absence of a mass and edema are key findings in an incidental myofascial defect.

Morel-Lavallée Lesion

- Separation of skin and subcutaneous fat from underlying muscle fascia caused by a closed shear ('degloving') injury.
- This interrupts the blood vessels and lymphatics supplying the overlying fat and skin.
- Lymph, blood products, and sometimes necrotic/liquified fat from the overlying more superficial tissues distend the potential space and block healing. This fluid may often be complex and may contain fat globules (Fig. 1.64).
- Size varies from a few millimeters to several centimeters in thickness.
- May develop a thick or thin pseudocapsule.
- The fluid may become infected.
- Overlying skin is vulnerable to necrosis.
- May exert mass effect on adjacent muscle, but adjacent muscle otherwise is unaffected.
- Most common sites: proximal lateral thigh and hip followed by other sites around the pelvis and the knee.
- CT, US, or MRI shows the fluid collection between superficial muscle fascia in a characteristic location in the lateral thigh, around the hip or pelvis, or by the knee.

Articular Cartilage Basics

- Articular cartilage covers the ends of bones in synovial joints.
- Function: cushions the bone ends and allows essentially frictionless motion in a joint.
- Composed of a complex matrix of collagen and large proteoglycan molecules, chondrocytes, and water that is bound by hydrogen bonds.
- A simplified model of articular cartilage anatomy consists of four layers, distinguished by the orientation of the collagen fibers (Fig. 1.65).
  - Most superficial layer (*superficial zone*): mainly collagen fibers oriented parallel to the cartilage surface. This layer is very thin.
  - Intermediate layer (*transitional zone*): collagen fiber orientation is overall relatively random as the fibers transition from perpendicular to parallel to the cartilage surface. Moderate proteoglycan concentration.
  - Deep layer (*radial zone*): collagen fibers are oriented radially—that is, mostly perpendicular to the subchondral bone. High proteoglycan concentration.
  - The *calcified zone* anchors the radial zone which is anchored to underlying subchondral bone by calcified collagen.
- Articular cartilage has no blood, lymphatic, or nerve supply and must rely on the diffusion of nutrients from the synovial fluid and, to a lesser extent, the extracellular space of subchondral bone.
  - Joint motion with normal loading assists in cartilage nourishment by driving in nutrients from the synovial fluid.

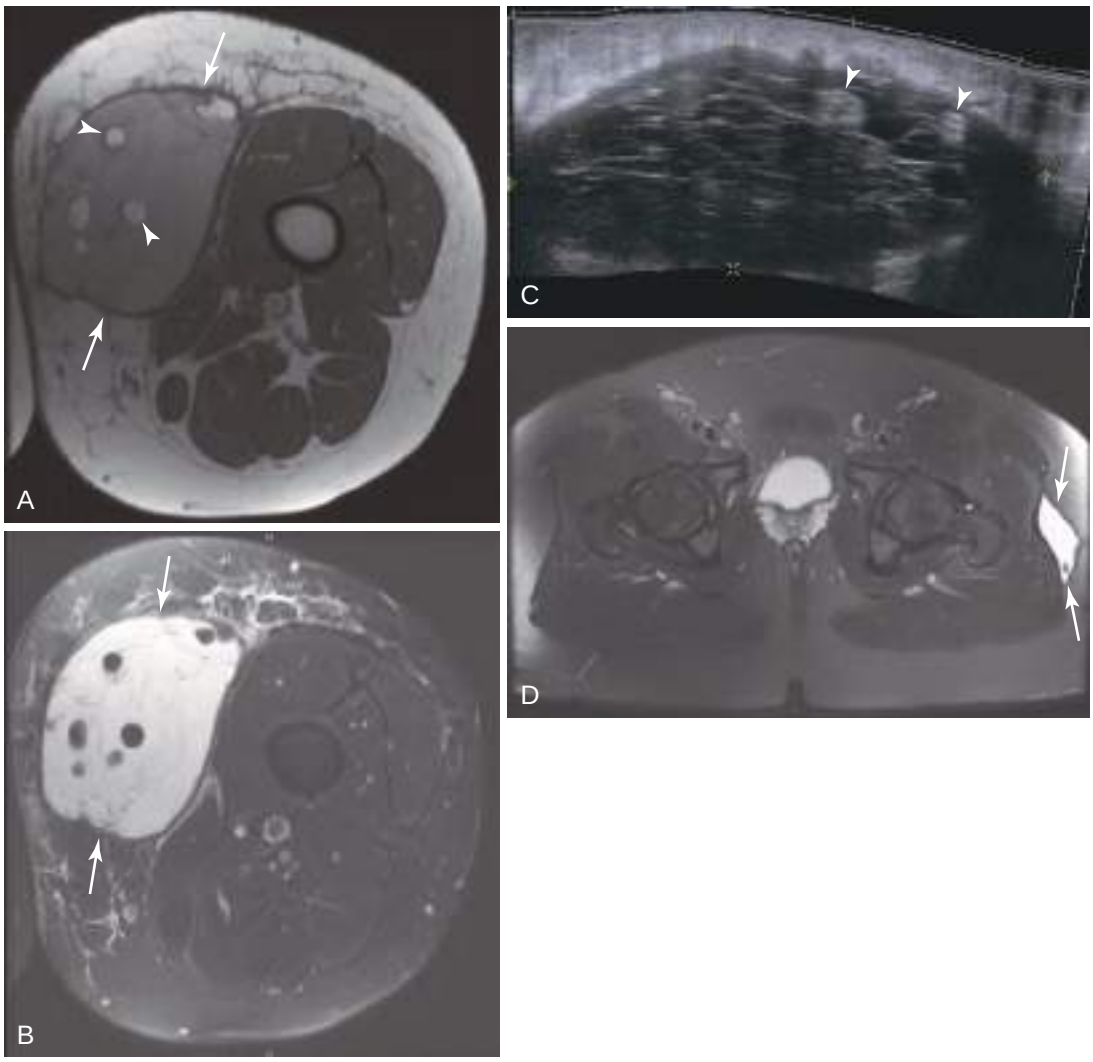

Fig. 1.64 Morel-Lavalée lesion in the thigh. (A) Axial T1-weighted and **(B)** fat-suppressed T2-weighted MR images and **(C)** longitudinal US. This lesion has many of the features that are variably present in Morel-Lavalée lesions, including a surrounding low-signal pseudocapsule *(arrows)*, innumerable internal thin septations, fat lobules within the lesion *(arrowheads)*, and mass effect on adjacent musculature. Note the characteristic location between subcutaneous fat and superficial muscle fascia. The medial location of this lesion is somewhat atypical, as most lesions occur laterally. **(D)** Smaller lesion in a different patient, lateral to the left hip.

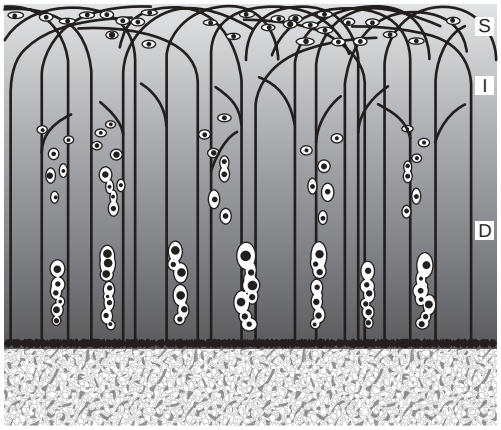

Fig. 1.65 Articular cartilage. Diagram shows the predominant orientation of collagen and proteoglycan fibers in the superficial, intermediate, and deep layers. This diagram exaggerates the thickness of the superficial layer, which is actually very thin. Calcified cartilage anchors the deep layer to underlying bone. *D*, Deep; *I*, intermediate; *S*, superficial.

IMAGING OF ARTICULAR CARTILAGE

MRI

- The gold standard imaging tool for articular cartilage.
- Lightly T2-weighted (intermediate) fast spin-echo.
  - The most widely used sequence.
  - An optimal TE is about 45 msec.
  - Often obtained with fat suppression.
    - Fat suppression increases dynamic range and reduces chemical shift artifact.
  - Normal articular cartilage has low to intermediate signal intensity on this sequence (Fig. 1.66A).
  - The deep cartilage layer may display slightly lower signal intensity because of its anisotropic ultrastructure.
- Fat-suppressed three-dimensional spoiled gradient-echo sequence (3D SPGR, FLASH).
  - Provides higher spatial resolution than a fast spin-echo sequence.

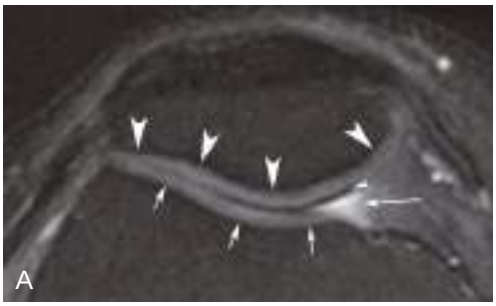

Fig. 1.66 Normal articular cartilage. (A) Axial fat-suppressed T2-weighted fast spin-echo (echo time, 45 msec) MR image obtained through the patella shows patellar *(large arrowheads)* and femoral trochlea *(short arrows)* cartilage. Careful observation shows slightly higher signal intensity in the intermediate layer (due to lack of anisotropy in this layer). The dark line between the patellar and trochlear cartilage *(small arrowhead)* is due to susceptibility artifact. Contrast the overall intermediate signal intensity of the normal articular cartilage with the high signal intensity of joint fluid *(long arrow)*. Cartilage defects are seen as high-signal regions. **(B)** Sagittal fat-suppressed three-dimensional spoiled gradient-echo MR image (repetition time, 60 msec; echo time, 5 msec; flip angle, 40 degrees) shows normal articular cartilage of the knee. Also note similar, normal signal of distal femoral and proximal tibial growth plates *(arrowheads)*. Hyaline cartilage is bright on this imaging sequence. Cartilage defects are seen as low-signal regions.

- Normal cartilage is bright on this sequence (see Fig. 1.66B).
- Downsides: long acquisition time, does not help in assessing other tissues, and displays only cartilage morphology. It is thus less widely used than fast spin-echo

Numerous other pulse sequences have been developed and validated for articular cartilage imaging. Example of more advanced techniques:

- T2 mapping.
  - Articular cartilage damage allows influx of free water, which prolongs T2.
  - Provides quantitative or semiquantitative assessment of cartilage T2 with high resolution.
  - Can detect cartilage degeneration earlier than fast spin-echo sequences.
  - Works best on 3T scanners.
  - Is becoming more available outside of research settings.

Other imaging options: both CT and MR arthrography can depict articular cartilage surface defects with excellent resolution.

Radiographs

- Poor sensitivity.
- The radiolucent cartilage space or joint space narrows with gross cartilage loss.
  - By the time such changes are visible on radiographs, cartilage loss is often extensive.

ARTICULAR CARTILAGE DEFECTS: DIAGNOSIS AT ARTHROSCOPY

- The current gold standard for articular cartilage assessment is arthroscopy.
- At arthroscopy, normal articular cartilage is smooth, firm, and glistening.
- The surgeon searches for visible articular cartilage defects and probes for abnormal cartilage softening.

Chondromalacia (Soft Cartilage)

- The earliest surgically detectable form of cartilage derangement is softness to a metal probe at arthroscopy. The cartilage may be swollen.
- More severe cartilage defects are classified by the defect *size* and *depth.*
- The most severe defects are full thickness with exposed subchondral bone.

Some cartilage defects have specific features that require additional terminology.

- *Fissure*: a crack in the cartilage surface of variable depth.
- *Fibrillation*: partial thickness cartilage loss with an irregular surface likened to crab meat.
- *Delamination*: separation of the cartilage from the subchondral bone.
  - These can be subtle or occult at arthroscopy if overlying superficial cartilage is intact.
  - Has high potential to progress to a full thickness defect.
  - MRI shows fluid signal intensity in deep articular cartilage (Fig. 1.67).
- *Flap tear*: delamination defect that extends to the cartilage surface at one or more sides.
  - The torn cartilage can be partially lifted off the bone.
- *Osteochondral fracture* (*lesion, defect)*: includes both cartilage and subchondral bone (Fig. 1.68).

Key Concepts

Describing Articular Cartilage Defects

Defect size, grade, location
Other features when applicable: fissure, flap tear, delamination, osteochondral lesion
Underlying subchondral bone: edema, sclerosis, cysts
Associated lesions such as synovitis, meniscal tears

IMAGING OF ARTICULAR CARTILAGE DEFECTS

- Easiest and most successful in the knee.
  - The knee has the thickest cartilage, up to 5 mm thick in the patella.

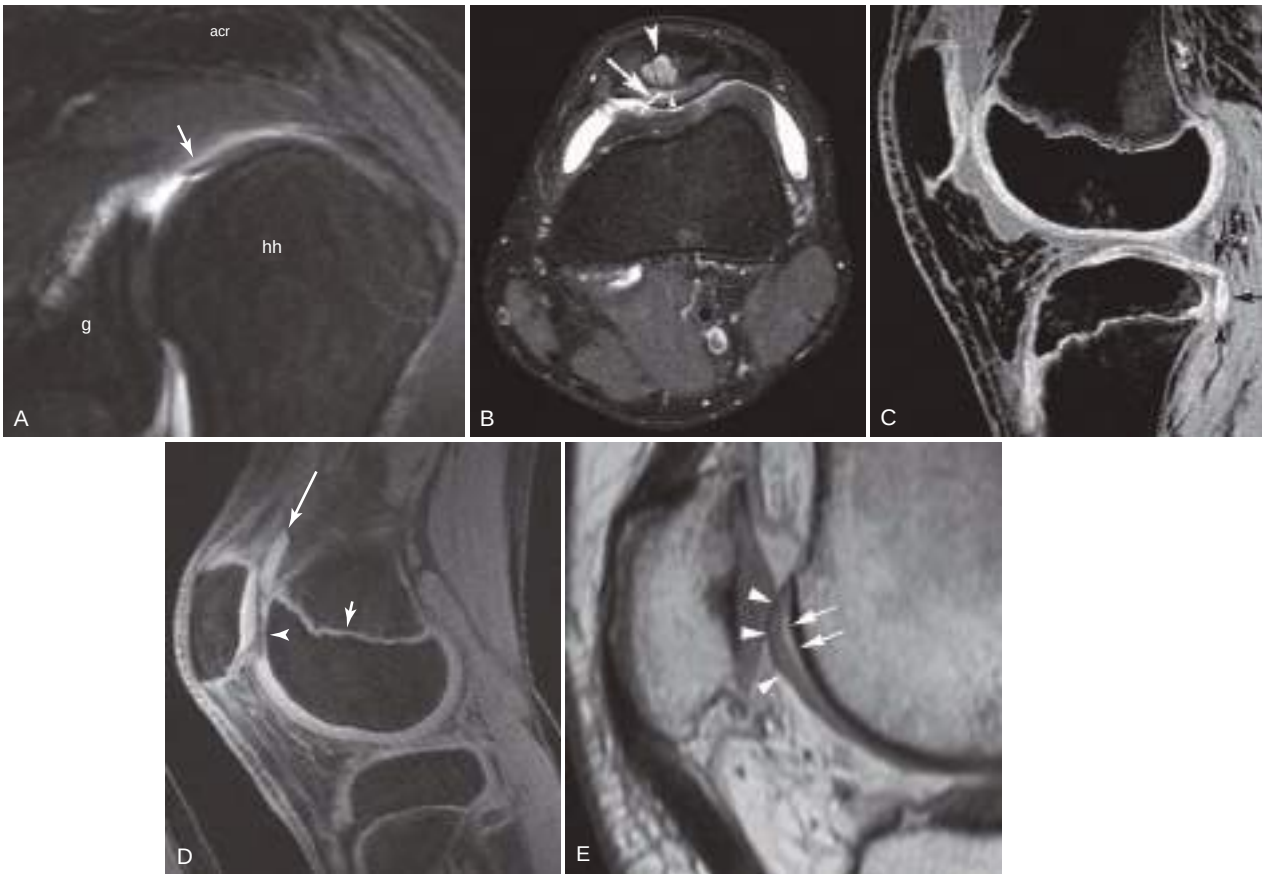

Fig. 1.67 Articular cartilage defects: flap tears and delamination. (A) Small humeral head flap tear. Oblique sagittal fat-suppressed T2-weighted fast spin-echo MR image shows flap tear *(arrow)* outlined by high-signal joint fluid. **(B)** Fissure with flap tear and partial delamination. Axial fat-suppressed fast spin-echo T2-weighted MR image (echo time, 60 msec) of a painful left knee shows an oblique fissure in the medial patellar facet *(arrow)* that extends laterally *(small arrowhead)*. Also note the adjacent patellar subchondral cyst *(large arrowhead)*. **(C)** Delamination of posterior lateral tibial plateau *(arrows)*. Sagittal fat-suppressed spoiled gradient-echo (SPGR) MR image in an adolescent who also sustained an anterior cruciate ligament tear with this injury. **(D)** Displaced full-thickness cartilage fragment. Fat-suppressed three-dimensional SPGR sequence. Recall that cartilage is bright on this sequence. Note the femoral trochlea chondral defect *(arrowhead)* and superiorly displaced fragment *(long arrow)*. Also note that the physis (growth plate) has similar bright signal, a normal finding *(short arrow)*. **(E)** Subtle delamination. Femoral trochlea cartilage *(arrowheads)* is separated from subchondral bone *(dark stripe)* by a thin layer of bright fluid signal *(arrows)*. *acr*, Acromion process; *g*, glenoid; *hh*, humeral head.

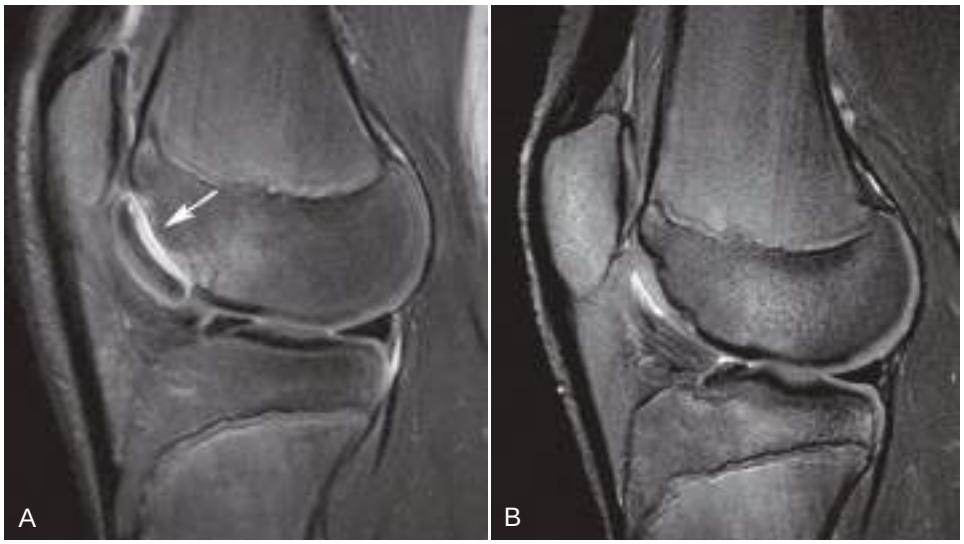

Fig. 1.68. Osteochondral fracture with successful repair. (A) Sagittal fat-suppressed lightly T2-weighted fast spin-echo MR image (echo time, approximately 45 msec) shows a detached lateral femoral trochlea osteochondral lesion *(arrow)*. **(B)** Follow-up MR study performed several months after surgical fragment reattachment shows successful repair, with healing of the bone fragments and smooth articular cartilage contour.

- In contrast, cartilage at the ankle joint, for example, is only about 1.5 mm on each surface and is harder to resolve.

MRI evaluation of focal cartilage defects:

- A cartilage defect may be seen as a region of increased T2 signal intensity or decreased cartilage thickness.
- Experience has shown that a reproducible and reliable MRI classification system of articular cartilage defects benefits from slight modification of the arthroscopic schemes.
- Defect evaluation includes defect signal intensity, depth and size, and signal change in the underlying bone.
- Most commonly used are adaptions of the arthroscopic grading system described by Outerbridge. Of these, the system adopted by the International Cartilage Regeneration and Joint Preservation Society (formerly known as the International Cartilage Repair Society and still goes by ICRS) is probably the most commonly used (Box 1.5 and Fig. 1.69; see also Fig. 1.67).
  - Grade 1 defect:
    - Mild irregularity and/or increased T2 signal of the cartilage surface on MRI images.
    - Most often due to cartilage surface degradation or microscopic disruption of the cartilage matrix deep to the cartilage surface. The damaged cartilage may *imbibe* (literally, 'drink') free water from the joint fluid.
  - Grade 2 defect:
    - Deeper than grade 1 but extends through less than 50% of the cartilage thickness or are localized areas of cartilage edema and swelling.
  - Grade 3 defect:
    - Greater than 50% thickness but not full thickness.
  - Grade 4 defect:
    - Full-thickness defects.
- Variations on the ICRS grading system are common. Examples:
  - Some authors consider any defect associated with a subchondral cyst or edema to be a grade 4 defect, regardless of the apparent depth of the defect on MR images.
  - Some authors simplify the ICRS system by lumping together grades 1 and 2 or grades 2 and 3 into a single grade, with a grade 3 being a full-thickness defect in these systems and grades 1 and 2 being something less.
- Simply describing a defect is another alternative.
  - Sample report: '12 by 7 mm 50% thickness articular cartilage defect posterior weight-bearing lateral femoral condyle. Underlying marrow signal is normal'.

Box 1.5 Magnetic Resonance Imaging Grading of Articular Cartilage Defects

Grade 0: Normal
Grade 1: Superficial edema and/or surface irregularity
Grade 2: Partial-thickness defect less than 50% thickness
Grade 3: Partial-thickness defect greater than 50% thickness
Grade 4: Full-thickness defect

Global joint evaluation systems such as WORMS (*Whole-Organ Magnetic Resonance Imaging Score*) and MOAKS (*MRI Osteoarthritis Knee Score*) combine assessment of articular cartilage loss with other knee pathology such as osteophytes, intraarticular bodies, effusion, and ligament and meniscal tears. These grading systems were developed as research tools to monitor potential effects of nonsurgical osteoarthritis therapies specifically in the knee, but in theory they could be modified to evaluate any joint.

MANAGEMENT OF ARTICULAR CARTILAGE DEFECTS

Articular cartilage is one of the few tissues of the musculoskeletal system that is incapable of regeneration.

The eventual response to articular cartilage injury is osteoarthritis. Osteoarthritis is the most common disability in the Western world and is associated with enormous direct and indirect costs to society, not only from treatment costs but also from economic loss of productivity. Ideal management arrests or reverses articular cartilage loss.

- *Delamination fragments* are sometimes successfully reattached to the subchondral bone. However, they may eventually break away or are resected when diagnosed, resulting in a full-thickness defect.
- An *osteochondral fracture fragment* has a higher likelihood of successful reattachment (see Fig. 1.68), because bone heals to bone much better than cartilage heals to anything.

Microfracture, Drilling, and Related Procedures

- Breaching subchondral bone in a full-thickness articular cartilage defect allows pluripotential cells to enter the exposed subchondral bone surface from underlying marrow.
- This allows for a cytokine-generated repair response that produces fibrocartilage in the defect. Fibrocartilage is inferior to articular (hyaline) cartilage but is better than no cartilage.
- Patients can increase their activity level with less pain.

Osteochondral Autologous Transplantation (OATS, Mosaicplasty, or Autologous Osteochondral Transplantation [AOTS], Fig. 1.70A)

- Cylindrical osteochondral plugs harvested from non–weight-bearing parts of the joint are transplanted to the site of a chondral or osteochondral lesion.
- Allografts made from biomaterials are also available.
- At present, this technique is limited to lesions that are about 2 cm^2 or less in size, although some surgeons use this approach for larger lesions.

Osteochondral Allograft Transplantation

- Used for large articular cartilage and osteochondral lesions.
- Requires careful matching of donor to recipient contours.
- Cadaver implants have not performed well.
- Grafts with living cells perform better, but availability is limited and these carry some risk of disease transmission.

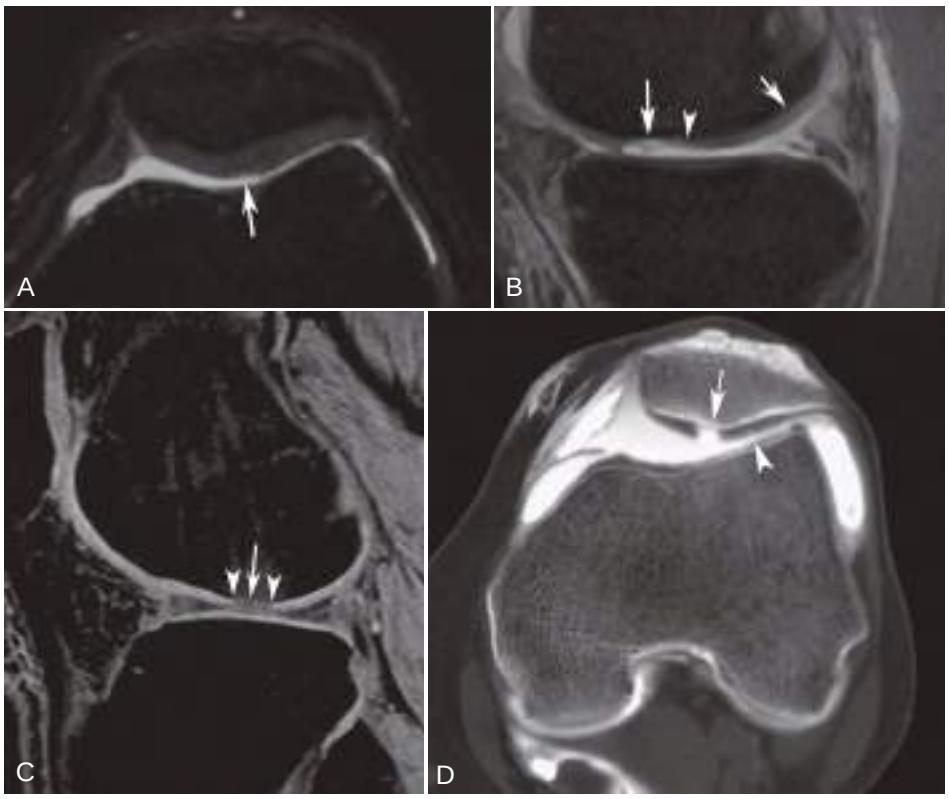

Fig. 1.69. Articular cartilage defects. (A) Axial fat-suppressed fast spin-echo T2-weighted MR image (echo time, 42 msec) shows grade 1 or shallow grade 2 defect of the median ridge of the patella *(arrow)*. **(B)** Sagittal fat-suppressed fast spin-echo T2-weighted MR image (echo time, 60 msec) of the knee shows grade 4 *(long arrow)* and grade 2 *(arrowhead)* defects of the lateral femoral condyle. Contrast this with the normal cartilage more posteriorly *(short arrow)*. **(C)** Sagittal fat-suppressed spoiled gradient-echo MR image shows grade 4 defect of the lateral femoral condyle *(arrow)*. The *arrowheads* mark the margins of this sharply marginated cartilage defect. **(D)** Axial computed tomographic arthrogram of the left knee shows grade 4 defect of the medial patellar facet *(arrow)*. Also note small, grade 1 defect of the lateral patellar facet *(arrowhead)*.

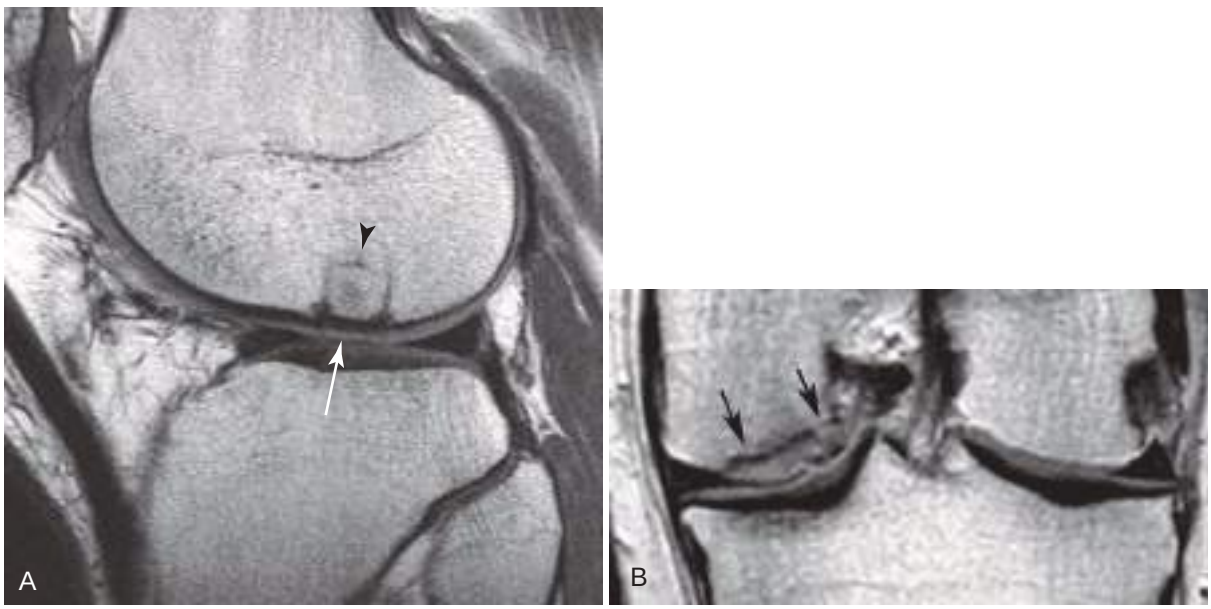

Fig. 1.70. Cartilage repair techniques. (A) Autologous osteochondral transplant (OATS). Sagittal proton-density MR image. *Arrowhead* marks the deep margin of the cylindrical bone and cartilage plug that was harvested from the high medial femoral trochlea and placed 6 months previously to repair a high-grade lateral condyle articular cartilage defect. The plug margin is visible as parallel low-signal lines perpendicular to the articular surface. The normal graft cartilage *(arrow)* blends smoothly with adjacent intact cartilage. **(B)** Autologous chondrocyte implantation (ACI). Coronal proton-density fast spin-echo MR image shows successful repair of a medial femoral condyle osteochondral lesion. Note the intermediate–signal-intensity new cartilage *(arrows)* filling the defect. The mildly irregular and raised articular surface is considered to be an acceptable finding.

Autologous Chondrocyte Implantation (ACI)

- Chondrocytes are harvested from the patient and cultivated ex vivo.
- The cultured chondrocytes are implanted into an articular cartilage defect under a protective periosteal flap (see Fig. 1.70B).
- The new cartilage requires months to mature, which requires long protected weight-bearing.
- Two operations required.

Matrix-associated ACI

- As with ACI, chondrocytes are harvested and cultured ex vivo.
- Cultured cells are embedded in a collagen scaffold that is glued into the cartilage defect.
- Two operations required.

ADDITIONAL ARTICULAR CARTILAGE PATHOLOGY

Acute Chondrolysis

- Sudden diffuse uniform loss of articular cartilage.
- Rare.
- May occur after trauma (including slipped capital femoral epiphysis) or arthroscopy.
- Also seen in immobilized patients.
- Most frequently in the hip joint, also the shoulder and elbow.
- Etiology is uncertain. Potential causes:
  - Increased intraarticular pressure and/or high intraarticular concentration of analgesics during arthroscopy.
    - Marcaine and related analgesics are toxic to chondrocytes in vitro.
  - Thermal capsule-tightening procedures used to manage shoulder laxity.
  - Lack of cyclic loading that nourishes cartilage in ambulatory patients might contribute in immobilized patients.
- Main differential diagnosis: infection, which can be identical in uniform, rapid, articular cartilage thinning and joint space narrowing. Large joint effusion suggests infection. Laboratory and clinical evaluation can distinguish.

Chondrocalcinosis

- Calcification of cartilage.
- Can be seen in association with:
  - Hypercalcemia in hyperparathyroidism.
  - Crystal deposition arthropathies, especially *calcium pyrophosphate deposition disease* (CPPD).
  - Hemochromatosis.
  - Various rare inborn errors of metabolism.
  - Older age as a degenerative but otherwise incidental finding.

Nerve Basics

- The peripheral nerves are composed of bundles of nerve fibers termed *fascicles*.
- Some of the major nerves of the extremities are part of a *neurovascular bundle* consisting of a nerve, artery, and vein or veins.

NORMAL NERVE IMAGING

- The myelin within the nerve sheaths has imaging features similar to fat.
  - CT: nerves have lower attenuation than muscle or water.
  - MRI: high signal intensity on T1- and T2-weighted MR images without fat suppression. Nerve signal intensity drops considerably on fat-suppressed or inversion recovery MR images.
  - High-resolution CT, MRI, and US demonstrate the individual fascicles within a peripheral nerve.

PERIPHERAL NERVE INJURY

Peripheral nerves are vulnerable to injury by direct trauma, compression, tension, tumor, autoimmune conditions, infection, radiation, and a variety of neuropathies.

- *Direct trauma* can be caused by an external source such as a knife wound or by a bone fragment following a fracture.
  - Example: the radial nerve of the arm is vulnerable to laceration or displacement by a humeral shaft fracture because it courses along the posterior margin of this bone. Surgeons may choose not to attempt to reduce a humeral midshaft fracture to avoid the risk of injuring this nerve while manipulating the fracture fragments.
- *Peripheral nerve entrapment* refers to a variety of clinical nerve dysfunction syndromes caused by nerve compression in relatively narrow anatomic spaces (Box 1.6; see Fig. 1.71).
  - The most common example is carpal tunnel syndrome, in which the median nerve is compressed within the carpal tunnel by a mass or mass effect—for example, by tendon sheaths enlarged by rheumatoid arthritis (see Chapter 4).
- *Tumors* may affect a nerve by compression or encasement. Some tumors such as a neurofibroma or schwannoma arise within a nerve. Careful attention to the status of nerves near a tumor is an essential part of evaluating surgical options for tumor treatment. Nerve and nerve sheath tumors are discussed in Chapter 12.
- *Neuritis* may be caused by peripheral nerve infection, notably by viral agents, or by immune-mediated inflammation, often following a systemic viral infection.
  - An injured or inflamed nerve may be associated with edema, enhancement, or swelling.
  - '*MR neurography*', using hybrid inversion recovery sequences in 3T scanners, can show nerve edema and swelling better than more conventional techniques on lower field strength magnets.
  - Muscle innervated by an injured motor nerve may show MRI findings of denervation (see Fig. 1.58).
  - Electromyelography is generally superior to imaging studies for assessing nerve injury or dysfunction, but can only be used in superficial nerves.

Box 1.6 Peripheral Nerve Entrapment Syndromes

Median nerve

Wrist: Carpal tunnel syndrome
Causes: Congenitally narrow tunnel, overuse, synovitis (e.g., rheumatoid arthritis), mass, hypothyroidism, fracture, idiopathic
Proximal forearm: Pronator syndrome
Cause: Compression within pronator teres
Distal arm: Ligament of Struthers
Cause: Anatomic variant, avian spur

Radial nerve

Proximal forearm: Posterior interosseous nerve syndrome
Cause: Compression of deep branch within the supinator muscle
Midarm: Compression or injury by humerus shaft fracture
Axilla: Sleep palsy
Cause: Compression while sleeping on side

Ulnar nerve

Elbow: Cubital tunnel syndrome
Cause: Nerve subluxation, mass, trauma, inflammation
Wrist: Guyon canal syndrome
Cause: Mass, trauma, inflammation

Axillary nerve

Quadrilateral space syndrome
Cause: Fibrotic bands, mass

Suprascapular nerve

Suprascapular notch syndrome
Cause: Mass or inflammation in spinoglenoid or suprascapular notch

Posterior tibial nerve

Tarsal tunnel syndrome
Cause: Nerve subluxation, mass, trauma, inflammation

Sciatic nerve

Piriformis syndrome

Lateral femoral cutaneous nerve

"Meralgia paresthetica"
Cause: Compression as nerve courses over inguinal ligament adjacent to anterior superior iliac spine

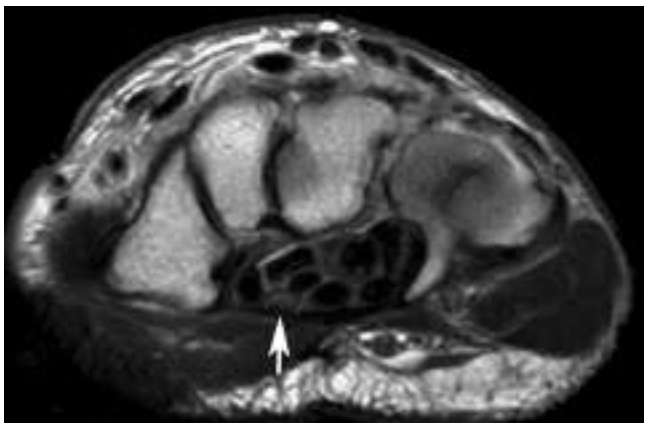

Fig. 1.71 Normal nerve. Axial T2-weighted fast spin-echo MR image obtained through the wrist shows the intermediate–signal-intensity median nerve *(arrow)* in the carpal tunnel. Contrast with the low signal of the carpal tunnel tendons.

Foreign Body Imaging

- The term *foreign body* includes both surgical implants and unwanted objects, such as metal or wood splinters that are usually introduced by direct penetration.
- Sufficiently radiodense foreign bodies including most glass fragments may be detected with radiographs (Fig. 1.72).
  - A skin marker at the penetration site is useful for localization.
- US is helpful for localization of superficial foreign bodies (Fig. 1.73).
- The MRI appearance of foreign bodies varies widely depending on their composition.
  - Microscopic metallic fragments are common after arthroscopy and can be numerous if a drill or burr

Fig. 1.72 Foreign bodies seen at radiography. (A) Bullet in soft tissues of the arm. **(B)** Smaller and less-dense foreign bodies can be subtle on radiographs. Oblique hand radiograph shows a linear foreign body in the soft tissues medial to the thumb *(arrow)*. This was the graphite core of a pencil. Foreign bodies with density similar to surrounding tissues such as most wood fragments can be invisible on radiographs.

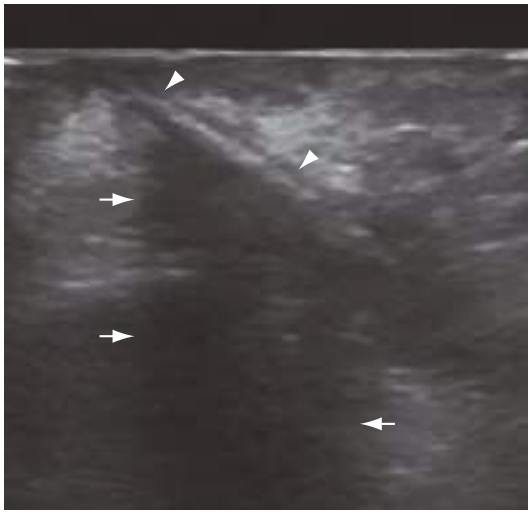

Fig. 1.73 Foreign body seen at US. Image of the calf shows an echogenic wood splinter *(arrowheads)*. Note the posterior acoustic shadowing *(arrows)*.

Box 1.7 Magnetic Resonance Imaging Techniques to Minimize Metal Artifact

Do

Increase receiver bandwidth.
Use fast spin-echo rather than conventional spin-echo.
Increase matrix.
Orient frequency encoding direction parallel to long axis of the metal object.
Use low field strength magnet.

Do not

Use gradient echo.
Use chemical fat suppression.

Note: The amount of metal artifact is greatly influenced by the type of metal alloy. Cobalt chromium steel alloys tend to cause much greater metal artifact than titanium and zirconium oxide alloys.

was used. These fragments are too small to be seen with radiography or CT. However, they cause susceptibility artifact and local field inhomogeneities that can be conspicuous on MR images, especially on gradient-echo images where they are seen as small areas of low signal intensity. This artifact can be minimized by using fast spin-echo sequences and other techniques (Box 1.7).

- Wood splinters are often simply invisible on MR images. When visible, they usually have low signal intensity on all sequences.
- Foreign bodies may develop a surrounding rim of granulation, sterile fluid, or pus with high T2 signal intensity that greatly increases lesion conspicuity on MRI (Figs. 1.74 and 1.75; see also Fig. 1.75).

Fig. 1.74 Radiographically occult foreign body seen at MRI. Axial T2-weighted MR image of the knee in a child who sustained an anterior left knee puncture wound by a tree branch 2 weeks previously shows a linear low–signal-intensity splinter with surrounding high–signal-intensity granulation tissue *(arrows)* at the level of the knee joint (note the localizer image at the *lower right corner* of the image). MRI is insensitive to small nonmetallic foreign bodies. However, reaction to the foreign body may include edema and granulation that can be detected with MRI.

Fig. 1.75 Radiographically occult foreign body seen at MRI. Sagittal T2-weighted spin-echo MR image of the foot demonstrates a long, thin low-signal foreign body *(long arrow)* with adjacent soft tissue edema *(arrowheads)* and a small fluid collection around the plantar end of the foreign body *(short arrows)*. The foreign body proved to be a wood fragment.

Part 3: Special Considerations in Imaging of Musculoskeletal Injury in Children

Children's bones are biomechanically different than adult bones

1. Children's bones are 'softer' (have greater plasticity), especially in younger children, and can permanently deform without fracturing into separate fragments. This plasticity decreases with age. Analogy: bones are like a bagel. Newborn bones are like a fresh bagel, soft and easily bent with only minimal disruption of the outer 'cortex'. As a child grows, the bones become progressively stronger and stiffer—like a bagel that has been left out on the kitchen counter for a few days. The analogous bagel is stiffer yet can still be bent, but with multiple cracks and circumferential disruption of the outer cortex. Adult bones are like a bagel that has been left out on the kitchen counter for weeks. The bagel is strong enough to support a stack of cookbooks, but it cannot bend, at least not perceptibly. If enough bending force is applied, the bagel, like an adult bone, will break into separate fragments rather than permanently bend. (Appreciation to the late pediatric radiologist Robert Wilkinson for this analogy.)
2. The *physis* (growth plate) is weaker than adjacent bone when exposed to shear or tension, so fractures often involve the physis.
3. Fractures in the immature skeleton have much greater potential for remodeling during later growth (see Fig. 1.32). Remodeling potential toward anatomic after a fracture depends upon:
   - The age of the child (younger is better, with more time to remodel toward normal during further growth).
   - Location (metaphyseal is best, best blood supply).
   - When present, the orientation of any angular deformity.
     - Angular deformity in the plane of motion of adjacent joints remodels better than angular deformity perpendicular to the plane of motion of adjacent joints.

- Example: a tibial shaft fracture with angular deformity in the coronal plane (valgus or varus) tends to remodel less than a fracture with angular deformity in the sagittal plane (apex anterior or posterior). This is unfortunate, because the knee and ankle can partially compensate for angular deformity in the sagittal plane but not in the coronal plane.

4. The periosteum of children's bones is loosely attached to the underlying bone except at the physis, where it is very tightly attached. This allows blood, pus, or tumor to accumulate between the periosteum and metaphyseal and/or diaphyseal cortex without extension into adjacent soft tissues.
   - *Periosteal reaction* (*periostitis, periosteal new bone formation*): New bone formed by periosteum displaced away from the cortex by tumor, hematoma, or pus. If the process elevates the periosteum then stops, early new bone that is created by the displaced periosteum may be seen on radiographs initially as a thin line or arc of calcification roughly parallel to the shaft (Fig. 1.76, see also Fig. 1.32). In contrast, sustained periosteal displacement, for example due to an enlarging tumor, results in different patterns that provide important clues to the nature of the underlying process. This is discussed further in Chapter 11.

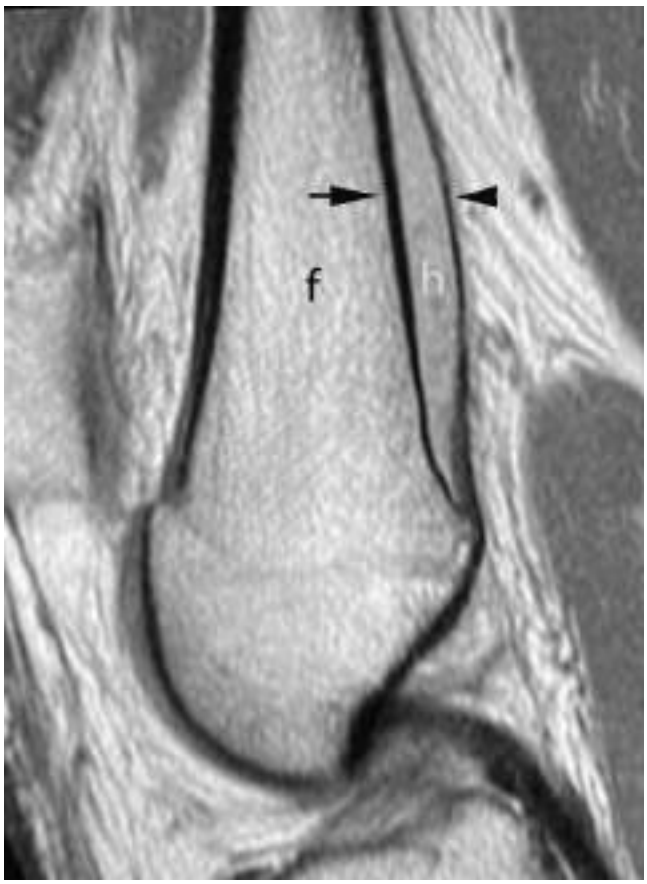

Fig. 1.76 Periosteal elevation by a traumatic hematoma. Sagittal PD-weighted MR image of the distal femur *(f)* in an adolescent shows a hematoma *(h)* between the posterior femoral cortex *(arrow)* and the elevated periosteum *(arrowhead)*.

Long Bone Growth and Remodeling

Longitudinal bone growth occurs at the physis.

THE PHYSIS IN GREATER DETAIL

- Also termed *growth plate, primary physis, epiphyseal growth plate*.
- Specialized site of enchondral ossification that allows long bone longitudinal growth (Fig. 1.77).
- The physis functions as a rolling assembly line that pushes the epiphysis away from the ossified metaphysis and diaphysis as it manufactures new bone in a multistep process.

A Summary of the Process

1. Chondrocytes are located along the epiphyseal margin of the physis (the *resting zone*).
2. These chondrocytes proliferate and produce a cartilage template.
3. This template becomes calcified (*zone of provisional calcification*, visible on radiographs and is a marker for some disease processes).
4. The chondrocytes die and the calcified cartilage is subsequently invaded by osteocytes. An intact metaphyseal blood supply is essential for this step.
5. The osteocytes convert the calcified cartilage to bone at the metaphyseal side of the physis.
   - The new bone deposited along the metaphyseal side of the physis is immature (woven) bone, and undergoes extensive remodeling to become cortex and trabeculae of mature lamellar bone
   - New cartilage is produced along the epiphyseal side of the physis at the same rate that it is converted to bone along the metaphyseal side. This equilibrium results in uniform width of the healthy physis throughout growth.

SECONDARY PHYSIS

Allows growth in the *secondary growth centers* (epiphyses and *epiphyseal equivalents*, i.e., apophyses and the small bones of the wrist and foot).

- Histologically similar to the primary physis.
- Not a linear plate like the primary physis, rather a thin circumferential shell around the ossified center of an epiphysis or epiphyseal equivalent.
- Creates radial rather than linear growth.
- Most do not appear until after birth.
- Not visible on radiographs but can be seen on high resolution T2-weighted MRI as a thin band of brighter signal around the ossified portion of the epiphysis.

LONGITUDINAL GROWTH RATE

- Depends on circulating hormones, notably growth hormone, and poorly understood local factors that maintain proportional skeletal growth.
- Fastest longitudinal growth in the appendicular skeleton occurs at the distal femur, where new bone is formed at up to 1–1.5 cm per year.

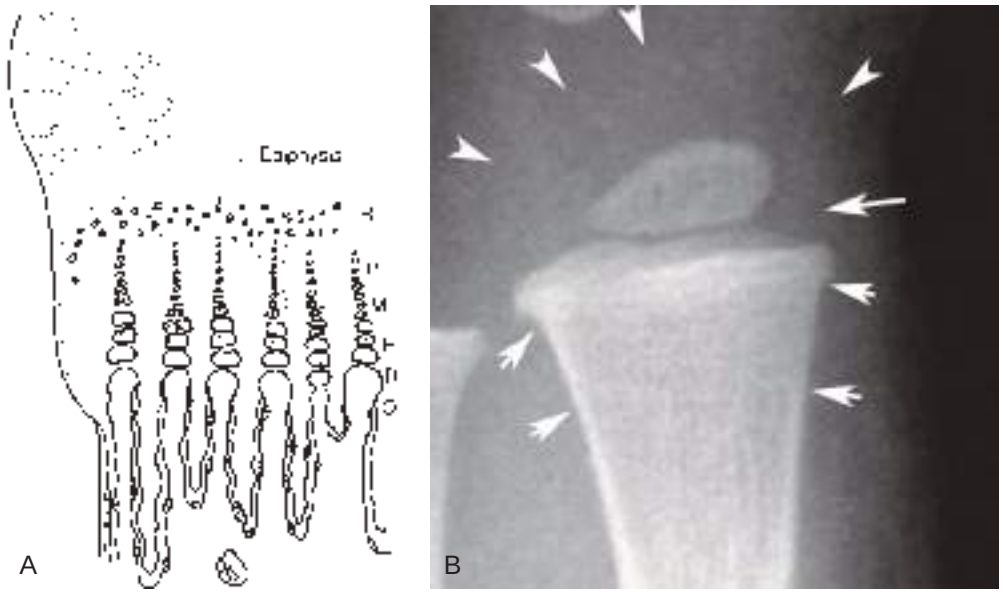

Fig. 1.77 The physis. (A) Diagram shows the histologic organization of the physis. The resting zone *(R)* adjacent to the epiphysis contains small clusters of cartilage cells. The proliferation zone *(P)* contains dividing and enlarging cartilage cells organized into longitudinal columns. Cell division ceases in the maturation zone *(M)*, but the cartilage cells continue to enlarge. The cells greatly enlarge in the hypertrophic zone *(H)*, and the surrounding cartilage becomes calcified (termed *provisional calcification* because it is not yet bone). The cartilage cells degenerate and die in the cartilage degeneration zone *(D)* and are replaced by osteoblasts. In the osteogenic zone *(O)* the osteoblasts begin the process of conversion of the calcified cartilage into bone. This zone marks the transition from the physis to the metaphysis. The term *bone bark* is sometimes used to describe the lateral margin of the physis, which occasionally calcifies and is seen on radiographs as a small spicule of bone extending distally from the metaphysis. **(B)** Radiograph of a child's distal radius shows the corresponding radiographic anatomy. The *long arrow* marks the physis. The convex contour of the metaphysis *(short arrows)* is the result of bone remodeling by osteoclasts and osteoblasts. If osteoclast activity is diminished, then this concave contour is not produced (undertubulation; see text and Fig. 1-79). The *arrowheads* mark the true margins of the epiphysis, which is composed mostly of cartilage in this young child.

CESSATION OF LONG BONE LENGTHENING

The chondrocytes in the resting zone of the physis stop dividing. Consequently, no new cartilage is formed and longitudinal growth ceases. The remaining cartilage is converted to bone as the physis closes.

- A dense transverse line on radiographs, sometimes termed a *physeal scar*, marks the final position of the physis.
  - This line may persist into adulthood but is eventually removed by normal adult bone remodeling.

The timing of physeal closure varies at different sites.

- Most bones stop lengthening by about age 14 in girls and 16 in boys.
- The medial clavicle physes are among the last to close, typically in the third decade, years after adult stature has been achieved.

Growth Arrest Lines

- Also termed *growth recovery lines, Park lines, Harris lines, or stress lines*
- Thin transverse sclerotic line across the metaphysis parallel to the physis.
  - Uniform, sharply defined, straight.
  - Does not abut the physis.
- Associated with periods of childhood stress such as illness, injury, or immobilization. Formed during the recovery phase after such episodes.
- Like the rings of a tree, the physis grows away from the line over time.
- Typically are single, but in the setting of repeated insults can be multiple (Fig. 1.78).
- Often persist into adulthood but are eventually removed by routine bone remodeling.

In contrast, *transverse metaphyseal bands* are broader, less well-defined, and abut the physis.

- *Sclerotic* transverse metaphyseal bands can be seen as a normal finding when found only in weight-bearing bones, or as an abnormal finding when found in all bones as a consequence of heavy-metal poisoning (see Fig. 13.53).
- *Lucent* transverse metaphyseal bands can occur in rickets, leukemia, and metastatic neuroblastoma.

LONG BONE LATERAL GROWTH AND REMODELING

- The periosteum produces bone that allows a bone to increase in diameter.
- *Tubulation*: As the bone lengthens, metaphyses are converted into a tube-like diaphyses.
  - Tubulation is mediated by coordinated function of osteoclasts and osteoblasts.
  - Disorders of tubulation may result in a wide metaphysis (*undertubulation*, *Erlenmeyer flask deformity*; Fig. 1.79 and Box 1.8; see Fig. 15.80), or a narrow, tubular metaphysis (*overtubulation*; Fig. 1.80 and Box 1.9).
  - For example, the diminished osteoclastic activity associated with osteopetrosis and marrow packing in storage diseases result in undertubulation.

Fig. 1.78 Growth arrest lines (Park lines, Harris lines). (A) AP radiograph of the distal radius in a 5-year-old shows multiple thin, sharp lines parallel to the physis. **(B)** Coronal T1-weighted MR image of the knee in a different patient shows similar findings, although extraordinarily prominent. This child has osteogenesis imperfecta that has been treated with periodic bisphosphonate injections. The growth recovery lines are formed by impaired osteoclast function during therapy. The growth recovery lines are more widely spaced in the femurs than in the tibias because the femurs grow more rapidly.

Fig. 1.79 Undertubulation. (A) Osteopetrosis. Failure of osteoclast function results in wide metaphyses. **(B)** Achondroplasia. Note the short, squat bones with wide metaphyses. **(C)** Hurler syndrome (mucopolysaccharidosis 1H). The marrow is packed with abnormal metabolites, causing expansion of the diaphyses and metaphyses. See also Fig. 15.80. (**B** courtesy of Stephanie Spottswood, MD.)

- Overtubulation is seen most commonly in neuromuscular conditions with absent or diminished weight-bearing, such as cerebral palsy.

Box 1.8 Common Causes of Undertubulation

Bones of normal length
- Rickets
- Osteopetrosis
- Fibrous dysplasia
- Multiple osteochondromas

Short, often squat bones
- Dwarfism (numerous types, achondroplasia most common)
- Storage diseases
- Multiple osteochondromas

Fig. 1.80 Overtubulation. Note the short transition from epiphysis to diaphysis in the forearm of this child with osteogenesis imperfecta. Also note the long, narrow diaphyses. This overall appearance is often described as 'gracile bones' and is most commonly seen in neuromuscular conditions with chronic absence of weight-bearing, such as cerebral palsy.

Box 1.9 Common Causes of Overtubulation (long, thin bones)

Neuromuscular conditions (e.g., cerebral palsy, myelomeningocele)
Osteogenesis imperfecta
Juvenile idiopathic arthritis
Marfan syndrome
Homocystinuria
Arthrogryposis

Key Concepts

Tubulation

Process of remodeling the shaft of a long bone into a normal configuration.
Overtubulation: cylindrical portion of the shaft is too long, with short and narrowed metaphysis (e.g., absent weight-bearing, neuromuscular conditions).
Undertubulation: cylindrical portion of the shaft is too short, with wide and long metaphysis (e.g., osteopetrosis, Gaucher disease).

Physeal Fractures

The physis is weaker than adjacent bone in resistance to shearing and torsional forces, but it is not weaker in resistance to compression. Fractures that cross or extend along a physis account for 15% of all pediatric fractures. The percentage is not higher because most pediatric fractures are caused by compression resulting from a fall.

SALTER–HARRIS SYSTEM OF FRACTURES INVOLVING THE PHYSIS (FIG. 1.81)

Salter–Harris I

- Involve only the physis, with displacement of the epiphysis relative to the metaphysis.
- Displacement may be minimal or imperceptible on radiographs. Comparison with the contralateral side and/or follow-up radiographs may make the diagnosis.
- MRI usually is definitive when needed.

Salter–Harris II

- Extend through a portion of the physis and a portion of the metaphysis.
- This is the most frequent pattern, 85% of physeal fractures.

Salter–Harris III

- Involve the physis and epiphysis. Thus, these are intraarticular fractures.

Salter–Harris IV

- Extend through the epiphysis, physis, and metaphysis.

Salter–Harris V

- Compression injury of the physis, which may be missed or resemble a Salter–Harris I fracture at initial diagnosis.
- Rare.

Some authors extend the Salter–Harris system with a variety of pure metaphyseal and epiphyseal fractures that do not extend into the physis. These additional Salter–Harris categories are not widely used.

IMAGING DIAGNOSIS OF FRACTURES INVOLVING THE PHYSIS

Radiography

- First-line test.

CT

- Mainly used for preoperative planning in some fractures in adolescents.

MRI

- Highly sensitive.
- Can show fractures in unossified epiphyseal cartilage.
- Requires sedation in younger children.

US

- Can show fractures in unossified epiphyseal cartilage.
- Can show cortical disruption and periosteal elevation by hematoma.

Bone Scan

- Hampered by normal intense tracer uptake at the physes. Pinhole imaging and careful comparison with the

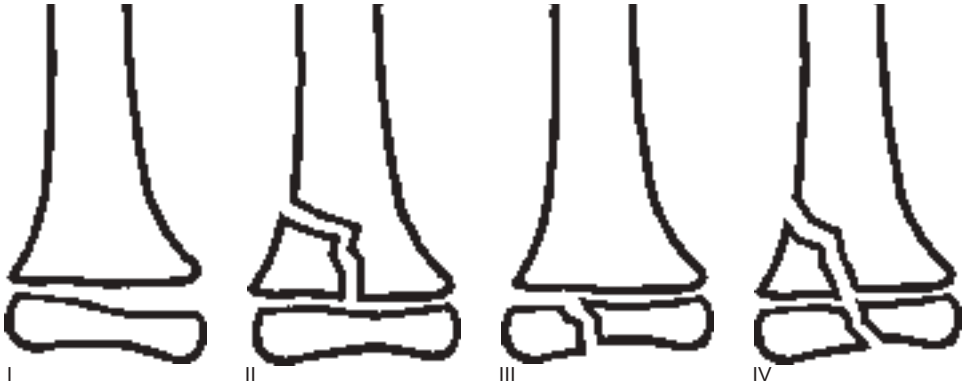

Fig. 1.81 Salter–Harris classification system of pediatric fractures that involve the physis. Salter–Harris V is a crush injury of the physis.

contralateral side improve the accuracy of bone scintigraphy, but this modality is inferior to MRI and US, and uses ionizing radiation.

PHYSEAL INJURY COMPLICATIONS

Direct trauma to the physis can result in osseous healing across the physis (*bone bridge* or *bone bar*) or injury to the chondrocytes that are needed to produce the cartilage model. Either complication can cause growth arrest or growth deformity (Figs. 1.82 to 1.85).

Bone Bridge Across the Physis (Bone Bar)

- Bone that crosses the physis and connects the epiphysis to the metaphysis.
- Can be large or small.
  - Large: growth arrest.
  - Small: the bridge tethers only a portion of the physis, resulting in a cup-like or angular deformity.

Fig. 1.82 Growth plate arrest after distal femur physeal fracture. **(A)** Frontal radiograph obtained at the time of injury shows Salter–Harris II fracture of the distal left femur *(arrows)*. **(B)** CT scanogram obtained 3 years later demonstrates shortening of left femur, the site of previous fracture. *Dashed lines* of each femur indicate the degree of left-sided shortening. **(C)** Coronal T1-weighted MR image shows substantial irregularity of distal femoral physis and focal absence of growth plate *(arrows)*. Note smooth contour of proximal tibial physis *(arrowheads)*. **(D)** Coronal fat-suppressed three-dimensional spoiled gradient-echo MR image (repetition time, 60 msec; echo time, 5 msec; flip angle, 40 degrees) shows cartilaginous irregularities of medial aspect of distal femoral physis *(arrowheads)* and focal absence of growth plate cartilage *(arrows)*. Note smooth contour of proximal tibial physis. (**D** adapted and reproduced, with permission, from Disler DG. Fat-suppressed three-dimensional spoiled gradient-recalled MR imaging: assessment of articular and physeal hyaline cartilage. *AJR*. 1997;169:1117-1123.)

Fig. 1.83 Physeal bar and deformity after distal tibial physeal injury. Coronal fat-suppressed spoiled gradient-echo MR image shows the bony bridge *(long arrows)*, old Salter–Harris IV fracture line *(short arrows)*, and the physis *(arrowheads)*. Note the angular deformity between the talar dome (T) and distal tibial epiphysis (E). M, metaphysis.

Main risk factors for development of a bone bridge:

- Vertical fracture.
  - Longitudinally oriented Salter–Harris IV fracture.
  - Just a few millimeter displacement along the fracture can allow a metaphyseal fragment to abut and heal directly to an epiphyseal fragment.
- Physis with a normally undulating contour.
  - The distal tibia and femur are the most common sites of growth arrest.
  - The physes at these sites have an undulating contour, which allows slight fracture displacement to appose metaphyseal and epiphyseal bone.

Imaging a Suspected Bone Bridge

Radiographs

- Obvious bone bridge across the physis and growth arrest or deformity are later findings.
- Earlier detection: observe any *growth recovery lines* (defined earlier).
  - The growth recovery line initiated by the fracture should uniformly separate from the physis on subsequent radiographs.
  - If focal physeal tethering is present, the growth recovery line may merge with the bone bridge (Fig. 1.85).
- A bone bridge in the center of the physis will cause growth arrest without an angular deformity but may cause a ball-in-cup appearance.
- A more peripheral bone bridge results in angular deformity as the uninjured portion of the physis continues to grow (see Fig. 1.85).

MRI

- Can confirm or exclude a bone bridge earlier and better than radiographs.
- Mature bone bridge:
  - Continuous marrow fat signal across the physis on T1w.
  - Pathognomonic but not always present.

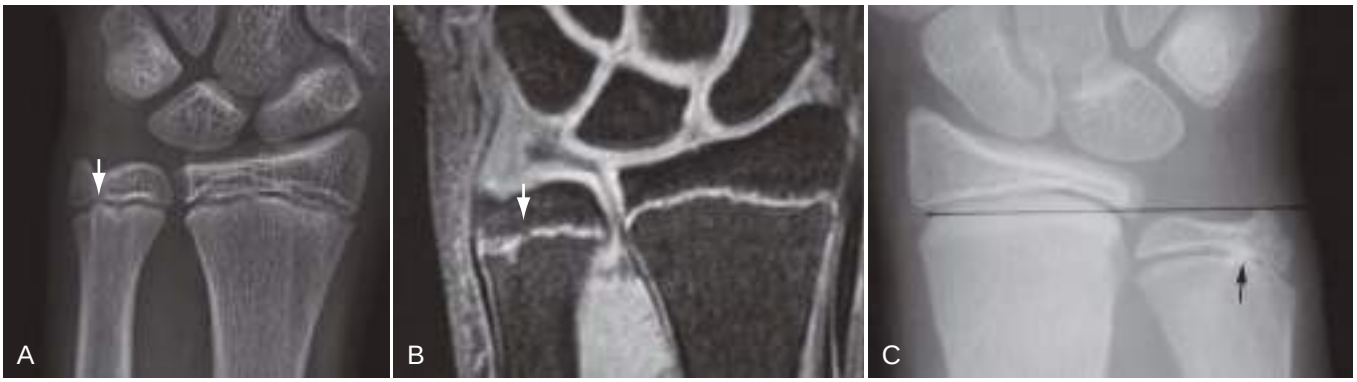

Fig. 1.84 Ulnar physeal bar. (A) Radiograph shows subtle narrowing of the ulnar growth plate, suspicious for a bony bar. **(B)** Coronal fat-suppressed spoiled gradient-echo MR image 4 weeks later confirms interruption of the bright growth plate by a small bar. This lesion was treated promptly with no resulting growth disturbance. **(C)** Similar lesion identified later, in a different patient. Note ulnar shortening without other deformity, due to a bony bridge *(arrow)*.

Fig. 1.85 Growth deformity after a distal tibial physeal injury. This AP view was obtained several months after a distal tibia fracture that healed with casting. Note the osseous healing across the medial physis, forming a continuous bony bridge between the metaphysis and epiphysis *(black arrowheads)*. Also note the growth recovery line in the distal tibial metaphysis, which was formed as a result of the fracture *(white arrowheads)*. Since the fracture, there has been normal growth laterally but absent growth medially due to physeal tethering by the bony bridge. As a result, the growth recovery line is seen to merge with the physis *(white arrows)* at the bony bridge.

- Earlier detection:
  - Fat-suppressed 3D SPGR (FLASH), the same sequence used for articular cartilage imaging.
    - Both articular and physeal cartilage are bright on this sequence.
    - A bone bridge is seen as an interruption of the bright signal of the normal physis (Figs. 1.82 and 1.83).
    - Allows precise localization of the bridge (Figs. 1.82 and 1.83). (For an excellent discussion of MRI for preoperative planning of growth plate injuries, see Ecklund and Jaramillo, 2002.).

Management of a Bone Bridge

- Goal is to prevent the development of deformity.
- If the bone bridge involves less than 50% of the physis, physeal growth may be salvaged by resection of the bridge with a drill, using an oblique approach through the metaphysis.
  - Preoperative MRI with fat-suppressed 3D SPGR allows precise localization of the bridge (Figs. 1.82 and 1.83).
  - This procedure is reserved for younger children with more growth potential.
- *Epiphysiodesis*
  - Fusion of the physis to arrest all growth, to prevent the development of angulation.
  - Can result in a leg length discrepancy.
  - Contralateral epiphysiodesis can keep the extremities of equal or at least length.
  - Alternatively, a bone lengthening procedure can be performed on the injured bone.
  - This is discussed further in Chapter 15.

OTHER CAUSES OF GROWTH ARREST

Injury to the chondrocytes that produce the cartilage model:

- Direct trauma (Salter V fracture), thermal injury (osteoid osteoma or osteoblastoma thermal ablation).
- Injury to the epiphyseal blood supply to the chondrocytes.
  - Trauma.
  - Focal infection.
  - Disseminated intravascular coagulation (DIC), as may result from *meningococcemia* (Fig. 1.86).
    - Limb amputation is a common sequela of meningococcemia but if a child survives with the limbs intact, growth deformities may become apparent over subsequent months.
    - The growth arrest in DIC often begins at the central portion of each physis, probably because of greater vulnerability of the blood supply, resulting in a cupped shape of the physes.
- Intact metaphyseal blood supply to the physis is essential to converting the cartilage model into bone.
  - Damage to metaphyseal blood supply by trauma, infection, or other insult can result in focal or generalized widening of the physis, because the newly

Fig. 1.86 Growth arrest after meningococcemia. Radiograph shows irregular, premature fusion of all physes.

produced cartilage cannot be transformed into bone. Growth disturbance and deformity may result.

PHYSEAL STRESS INJURY

- Can be considered a chronic Salter–Harris I injury.
- Radiographs: widening and irregularity of the growth plate.
- MRI: widening and irregularity of the growth plate and adjacent marrow edema, especially in the metaphysis.
- Overuse injuries in high-performance child and adolescent athletes.
  - Gymnasts: distal radius and ulna (Fig. 1.87).
  - Baseball pitchers: proximal humerus, humeral medial epicondyle.
  - Runners: lower extremities.
- These injuries usually resolve with conservative therapy.

GROWTH CARTILAGE

- Unossified epiphyseal (and apophyseal) cartilage in younger children located between the superficial articular cartilage and the ossified central portion of the epiphysis (the *ossific nucleus*).
- Mainly fibrocartilage.
- MRI of growth cartilage.
  - Lower signal intensity on T2-weighted MR images than articular cartilage.
  - Highly vascular and enhances following gadolinium administration.
  - Absent enhancement is a sign of injury or infection.
- Fractures that involve unossified growth cartilage can be invisible on radiographs.
- Detection of a fracture through unossified cartilage requires MRI, US, or intraoperative arthrography (for intraarticular fractures).

Fig. 1.87 Chronic Salter–Harris I injury of the distal radius in a young female gymnast. Note the sclerosis and irregularity around the physis.

Key Concepts

Osteochondritis dissecans (OCD)

Distinctive form of osteochondral injury of older children and adolescents

Subchondral stress injury

May heal with or without deformity or result in a fragment that is loose in situ or displaced into the joint

Osteochondritis Dissecans

- OCD overlaps with but is not exactly the same as *osteochondral* lesion or OCL.
- Distinctive type of osteochondral injury that occurs in older children and teenagers.
- Likely cause is chronic/repetitive shear stress injury, and specifically injury to the secondary physis, with subsequent disturbed enchondral ossification. Advanced cases result in fragmentation and involve the overlying articular cartilage.
- Becoming more prevalent in younger children due to increased participation in high-level sports at a younger age.
- Present with joint pain of months or longer duration.
- More advanced cases present with joint pain, swelling, clicking, and locking.
- The knee is by far the most common site for OCD, especially at the lateral aspect of the medial femoral condyle.
  - Mnemonic: LAME, for **l**ateral **a**spect of the **m**edial femoral (**e**pi)condyle (Fig. 1.88)
  - Other sites are listed in Box 1.10

The disease process and imaging findings in OCD are mostly similar at all sites, but most literature is focused on the knee.

OCD is a process:

- Begins as a subchondral injury with intact overlying articular cartilage.
  - MRI may initially show only edema in unossified subchondral cartilage, which is nonspecific because

Fig. 1.88 Osteochondritis dissecans (OCD), knee. (A and B) Classic radiographic appearance. AP **(A)** and lateral **(B)** radiographs demonstrate typical location of osteochondritis dissecans along lateral aspect of the medial femoral condyle. Note osteochondral fragment *(arrows)* and linear lucency separating fragment from underlying bone. Note also adjacent cystlike bone lucencies (*black arrowheads* in **A**), which suggest instability of bone fragments. Incongruence of osteochondral fragment and underlying bone (*white arrowhead* in **A**) also suggests instability of fragment. **(C)** Sagittal CT reformat in a different patient shows similar findings: sclerotic OCD fragment separated from the host femur by soft tissue attenuation that could be fluid, granulation tissue, or fibrous or cartilaginous connective tissue.

Box 1.10 Osteochondritis Dissecans: Sites

Knee (most common site):
- Lateral aspect of medial femoral condyle (mnemonic: LAME)
- Less common: patella, any surface of the femoral condyles

Elbow: Distal capitellum
Shoulder: Humeral head
Ankle: Talar dome, most often medial

edema can be seen as a benign transient finding (see Fig. 1.89).
- If the normal thin high T2-signal signature of the secondary physis is no longer visible at the adjacent chondro-osseous junction, secondary physeal injury may be present. This is associated with risk for progression.

- If the process continues in younger children:
  - Fragmentation of unossified growth cartilage and/or epiphyseal bone.
  - Eventual extension into overlying articular cartilage, creating fragments.
  - Fragment displacement.
- If the process continues in older children, classic OCD findings develop:
  - Thickening of unossified cartilage due to the secondary physis injury.
  - Epiphyseal trabecular microfractures develop and may coalesce into a subchondral fracture line that is roughly parallel to the subchondral cortex (see Figs. 1.90 to 1.92).
  - The fracture can focally extend to the joint surface (see Figs. 1.91 and 1.92).
  - This may progress to a complete separation of the osteochondral fragment. The fragment may remain in place ('loose in situ' *or* '*in situ loose*') (Figs. 1.92 to 1.95), or may displace into the joint (Fig. 1.96).

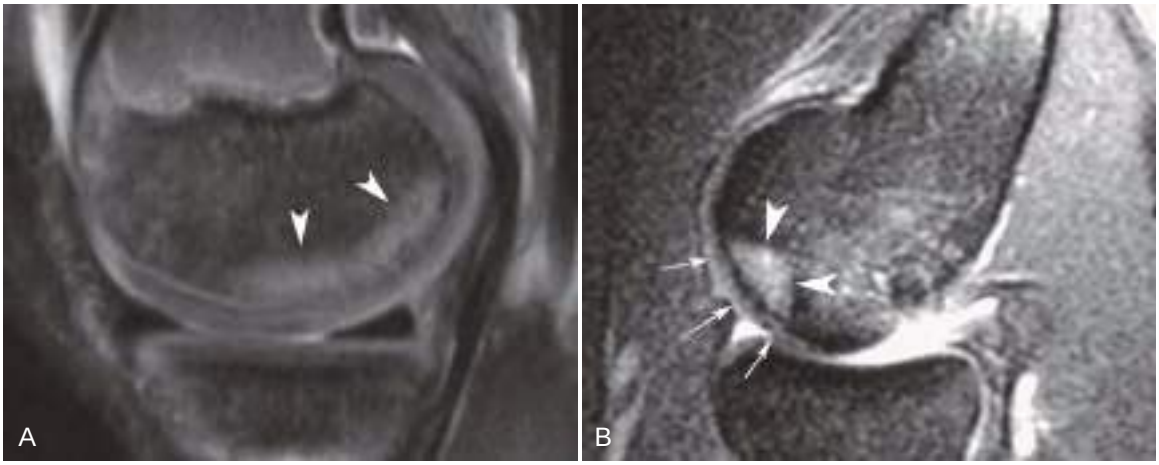

Fig. 1.89 Early osteochondritis dissecans (OCD). (A) Very early OCD. Sagittal fat-suppressed T2-weighted MR image shows subchondral marrow edema in the medial femoral condyle *(arrowheads)*. This edema is not specific and may resolve. In this child, painful subchondral fragmentation typical of OCD subsequently developed. **(B)** Early OCD of the humeral capitellum (Panner disease). Sagittal fat-suppressed T1-weighted MR image obtained after administration of intravenous contrast medium and elbow exercise shows enhancement of the OCD lesion *(arrowheads),* which indicates an intact blood supply and thus a good potential for resolution without further progression. Note the intact overlying cartilage *(small arrows)*. This image also illustrates the technique of indirect arthrography, which delivers gadolinium to the joint via diffusion through the synovium.

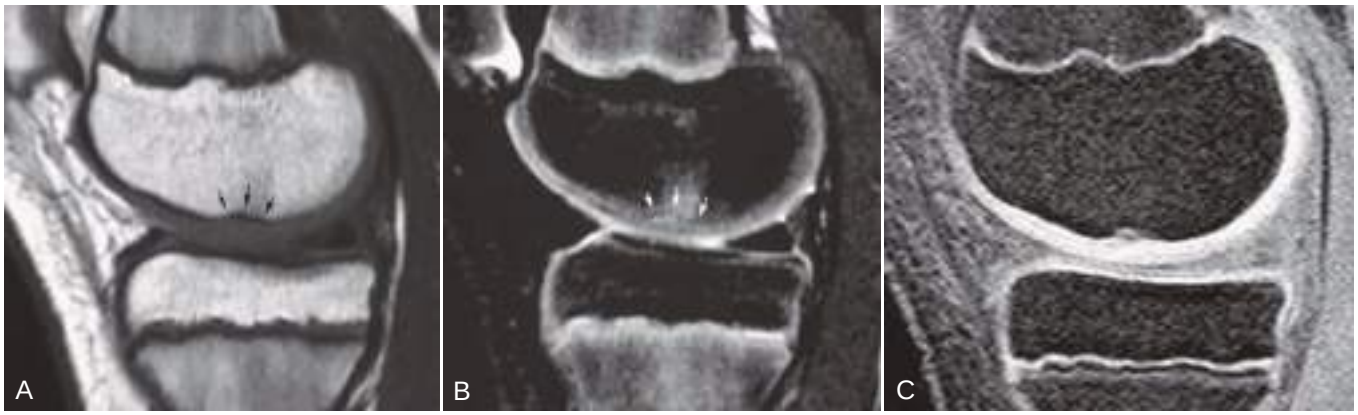

Fig. 1.90 Early osteochondritis dissecans with intact overlying articular cartilage. Sagittal T1-weighted **(A)**, fat-suppressed T2-weighted **(B)**, and sagittal fat-suppressed spoiled gradient-echo MR images **(C)** show subchondral irregular low-signal line *(small arrows)* with adjacent marrow edema. Note intact overlying articular cartilage, best seen in **C**, with normal signal intensity. This could be a subchondral impaction fracture along with early osteochondritis dissecans.

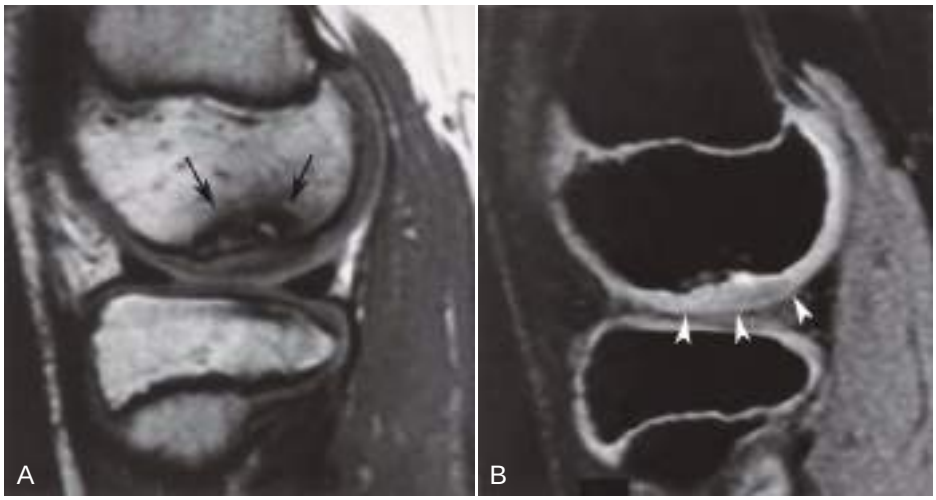

Fig. 1.91 Osteochondritis dissecans with intact overlying articular cartilage. (A and B) Sagittal T1-weighted **(A)** and fat-suppressed spoiled gradient-echo **(B)** MR images show the osteochondral fracture lines (*arrows* in **A**). The overlying articular cartilage is intact (*arrowheads* in **B**).

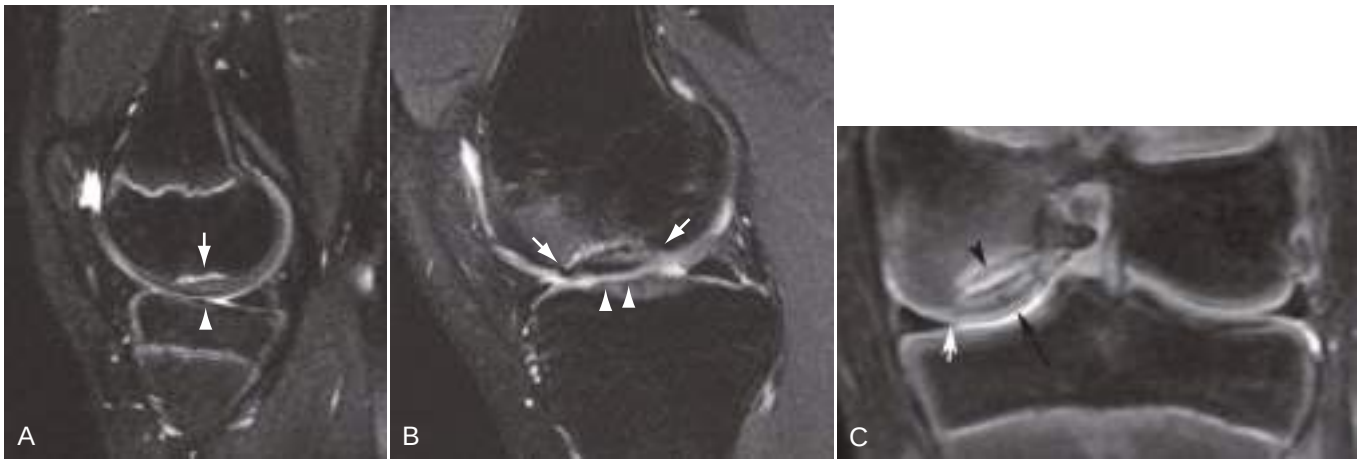

Fig. 1.92 Osteochondritis dissecans (OCD) progression over time to loose in situ fragment. (A) Sagittal fat-suppressed T2-weighted MR image shows incomplete transverse fracture in subchondral trabecular bone *(arrow)* with completely intact overlying articular cartilage *(arrowhead)*. **(B)** Same patient 7 years later, now a young adult. The OCD lesion has progressed to a loose in situ fragment. Edema completely separates the host bone from the OCD fragment, including through articular cartilage at the lesion margins *(arrows)*. Also note edema in degenerating fragment cartilage *(arrowheads)*. **(C)** Coronal fat-suppressed proton-density MR image of the left knee in a different child shows medial femoral condyle OCD fragment *(long arrow)* and high T2 signal between the fragment and the host femur *(arrowhead),* indicating that the fragment is loose, despite intact medial articular cartilage *(short white arrow)*.

Fig. 1.93 Osteochondritis dissecans (OCD) with loose in situ fragment. Sagittal fat-suppressed T2-weighted MR image shows medial femoral condyle OCD fragment *(long arrow)* with uniform high signal intensity consistent with fluid *(short arrows)* surrounding the fragment. Also note the intense marrow edema in the adjacent femur *(arrowhead)*. Same patient as shown in Fig. 1.88C.

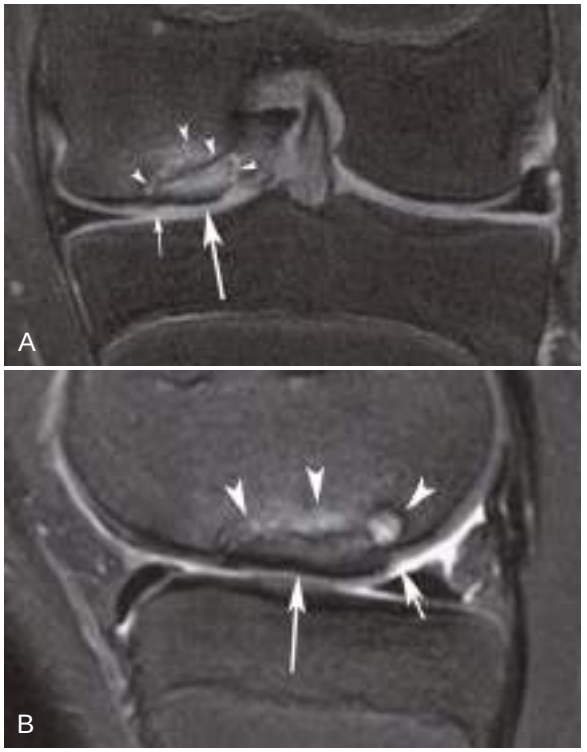

Fig. 1.94 Osteochondritis dissecans (OCD) with loose in situ fragment. MRI findings in a loose fragment are not always as unambiguous as seen in Fig. 1.93. Coronal fat-suppressed proton-density **(A)** and sagittal fat-suppressed T2-weighted **(B)** MR images of the left knee show medial femoral condyle OCD fragment *(large arrow),* with surrounding high signal, small cystlike lesions, and marrow edema at the margin of the fragment and the host bone *(arrowheads)*. Also note the small articular step-off posteriorly *(short arrows)*. These findings are highly suggestive of a loose fragment, but a fragment that is healing in place could have a similar appearance. Arthroscopy was needed to confirm that this fragment was loose in situ.

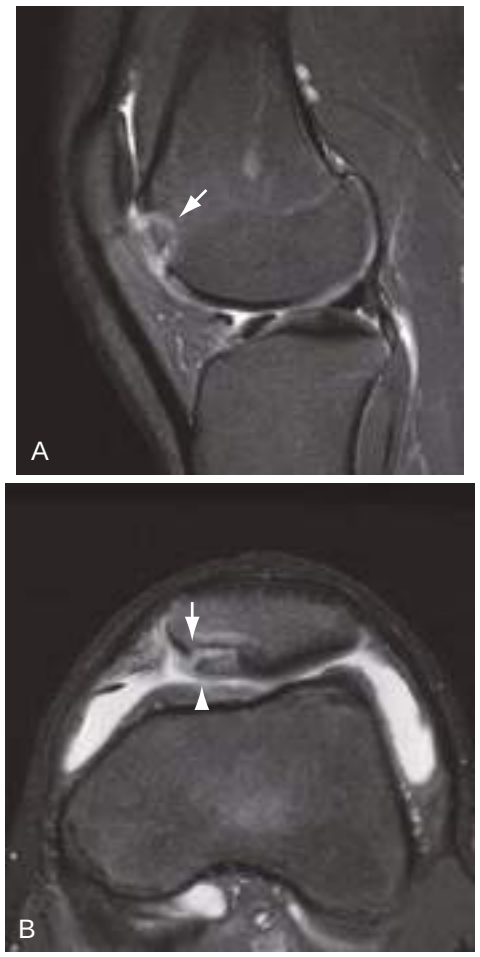

Fig. 1.95 Patellofemoral osteochondritis dissecans (OCD). (A) Sagittal fat-suppressed T2-weighted MR image shows lateral femoral trochlea OCD lesion *(arrow)*. **(B)** Axial T2-weighted spin-echo MR image obtained after intraarticular saline injection in a different patient shows partially displaced patellar OCD fragment *(arrowhead)*. Note that the intermediate signal material between the fragment and the host patella *(arrow)* has lower signal than the joint fluid. This tissue may be granulation, fibrous tissue, cartilage, or a combination. Joint fluid does not flow between the fragment and the host bone. At arthroscopy, the fragment was fixed in position.

Imaging of Osteochondritis Dissecans

Radiographs

- Subchondral fracture in a characteristic location (Box 1.10).
- Notch (tunnel, intercondylar) view, i.e. an anteroposterior view with the knee flexed at 40 degrees is the best view for detection.
- Fragment and/or adjacent epiphysis may be sclerotic (associated with a worse outcome).
- Note that some apparent fragmentation of epiphyseal bone can be a normal variant in the posterior femoral condyles in younger children (further discussed later).
- MRI findings range from subchondral bone marrow edema and thickened unossified cartilage to subchondral fractures and fragmentation to displacement of an osteochondral fragment.
- A main indication of MRI in OCD is to evaluate the stability of the osteochondral fragment. Fragments that are prone to displacement are managed surgically.

Fig. 1.96 Osteochondritis dissecans (OCD) with displaced fragments. (A) Coronal T2-weighted MR image of the right knee shows fluid filling medial femoral condyle OCD defect *(arrow)*. The fragment was displaced into the joint. (Same patient as shown in Fig. 1.88A.) Anteroposterior radiograph **(B)** and coronal fat-suppressed proton-density MR image **(C)** in a different patient show severe fragmentation of the medial femoral condyle *(arrows)*.

- Findings indicating an unstable ('loose in situ') fragment are less well defined in OCD than for an adult osteochondral lesion:
  - Bright T2 signal that surrounds the fragment (may be joint fluid, granulation, or edematous fibrous tissue, but the distinction is not important). This finding is highly specific for a loose fragment in an adult but less so in OCD.
  - Cystlike change in adjacent epiphyseal bone.
- MRI arthrography or high-resolution CT arthrography is occasionally requested. Joint contrast that surrounds part or the entire fragment is evidence of an unstable fragment.
- Additional findings in advanced OCD:
  - Fragment signal varies, but frequently has decreased T1 signal and sclerosis on CT.
  - Fragment may be mildly displaced, resulting in articular surface contour step-off.
  - Overlying articular cartilage may be intact, fractured at the fragment margin, and/or degenerated with decreased thickness and increased T2 signal.
  - Enhancement with intravenous contrast early in the process suggests better potential for healing.

OCD Management

- Based on the stability of the OCD lesion.
- Stable lesions are treated with non–weight-bearing and have a good prognosis.
- Unstable lesions require surgery.
  - Fragment stabilization with a pin or screw.
  - Fragment debriding or resection.
  - Osteochondral graft (see previous section).
  - Less severe lesions may be managed with drilling through the fragment into underlying host bone. This stimulates fibrocartilage growth and potentially bone that may adequately stabilize the fragment.
  - Prognosis of unstable lesions is better in OCD than in adult osteochondral lesion.

IMPORTANT OCD MIMIC

- Normal variation in epiphyseal ossification can overlap the imaging appearance of OCD (Fig. 1.97).
- Radiographs frequently show irregularity of the margin of the condylar ossification centers in 3- to 6-year-olds. Magnetic resonance images often show elevated T2 signal in the unossified growth cartilage in the posterior femoral condyles of younger children.
- In 10- to 13-year-olds, mild apparent fragmentation of the posterior portion of the femoral condyles may be seen as a normal variant.
  - Incidental cases usually are bilaterally symmetric and asymptomatic, with intact overlying cartilage and no edema on MRI.
  - However, this normal variant occasionally progresses to OCD, especially if the fragmentation is extensive, the joint is painful, and the child maintains a high level of activity. MRI shows edema in the fragments and unossified cartilage.

Child Abuse

- Inflicted or nonaccidental trauma, battered child syndrome, shaken baby syndrome, trauma X.
- Imaging findings in child abuse is essential knowledge for any radiologist who interprets pediatric images.
- This discussion briefly reviews the skeletal findings that are most specific for child abuse. Other organ systems, notably the central nervous system, may also sustain injuries that are fairly specific for child abuse.

IMAGING ASSESSMENT OF CHILD ABUSE

Techniques

- Radiographic skeletal survey.
  - First-line exam in children younger than 2 years.
  - Complete set of high-quality radiographs of the entire body, as recommended by the American College of Radiology (Box 1.11).
  - Adding lateral views of the extremities increases fracture detection but adds radiation.
  - High-detail equipment is required.
  - Obtaining these radiographs is time-consuming and requires a highly skilled and diplomatic technologist.

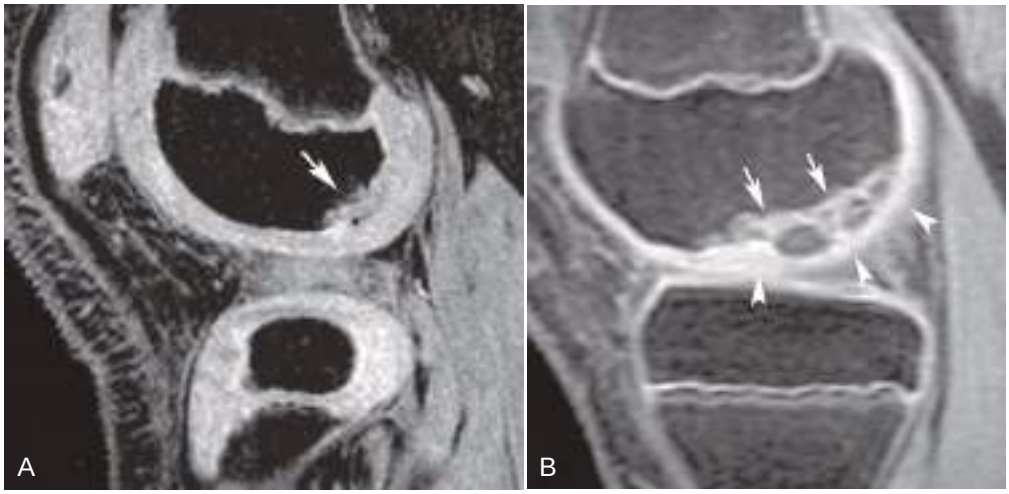

Fig. 1.97 Disorders that mimic osteochondritis dissecans (OCD). Subchondral bone irregularity or fragmentation is a frequent finding in the posterior femoral condyles of children. **(A)** Sagittal fat-suppressed spoiled gradient-echo MR image shows corresponding finding of subchondral irregularity, with cartilage filling the defect. Note the normal contour of overlying articular cartilage. Also, fluid-sensitive sequences showed no marrow edema, which is another clue to a benign process. **(B)** More extensive fragmentation *(arrows)* in a different child, in this case with potential to progress to OCD. Note the intact overlying cartilage *(arrowheads)*. Other sequences showed normal marrow signal, and the child had only minimal symptoms. These rather extreme findings resolved with restriction of the child's activities.

Box 1.11 Radiographic Series for Suspected Child Abuse

AP skull and lateral skull, additional skull views if needed
AP and lateral cervical spine
AP and lateral thorax
Oblique rib views optional but recommended
Lateral lumbosacral spine
AP pelvis
AP humeri
AP forearms
PA hands
AP femurs
AP tibias
PA or AP feet

AP, anteroposterior; *PA,* posteroanterior.

- In children younger than 2 years of age, a repeat examination after 2 weeks can be helpful to detect healing fractures that were originally occult.
- In older children, the examination can be tailored to 'where it hurts', but some sort of whole-body screening may still be appropriate.
- Bone scintigraphy.
  - Used as a complement to the skeletal survey.
  - Improves sensitivity for detecting periosteal reaction and rib, spine, pelvic, and acromion fractures.
  - Used when skeletal survey is negative but clinical suspicion remains high, either at presentation or more optimally 2 weeks later.
  - Normal physeal tracer uptake limits detection of adjacent fractures. Pinhole collimator imaging improves sensitivity.
- CT improves the detection of rib and spine fractures, but requires additional radiation and may require sedation.
- MRI can be helpful in detecting marrow and subperiosteal edema.
- Both MRI and US can detect fractures of unossified epiphyseal cartilage that are not visible on radiographs.

Findings

- The most specific fractures associated with child abuse are summarized in Box 1.12. Other fractures are less specific but still may be nonaccidental.
- The *classic metaphyseal lesion* (CML) is also known as the metaphyseal corner fracture and the bucket handle fracture. These are actually the same injury as seen from different perspectives (Fig. 1.98A and B).
  - The CML is radiographically similar to a Salter–Harris II fracture, but the transverse component extends through the immature bone of the distal metaphysis rather than through the cartilaginous physis as in a true Salter–Harris II fracture.
  - The mechanism is a combination of twisting and tension, as can occur when a child is violently shaken or when an extremity is violently pulled and twisted.
- Fractures around the infant thorax, especially the posterior ribs, result from forceful squeezing of the thorax by adult hands (Fig. 1.98C).
  - Highly specific for child abuse.

Box 1.12 Fractures Highly Suggestive of Physical Abuse

Classic metaphyseal lesions
Rib fractures, especially posterior
Scapular fractures
Spinous process fractures
Sternal fractures
Skull fractures that are complex or involve bones other than the parietal bone
Multiple fractures involving more than one skeletal area
Fractures of different age

Fig. 1.98 Child abuse, skeletal findings. (A and B) Classic metaphyseal lesions *(arrows)*. Also note the periosteal new bone formation in **A** *(arrowheads)*. **(C)** Posterior rib fractures. The fracture lines are not visible, but the callus formation indicates their presence *(arrowheads)*. These can be undetectable at the time of injury, illustrating the usefulness of follow-up radiographs. Even on delayed radiographs, subtle fractures of child abuse may remain nearly occult and must be carefully sought. **(D)** Multiple skull fractures. This finding is less specific for child abuse than the classic metaphyseal lesion and posterior rib fractures.

- Cardiopulmonary resuscitation of infants does not cause posterior rib fractures.

FRACTURE DATING

Fractures of different of ages is highly suspicious for child abuse. Also, precise fracture dating would provide important forensic evidence.

- As a result, radiologists are often asked to date healing fractures.
- Radiographs: callus usually first appears within 7–14 days but can be seen as early as 4 days.
- Most other generalizations are not reliably applied to an individual fracture, especially a fracture that has not been treated with immobilization. Therefore the following should be considered only as vague generalizations.
- Immature endosteal callus develops along the fracture, resulting in increased density within 10–14 days, and is maximal at 2–3 weeks.
- The endosteal callus matures and is subsequently removed by remodeling by 7–13 weeks after the fracture.
- Remodeling of a deformity begins by 3 months and can take up to 2 years.
- Repeated injury can prolong all of these time periods.

POTENTIAL MIMICKERS OF CHILD ABUSE

- Birth injury.
  - Often associated with shoulder dystocia or breech vaginal delivery.
  - Can cause clavicle and rib fractures and the CML in the extremities.
  - Review of the birth history and clinical follow-up are usually adequate to exclude abuse.
- Vigorous physical therapy in disabled children can cause fractures, including the CML.
- Other types of fractures are frequently seen in child abuse but are less specific (see Fig. 1.98D).
- Rickets.
  - Has characteristic radiographic and features such as rachitic rosary and metaphyseal flaring, reviewed in Chapter 13.
  - Rib fractures are rare in rickets.
- Metabolic bone disease of prematurity.
  - Basically rickets.
  - Very low birth weight infants are born without adequate stores of calcium, phosphate, and vitamin D. Oral delivery after birth is inadequate at first.
  - Most evident between 6 and 12 weeks postnatal.
- Osteogenesis imperfecta (OI), which is discussed in Chapter 15.
  - 95% of children with OI have blue sclerae.
  - Genetic evaluation for the associated mutation.

Other exceedingly rare syndromes also may produce findings suggestive of child abuse in the absence of true abuse, including Schmid-type metaphyseal chondrodysplasia, Langer-type spondyloepiphyseal dysplasia, Caffey disease (discussed in Chapter 15), Menkes syndrome (abnormal copper metabolism leading to weak bones), and congenital indifference to pain.

Box 1.13 Periosteal New Bone Formation in Children

Infection/inflammation
Healing fracture
Healing subperiosteal hematoma
Metabolic (scurvy, hypervitaminosis A and D, Gaucher disease, others)
Juvenile rheumatoid arthritis
Physiologic (during rapid growth, symmetric)
Solid tumors (often aggressive periosteal reaction)
Leukemia
Premature birth (prostaglandin E, physiologic, metabolic disease of prematurity)
Caffey disease (Chapter 15)
Melorheostosis (Chapter 15) can mimic periosteal new bone formation

Periosteal elevation in children can be associated with trauma, but there are numerous other potential causes (Box 1.13).

Congenital infection (e.g., due to syphilis) and scurvy, like rickets, also may produce features suggestive of child abuse. Clinical and laboratory workup and/or follow-up skeletal surveys are usually adequate to diagnose or exclude these conditions. Other entities such as 'brittle bone disease' and radiographically occult rickets due to vitamin D deficiency have been hypothesized but are not generally accepted.

Measuring Skeletal Maturity

- Essential information for diagnosis and management of many pediatric conditions.
  - Important examples:
    - Growth or sex hormone deficiency or excess.
    - Timing of surgery for childhood growth disturbances or scoliosis.
- The process of skeletal maturation tends to follow an orderly progression, even when accelerated or delayed by endocrine conditions, nutritional deficiencies, or other disease states.
- Thus, evaluation of just one part of the skeleton can serve as a reasonable surrogate for the entire skeleton.

GREULICH AND PYLE'S RADIOGRAPHIC ATLAS OF SKELETAL DEVELOPMENT OF THE HAND AND WRIST

- Widely adopted in the US as a standard reference for determining the skeletal age of children older than 1 year.
- Atlas of reference images of the maturing left hand.
- Derived from a longitudinal study of healthy children of northern European decent living in the Cleveland area during the 1930s.
  - This may not represent an optimal data set, but current appreciation of the potential harm of ionizing radiation makes it unlikely that a similar study will ever be performed in other racial or ethnic groups.
- Contemporary evaluations of this atlas have verified its accuracy, at least in children of European descent.
- Provides bone age and standard deviations. Chronologic age within two standard deviations of bone ages is considered to be normal.
- Automated versions are available.
- As a general rule, children of African descent tend to skeletally mature faster than white children. Girls mature faster than boys, and the difference becomes greater as they grow.

TANNER–WHITEHOUSE METHODS 2 AND 3

- Evaluates the hand and wrist.
- Based on a data set of British children from the 1950s and 1960s.
- This method is used more commonly in Europe.
- Arguably more precise than Greulich and Pyle, but time-consuming when done manually.
- Artificial intelligence apps reduce the analysis time to a few seconds with either technique.

METHOD OF SONTAG, SNELL, AND ANDERSON

- For infants and very young children not covered by Greulich and Pyle.
- Radiographs of one upper and one lower extremity are evaluated for the number of secondary growth centers (epiphyses, apophyses, and small round bones) that have started to ossify.
- Relies on a yes-or-no determination of the presence of visible ossification in each secondary growth center (Table 1.1).
  - The *Elgenmark method* is similar, but it uses only unilateral carpal and tarsal bones.

RISSER TECHNIQUE

Is used to estimate skeletal maturity of the spine in adolescents with scoliosis.

- Based on the radiographic appearance of the iliac crest apophyses.
- The iliac crest apophyses ossify in an orderly sequence from lateral to medial before fusing to the crest when or shortly after spinal growth is complete.
- Discussed further in the Scoliosis Management section in Chapter 15.

Table 1.1 Skeletal Age in Infants: the Method of Sontag, Snell, and Anderson

MEAN TOTAL NUMBER OF CENTERS ON THE LEFT SIDE OF BODY OSSIFIED AT GIVEN AGE LEVELS

	Boys		Girls	
Age (months	Mean No.	SD	Mean No.	SD
1	4.11	1.41	4.58	1.76
3	6.63	1.86	7.78	2.16
6	9.61	1.95	11.44	2.53
9	11.88	2.66	15.3	4.92
12	13.96	3.96	22.40	6.93
18	19.27	6.61	34.10	8.44

SD, standard deviation.

Sample Report

History: short stature.

Comparison: 6 months previously.

The child's chronologic age is 9 years, 4 months.

Using the standards of Greulich and Pyle, the child's skeletal age is 8 years, 5 months. The standard deviation is 8 months.

Skeletal age on the prior exam was 8 years.

Impression: Normal skeletal maturation.

Sources and Suggested Readings

Adamsbaum C, Méjean N, Merzoug V, Rey-Salmon C. How to explore and report children with suspected non-accidental trauma. *Pediatr Radiol*. 2010;40(6):932–938.

American College of Radiology ACR Appropriateness Criteria® Suspected Physical Abuse–Child. https://acsearch.acr.org/docs/69443/Narrative/.

Beaman FD, Bancroft LW, Peterson JF, et al. Imaging characteristics of bone graft materials. *RadioGraphics*. 2006;26:373–388.

Beaty JH, Kasser JR, Shaggs DL, et al., eds. *Rockwood and Green's Fractures in Children*. Philadelphia: Lippincott-Raven; 2009.

Beck BR, Bergman AG, Miner M, et al. Tibial stress injury: relationship of radiographic, nuclear medicine bone scanning, MR imaging, and CT severity grades to clinical severity and time to healing. *Radiology*. 2012; 263(3):811–818.

Brittberg M, Winalski CS. Evaluation of cartilage injuries and repair. *J Bone Joint Surg Am*. 2003;85-A(Suppl 2):58–69.

Bucholz RW, Court-Brown CM, Heckman JD, Tornetta P, eds. *Rockwood and Green's Fractures in Adults*. Philadelphia: Lippincott-Raven; 2009.

Christian CW, States LJ. Medical mimics of child abuse. *Am J Roentgenol*. 2017;208(5):982–990.

Crema MD, Roemer FW, Marra MD, et al. Articular cartilage in the knee: current MR imaging techniques and applications in clinical practice and research. *Radiographics*. 2011;31(1):37–61.

Deshmukh S, Carrino JA, Feinberg JH, et al. Pins and needles from fingers to toes: high-resolution MRI of peripheral sensory mononeuropathies. *AJR Am J Roentgenol*. 2017;208(1):W1–W10.

Disler DG. Articular cartilage in the knee: current MR imaging techniques and applications in clinical practice and research. Invited commentary. *Radiographics*. 2011;31(1):61–62.

Ecklund K, Jaramillo D. Patterns of premature physeal arrest: MR imaging of 111 children. *AJR Am J Roentgenol*. 2002;178:967–972.

Gold GE, Chen CA, Koo S, et al. Recent advances in MRI of articular cartilage. *AJR Am J Roentgenol*. 2009;193(3):628–638.

Gorbachova T, Melenevsky Y, Cohen M, Cerniglia BW. Osteochondral lesions of the knee: differentiating the most common entities at MRI. *Radiographics*. 2018;38:1478–1495.

Guermazi A, Roemer FW, Alizai H, et al. State of the art: MR imaging after knee cartilage repair surgery. *Radiology*. 2015;277(1):23–43.

Hu H, Zhang C, Chen J, et al. Clinical value of MRI in assessing the stability of osteochondritis dissecans lesions: a systematic review and meta-analysis. *AJR Am J Roentgenol*. 2019;213:147–154.

Jaimes C, Jimenez M, Shabshin N, et al. Taking the stress out of evaluating stress injuries in children. *Radiographics*. 2012;32:537–555.

Jarraya M, Hayashi D, de Villiers RV, et al. Multimodality imaging of foreign bodies of the musculoskeletal system. *Am J Roentgenol*. 2014;203(1): W92–W102.

Jo S, Sammet S, Thomas S, et al. Musculoskeletal MRI pulse sequences: a review for residents and fellows. *Radiographics*. 2019;39:2038–2039.

Joint ACR/Society for Pediatric Radiology/Society of Skeletal Radiology guidelines. https://www.acr.org/-/media/ACR/Files/Practice-Parameters/Scoliosis.pdf.

Kleinmann P, ed. *Diagnostic Imaging of Child Abuse*. 3rd ed. Cambridge: Cambridge University Press; 2015.

Laor T, Zbojniewicz AM, Eismann EA, Wll EJ. Juvenile osteochondritis dissecans: is it a growth disturbance of the secondary physis of the epiphysis? *AJR Am J Roentgenol*. 2012;199(5):1121–1128.

Lonergan GJ, Baker AM, Morey MK, Boos SC. From the archives of the AFIP. Child abuse: radiologic-pathologic correlation. *Radiographics*. 2003;23:811–845.

Marshall RA, Mandell JC, Weaver MJ, et al. Imaging features and management of stress, atypical, and pathologic fractures. *Radiographics*. 2018; 38:2173–2192.

May DA, Disler DG, Jones EA, et al. Abnormal signal within skeletal muscle in magnetic resonance imaging: patterns, pearls, and pitfalls. *Radiographics*. 2000;20:S295–S315.

McCarthy EF, Sundaram M. Heterotopic ossification: a review. *Skeletal Radiol*. 2005;34:609–619.

Miller TT, Reinus WR. Nerve entrapment syndromes of the elbow, forearm, and wrist. *AJR Am J Roentgenol*. 2010;195(3):585–594.

Narayanasamy S, Krishna S, Sathiadoss P, et al. Radiographic review of avulsion fractures. *Radiographics*. 2018;38:1496–1497.

Nguyen JC, Markhardt BK, Merrow AC, et al. Imaging of pediatric growth plate disturbances. *Radiographics*. 2017;37:1791–1812.

Offiah A, van Rijn R, Perez-Rossello JM, Kleinman P. Skeletal imaging of child abuse (non-accidental injury). *Pediatr Radiol*. 2009;39(5):461–470.

Outerbridge RE. The etiology of chondromalacia patellae. *J Bone Joint Surg Br*. 1961;43-B:752–757.

Pathria MN, Chung CB, Resnick DL. Acute and stress-related injuries of bone and cartilage: pertinent anatomy, basic biomechanics, and imaging perspective. *Radiology*. 2016;280:21–38.

Peterfy CG, Guermazi A, Zaim S, et al. Whole-organ magnetic resonance imaging score (WORMS) of the knee in osteoarthritis. *Osteoarthritis Cartilage*. 2004;12(3):177–190.

Sargar KM, Singh AK, Kao SC. Imaging of skeletal disorders caused by fibroblast growth factor receptor gene mutations. *Radiographics*. 2017;37: 1813–1830.

Schulze M, Kötter I, Ernemann U, et al. MRI findings in inflammatory muscle diseases and their noninflammatory mimics. *AJR Am J Roentgenol*. 2009;192(6):1708–1716.

Smitaman E, Flores DV, Mejía Gómez C, Pathria MN. MR imaging of atraumatic muscle disorders. *Radiographics*. 2018;38:500–522.

van Vucht N, Santiago R, Lottmann B, et al. The Dixon technique for MRI of the bone marrow. *Skeletal Radiol*. 2019;48:1861.

Vassalou E, Zibis AH, Raoulis VA, et al. Morel-Lavallée lesions of the knee: MRI findings compared with cadaveric study findings. *AJR Am J Roentgenol*. 2018;210(5):W234–W239.

White CL, Chauvin NA, Waryasz GR, et al. MRI of native knee cartilage delamination injuries. *Am J Roentgenol*. 2017;209(5):W317–W321.

Winalski CS, Rajiah P. The evolution of articular cartilage imaging and its impact on clinical practice. *Skeletal Radiol*. 2011;40(9): 1197–1222.

Wooten-Gorges SL, Soares BP, Alazraki AL, et al. ACR appropriateness criteria: suspected physical child abuse. Expert Panel on Pediatric Imaging. *J Am Coll Radiol*. 2017;14:S338–S349.